PHYSICAL MODELS OF NONCOVALENT INTERACTIONS INVOLVING AROMATIC RINGS

A Dissertation

by

JACOB WALTER GOLDSTEIN BLOOM

Submitted to the Office of Graduate and Professional Studies of
Texas A&M University
in partial fulfillment of the requirements for the degree of

DOCTOR OF PHILOSOPHY

Chair of Committee,	Steven E. Wheeler
Committee Members,	Robert R. Lucchese
	Michael B. Hall
	Perla B. Balbuena
Head of Department,	David H. Russell

May 2014

Major Subject: Chemistry

ABSTRACT

Noncovalent interactions involving π-systems play a vital role throughout chemical and biological processes. These π-interactions can be found in organic photovoltaics and electronics as well as govern many protein and DNA interactions. A fundamental and physically meaningful model of these interactions is necessary for the efficient exploitation of these materials and rational drug design. First, the role of aromaticity in π-stacking, cation/π, and anion/π interactions is investigated. Aromaticity weakly hinders π-stacking and greatly hinders anion/π interactions, while greatly enhancing cation/π interactions. Nonaromatics, therefore, present themselves as a new target in design for π-stacking and anion/π interactions.

The well-established local direct interaction model for π-stacking that substituent effects are due solely to local electrostatic changes has also been expanded herein. First, we show that the local direct model for substituent effects in π-stacking also applies to polar XH/π interactions. The nonpolar XH/π interactions vary little with substituent, depending only on changes in dispersion. The energetic changes of both sets of XH/π interactions follow well-known substituent constants. Next, the local direct interaction model is expanded to the use of electric fields to reconcile unusual similarity in the substituent effects between benzene, triazine, and borazine. Substituent effects for different rings are similar as long as the electric fields of those rings are similar in the location of the substituent. In fact, the substituent effect scales proportionally to the

relative strength of those fields. Lastly, in an analysis on anion/π complexes with a variety of azines and benzene, it is shown that changes induced through the substitution of a carbon-hydrogen bond with nitrogen are almost exclusively from the nuclear charge differences. This reconciles well with the local direct interaction model.

DEDICATION

This dissertation is dedicated to Mr. J. Bloom.

ACKNOWLEDGEMENTS

Thanks to all my friends, family, professors, and staff who helped me get here. Particular thanks to Sandy Manning for helping me get my ducks in a row. Thanks to Dr. Johnson for inspiring my career as a chemist and for all of those extra Saturdays dedicated toward teaching me AP Chemistry.

Chapter II was supported by the ACS Petroleum Research Fund (ACS PRF 50645-DNI6) and we acknowledge the Texas A&M Supercomputing Facility for computational resources. S. Steinmann and C. Corminboeuf are thanked for fruitful discussions.

Chapter III was supported in part by the ACS Petroleum Research Fund (ACS PRF 50645-DNI6). We also thank the Texas A&M Supercomputing facility for providing computational resources.

Chapter IV was supported in part by the National Science Foundation (Grant CHE-1254897) and we acknowledge the Texas A&M Supercomputing Facility for computational resources. J. S. Siegel and T. Lu are thanked for fruitful discussions.

Chapter V was supported by the National Science Foundation (Grant CHE-1254897). We also acknowledge the Texas A&M Supercomputing Facility for computational resources and H. T. Chifotides, J. Frank, and K. R. Dunbar for fruitful discussions.

TABLE OF CONTENTS

Page

Page

LIST OF FIGURES

Page

Page

Page

LIST OF TABLES

Page

Page

CHAPTER I

INTRODUCTION

Interactions involving π-systems (See Fig. 1.1), known as π-interactions, can be found throughout chemistry and biology including molecular recognition, crystal packing, tertiary structures and active sites of proteins, and even DNA.[1-26] In biological systems, rational drug design is highly dependent on a thorough understanding of the target system for the selection of viable candidate ligands.[27] Furthermore, π-interactions have been shown to play a significant role in the damage and repair processes in DNA.[28] These interactions also play a large role in more industrial applications. Many of the routes toward improvement of organic electronic devices are focused on tuning the intramolecular properties such as the HOMO-LUMO gap.[29,30] The tuning of π-interactions can improve charge transport between chains as well as flatten oligothiophenes and similar systems to narrow the HOMO-LUMO gap.[31] A better understanding of π-interactions should be useful for a variety of important applications.

The term π-interactions has not been fully accepted by the scientific community. In 2006, Grimme critiqued these terms by comparing stacked arenes and their fully saturated analogues.[2] He noted that for small systems, there was no significant difference in the interactions and the term π-stacking should be reserved as a geometric description. Martinez and Iverson recently challenged π-stacking and π-π interactions as terms due to the repulsive nature of the two π-systems.[1] They note that the local direct interaction model (see below) supplants any thoughts of the π-systems having a

significant role. They argue to not use these terms despite their provision of a useful geometric description as they are too often confused as an energetic description. Within this work, π-interactions and related terms are used solely as a geometric description.

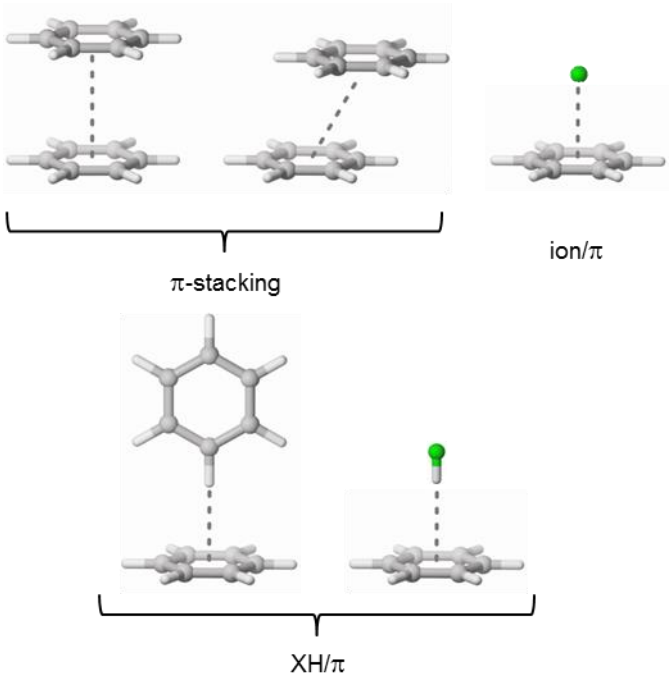

Figure 1.1: Prototypical π-interactions

A similarly confusing term, aromatic interactions, has also appeared throughout the literature. This label limited studies and designs around this peculiar motif to those of aromatic molecules. Chapter II focuses on whether the term aromatic interactions should indeed be used at all, showing that not only should the label aromatic interactions be broadened to at least π-stacking interactions, but aromaticity actually hinders some of

these interactions. Since publication of this chapter, there have been several experimental examples of nonaromatic π-interactions.[32-35]

π-stacking interactions are the most studied of the various π-interactions. In fact, the early work on stacking is foundational for many of the other π-interaction models. Hunter and Sanders first proposed a profusely used model for describing π-stacking interactions.[36] Their model posited that the geometries found in π-stacking interactions are driven by electrostatic forces. Though these are not the strongest forces involved in these interactions, Hunter and Sanders showed that qualitative predictions could be made using a distributed quadrupole based on the π-system; the most favorable configuration occurs when electron deficient and electron rich atomic quadrupole moments of the opposing rings are in proximity as this reduces the π-repulsion. One assumption that differs drastically from the local direct model for substituent effects is that the effect of substituents is included in these quadrupole moments with the assumption that the π-system of the ring is being changed.

A modified version of the Hunter-Sanders model proposed by Hunter et al is oversimplified.[37] Rather than comparing the atomic π-densities through distributed quadrupole moments, this new version uses the molecular quadrupole moment Q_{zz}. In addition to losing information about orientation, the connection between π-density and quadrupole moment established by the original model is continued. Thus, electron-donating substituents cause an increase in π-density and electron-withdrawing substituents decrease the π-density, where more favorable interactions occur when one

ring is π-electron rich and the other deficient. This newer model is qualitatively valid for benzene interacting with hexafluorobenzene, but easily fails for 1,3,5-trifluorobenzene, a regime where the original Hunter-Sanders model predicts the correct geometry.[38,39] This failure is due to Q_{zz} lacking any information involving the orientation and about the z axis. Inclusion of more molecular multipole terms may appear to correct this deficiency; however, this ignores an important aspect of the multipole expansion.

Formally, the multipole expansion is always convergent only at distances greater than the charge distribution it is describing. This definition is incompatible with a quantum mechanical description of a molecule where the wavefunction, and therefore the location of the charge being described, continues infinitely. Fortunately, it has been shown that the multipole expansion is always convergent as long as two spheres, each enclosing all the nuclei of two monomers, do not overlap.[40,41] Unfortunately for the modified Hunter model utilizing Q_{zz} values, π-stacking interactions occur at distances where these spheres overlap; for the case of benzene stacked with hexafluorobenzene, the equilibrium distance of 3.5Å is within the 5.2Å of separation required.[42] This is the realm where distributed multipole analysis is required for a valid description.

The simplified Hunter model was shown to be not predictive by Lewis and coworkers.[43] They showed that not only are quadrupole moments not correlated with the interaction energies of a variety of substituted arenes, but that Hammett constants had surprising predictive ability. In a similar study, Kim et al showed that a correlation exists between the electrostatic energies and the total energies of π-stacked substituted

benzene dimers.[44] The other terms involved, exchange-repulsion, induction, and dispersion, cancelled each other out in each dimer. Sherrill and coworkers have shown that interpenetration, where the charge clouds of the two molecules have significant overlap at close range, leads to an always favorable interaction regardless of the nature of the substituent.[45] Interpenetration is always favorable until the extremely close distances where the nuclei start to collide.[42]

Wheeler and Houk have expanded on this attack on the simplified Hunter model and the original Hunter-Sanders model.[46] They have shown that almost all of the substituent effects can be explained as through-space electrostatic interactions between the substituents and the unsubstituted ring often referred to as the local direct model. This explanation refrains from any invocation of changes to the π-density, whether the whole molecule as in the simplified Hunter model or localized as in the original Hunter-Sanders model. In fact, the changes in interaction energies can be reproduced with the substituents bound to hydrogen instead of benzene. Subsequent work has expanded this model to include substituents on both arenes, finding that substituent effects are dependent only on the proximal apex of the interacting ring.[47]

Chapters III and IV expand the local direct interaction model. First, a comprehensive analysis of XH/π interactions for small model systems in performed. Using Symmetry-Adapted Perturbation Theory (SAPT, see section 1.1) to analyze the physical cause for these systems, it was determined that electrostatic interactions drive the more polar FH/π, OH/π, and NH/π interactions, while dispersion controls, albeit subtly, the CH/π and BH/π interactions. These polar XH/π interactions follow a similar

trend as that found in π-stacking. Additionally, correlations with known substituent constants were produced for potential use in future work. The other chapter focuses back on π-stacking itself to determine if substituent effects are transferable among benzene, triazine, and borazine. Not only were these found to be transferable when the proximal apex of the unsubstituted ring was the same, but also when the unsubstituted rings produced similar electric fields at the location of the substituent. This discovery has led to a refinement and broadening of the local direct model for substituent effects in π-stacking.

Chapter V challenges the existing models when applied to anion/π interactions and further support the local direct interaction model. In this chapter, benzene's and several azines' electrostatic potentials (ESP) and Q_{zz} values are separated into σ-system and π-system components. In addition, the nuclear component is analyzed separately from the electronic components. This work is a direct challenge to the assumptions of both the Hunter-Sanders and simplified Hunter model. For an anion/π interaction involving a chloride, the simplified Hunter model should be suitable if the basic assumptions of the overall π-density in these dramatically altered arenes hold. However, as is shown, the vast majority of the system changes occurs from the nucleic changes when going from a carbon-hydrogen bond to just a nitrogen. This is reconciled with the local direct interaction mode through a local dipole model of this change.

These chapters on aromaticity, substituent effects, and anion/π interactions provide much needed and insightful challenges to some of the remaining areas of confusion surrounding the noncovalent interactions of π-systems. Though some more

nuanced areas are currently being explored to fill the few gaps that remain, the Hunter-Sanders model appears to be invalid for these interactions and should be replaced with the more physically and chemically sound local direct interaction model. These noncovalent interactions are entirely the result of local molecular changes.

1.1 DFT-D AND SAPT

A variety of methods can be used for analyzing noncovalent interactions including SAPT, Density Functional Theory with an empirical dispersion correction (DFT-D), and more conventional Hartree-Fock (HF) based methods. As SAPT and DFT-D are the newer and lesser used methods, a discussion is warranted. The SAPT method is one of a few routes to determine the origin of the interaction energies through decomposition into known physically meaningful terms. The four components found are referred to as exchange-repulsion, electrostatic, induction, and dispersion. Most discussions on noncovalent interactions will refer to these terms at least qualitatively, but with SAPT analyses, one can quantify these terms. DFT-D, meanwhile, is not as easily decomposable. Though the final D of DFT-D is an empirical "dispersion" correction that can be added to any variant of DFT, it is not necessarily only or all of the dispersion. In fact, the correction is scaled depending on the needs of the functional and can therefore vary depending on the functional used. The particular variant of DFT-D used herein is B97-D; as such, a brief discussion of the formulation of B97-D.

The Hohenberg-Kohn theorem uses density as a replacement for the wavefunction found in HF based methods.[48] To do this, the energy of the system can be

separated into three main components: the non-interaction kinetic energy, the electrostatic energy, and the exchange-correlation energy:

$$E_{HK} = E_{ni} + E_{es} + E_{xc}.$$

The electrostatic energy has a well-known form:

$$E_{es} = \frac{e^2}{2}\int \frac{\rho(r)\rho(r')}{|r - r'|} dr dr',$$

where ρ is the density of the system. The non-interacting kinetic energy can be solved through the Kohn-Sham formulation of DFT by reintroducing orbitals. To do this, the Schrödinger equation is evaluated for a system on noninteracting electrons:

$$\left(-\frac{\hbar^2}{2m}\nabla^2 + v_{ni}\right)\psi_{i(r)} = \epsilon_i \psi_i(r),$$

where $\rho(r) = \sum_{i=1}^{N} |\psi_i(r)|^2$. The operators corresponding to the Hohenberg-Kohn energy formula is then rearranged such that $v_{ni} = v_{es} - v_{HK} + v_{xc}$. The energy of the system and the wavefunction, and density, can be solved self-consistently as long as the exchange-correlation has an appropriate form. The variants of DFT that exist are all different attempts at finding an approximation to the exchange-correlation operator that yields an accurate energy.

The first approximation made for the exchange-correlation term is that of the local spin density approximation (the spin component accounts for any differences due to electron spin).[48] This approximation assumes that the electron density of the system changes little, leading to an incorrect behavior in the asymptotic limit of infinity. This can pose problems both in bond dissociation energies and non-covalent interactions, both of which can be thought of as the interaction of densities far from their centers.[49]

To correct this deficiency, a generalized gradient approximation (GGA) is added to this term, which, by design, reproduces the infinite limit behavior. This gradient term now incorporates rapid changes in the electron density and makes DFT an attractive solution for many molecular simulations. Two other additional corrections can be made referred to as meta-GGA and hybrid. These corrections increase computational costs, but do not appear to be necessary for reasonably accurate energies in these non-covalent interactions.

Becke's B97 style functional is one of many functionals utilizing gradients.[50] Becke designed B97 to be tuned to any data set, splitting the exchange-correlation energy as follows:

$$E_{XC} = E_X + E_{C_{\alpha\beta}} + \sum_{\sigma=\alpha,\beta} E_{C_{\sigma\sigma}} \ ,$$

$$E_X = \sum_{\sigma=\alpha,\beta} \int e\big(\rho_\sigma(r)\big) g_{X_\sigma}(s_\sigma^2) dr$$

$$E_{C_{\alpha\beta}} = \int e\left(\rho_\alpha(r), \rho_\beta(r)\right) g_{C_{\alpha\beta}}\left(\frac{1}{2}(s_\alpha^2 + s_\beta^2)\right) dr$$

$$E_{C_{\sigma\sigma}} = \int e\big(\rho_\sigma(r)\big) g_{C_{\sigma\sigma}}(s_\sigma^2) dr$$

where $g(s^2) = \sum_{j=0}^{k} c_j u^j(s^2)$. With this in mind, Grimme took the burgeoning concept of DFT-D and reparameterized B97 with an explicit dispersion correction he called B97-D and a k value of 2.[51] The dispersion component itself is approximated by the first order multipole expansion of a dispersion interaction:

$$E_{disp} = -s_6 \sum_i \sum_{j=i+1} \frac{C_6^{ij}}{R_{ij}^6} f\big(R_{ij}\big) ,$$

where $f(R_{ij})$ is a damping function to prevent double counting intramolecular dynamic correlation and C_6^{ij} is a coefficient for the atom pair i and j. A noteworthy aspect of this form is that molecular anisotropy is inherently included through the atom centered equation.[52] By including the dispersion correction during the functional fitting process, B97-D performs remarkably well through avoidance of double counting of close range dynamic correlation and inclusion of the long range.[51] The errors associated with π-systems were found to be within the errors of the reference energies when paired with a TZV style basis set.[51] It is for this reason that B97-D/TZV(2d,2p) is used for much of this work, though a more recent B97-D3 may prove more accurate through the inclusion of atomic hybridization states and a second order multipole expansion.[52]

This empirical dispersion correction is a preferred choice over other DFT dispersion methods for several reasons. The first being that it can be added to any functional with little effort, normally by scaling the above equation and adding it as a correction.[52] As mentioned, in the case of B97-D, it was parameterized with the functional as opposed to being a scaled correction. Secondly, it can be easily implemented in optimizations as its simple form has an analytical gradient. The last advantage is due to the atom centered nature of this correction; individual atomic interactions related to dispersion can be teased from this calculation, though this is not performed herein.

A more illuminative theory for intermolecular interactions is SAPT, which can predict interaction energies to within a few percent for 100 atoms.[53] The current state and direction of SAPT is very exciting with recent developments including three-

monomer SAPT and DFT-SAPT. SAPT itself is twice based on Rayleigh-Schrödinger perturbation theory. The first basis constitutes the most unique aspect and is an adaptation of polarization theory. The Hamiltonian found in SAPT and polarization theory is composed of the Hamiltonians for the individual monomers and a perturbation, V, of the coulombic interactions between the electrons and nuclei of each monomer with the other yielding the following Schrödinger equation:

$$(H_A + H_B + \zeta V)\Phi_{AB} = E_{AB}\Phi_{AB},$$

where

$$\Phi_{AB}(\zeta) = \sum_{n=0}^{\infty} \zeta^n \Phi_{pol}^{(n)}.$$

The electrostatic energy is resultant when $\zeta = 1$. The induction of monomer A by electrostatic environment of monomer B, and vice versa, as well as the first, and usually largest, dispersion term is found when $\zeta = 2$. The second dispersion term and a term corresponding to the coupling of induction and dispersion occur when $\zeta = 3$, however the expansion is normally truncated at $\zeta = 2$.[54] The unperturbed Hamiltonian, where V is zero, has a solution in the form of the product of the monomer wavefunctions. Unfortunately, this does not fulfill the Pauli Exclusion Principle for a perturbed many-electron system and needs to be antisymmeterized, but this antisymmeterization would then no longer be an eigenstate for the unperturbed system.[53] SAPT solves this by first calculating the unperturbed system and then antisymmerterizing the wavefunction prior to using polarization theory. The antisymmeterization also yields exchange terms, of which only the first order is considered exchange, while higher orders are corrections to

induction and dispersion.[54] As such, SAPT yields overall exchange, electrostatic, induction, and dispersion energies to enable a more thorough analysis. The second Rayleigh-Schrödinger perturbation theory found in SAPT in the addition of Møller-Plesset Perturbation Theory (MP) to give the following Hamiltonian:

$$H = F_A + F_B + W_A + W_B + V,$$

where F_A is the Fock operator for molecule A, W_A is the MP perturbation operator, and V is, again, the intermolecular coulombic perturbation operator. This inclusion of MP perturbation theory provides a more accurate monomer wavefunction and energy for use in the SAPT equations.

CHAPTER II

TAKING THE AROMATICITY OUT OF AROMATIC INTERACTIONS*

The phrase "aromatic interactions" is widely used to describe π-stacking, cation/π, and anion/π interactions, among others.[37,55] These interactions are central to many areas of modern chemistry and molecular biology,[22,56-59] and are vital tools in the supramolecular armamentarium.[56] The concept of aromaticity appears almost universally in definitions of these interactions, implying that they are somehow dependent on aromatic π-delocalization in the interacting monomers. But does aromaticity actually enhance these interactions, or can stronger noncovalent interactions be achieved, for example, by using planar, non-aromatic polyenes?

We show below, through robust *ab initio* studies of model systems, that the cyclic π-electron delocalization associated with aromaticity often hinders π-stacking and anion/π interactions, although it strengthens cation/π interactions. The implication is that more favourable stacking interactions can be achieved in supramolecular complexes by exploiting interactions with non-aromatic polyenes rather than aromatic systems.

In 2008, Grimme[60] showed that stacking interactions in the parallel-displaced benzene and naphthalene dimers are comparable in magnitude to the corresponding saturated cyclic systems. However, for larger acenes (*i.e.*: anthracene and tetracene), Grimme reported enhanced stacking interactions in the aromatic dimers that are not

mirrored in the saturated systems. This was attributed to long-range correlation effects.[60] The impact of *aromaticity* on these stacking interactions, however, was not directly addressed.

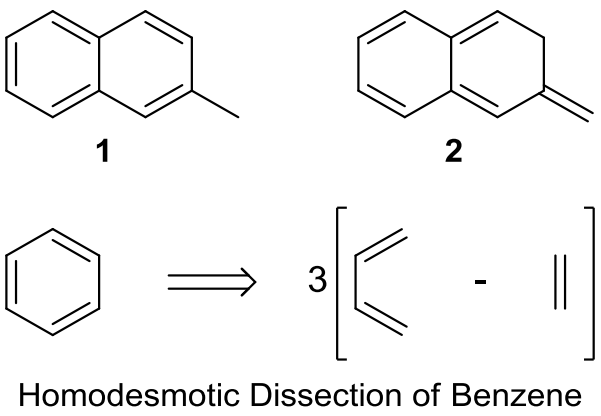

Figure 2.1: Molecular systems used to quantify the effect of aromatic π-delocalization on stacking and other aromatic interactions: 2-methylnaphthalene (1), 2-methylene-2,3-dihydronaphthalene (2), and dissected benzene. In the dissected benzene, the nuclear positions are such that all interatomatic distances exactly match those in benzene.

Here, we quantify the effect of aromatic π-electron delocalization on the strength of π-stacking, cation/π, and anion/π interactions. We first consider the sandwich dimers of benzene with the unsubstituted rings of 2-methylnaphthalene (**1**) and 2-methylene-2,3-dihydronaphthalene (**2**) (see Fig. 2.1 and Fig. 2.2a). Isomer **2** provides a means of quenching the aromaticity present in **1** while conserving the number of π-electrons.[61] Isomers **1** and **2** can thus be used to quantify the electronic effects of aromatic π-

delocalization on stacking interactions.[a] SCS-MP2/TZVPP interaction energies at equilibrium separations are provided in Fig. 2.2, and are plotted as a function of inter-monomer distance (*R*) in the appendix Fig. A.1. Across the full range of distances, the stacking interaction of benzene with the non-aromatic isomer **2** is more favourable than with **1**. In other words, the non-aromatic isomer engages in stronger stacking interactions with benzene than does the aromatic isomer. This difference is not attributable to differential direct interactions[46] between benzene and the methyl/CH or methylene/CH_2 groups in **1** and **2** (see Appendix A), but instead results from the localization of the π-system in isomer **2**.

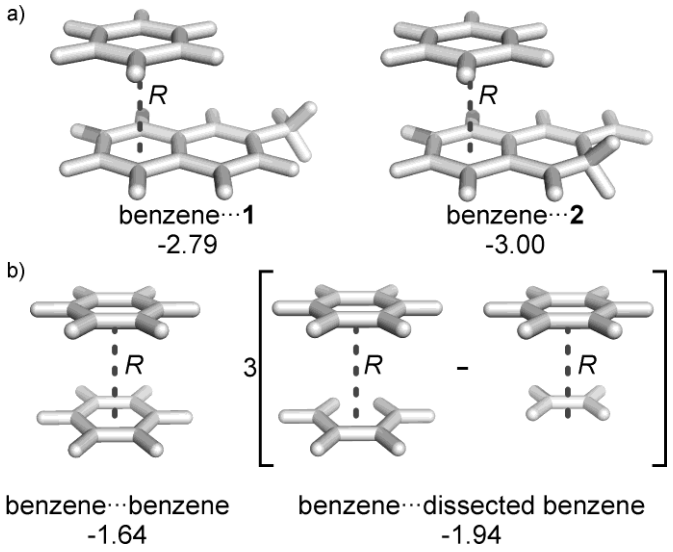

Figure 2.2: Sandwich dimers and interaction energies (kcal mol–1) for benzene with a) 2-methylnaphthalene (1) and 2-methylene-2,3-dihydronaphthalene (2) at the SCS-MP2/TZVPP level of theory and b) benzene and dissected benzene at the CCSD(T)/AVTZ level of theory.

[a] To avoid complications from changes in nuclear arrangements, the conserved atoms in 2 are fixed at the equilibrium geometry of 1, and only the positions of the added hydrogens optimized.

The homodesmotic[62-64] dissection of benzene depicted in Figure 2.1 provides an alternative means of quantifying the effect of aromatic π-delocalization on stacking interactions (see Fig. 2.2b and Table 2.1).[65] Comparing CCSD(T) interaction energies in the benzene sandwich dimer with the interaction between benzene and dissected benzene yields the same conclusion as above; π-localization stabilizes sandwich stacking interactions by 0.31 kcal mol^{-1} at the corresponding equilibrium inter-monomer separations (3.92 and 3.84 Å for benzene and dissected benzene, respectively).

Table 2.1: Estimated CCSD(T)/AVTZ interaction energies (kcal mol–1) of benzene, Cl–, and Na+ with benzene and dissected benzene.[a]

	C_6H_6 (S)	C_6H_6 (P)	Cl^-	Na^+
Benzene	–1.64	–2.60	+0.86	–23.5
Dissected Benzene	–1.94	–3.60[b]	–1.10	–18.2

[a] (S) = sandwich dimer; (P) = parallel-displaced dimer. [b] Interaction energy is –3.09 kcal mol^{-1} if the dissected benzene is rotated 60°.

These effects are even larger for the parallel displaced dimer.[b] In this configuration, replacing benzene with dissected benzene increases the interaction by 1.0 kcal mol^{-1}, or nearly 40% of the total interaction energy! Moreover, the magnitude of this energy difference is dependent on the regiochemistry of the localized π-system (see Table 2.1). This suggests a potential means of controlling the orientation of parallel displaced stacking interactions in the case of localized π-systems.

Cation/π and anion/π interactions are also affected by π-localization. Indeed, the differences between the interaction of Na^+ or Cl^- with benzene and the dissected benzene

[b] Vertical separation of 1.69 Å and horizontal displacement of 3.52 Å

are substantially larger than in the stacking interactions, as seen in appendix Figs. A.3 and A.4 and in Table 2.1. Intriguingly, localization of the benzene π-system enhances the interaction with Cl^- to such an extent that this model system is actually bound in the gas phase, unlike benzene-Cl^-.[66] In the case of the cation/π comlexes, π-localization diminishes the interaction by more than 5 kcal mol^{-1}.

The enhanced stacking interaction in the sandwich dimer of benzene with dissected benzene extends over the full range of inter-monomer distances (see Fig. 2.3a). These differences are reproduced at the Hartree-Fock (HF) level (grey curves), indicating that electron correlation effects (*e.g.* dispersion interactions) have little net impact. This is corroborated by SAPT2 analyses,[c,50,54] the results of which are plotted in Fig. 2.3b as a function of *R*. The enhanced interaction of benzene with dissected benzene arises from a reduction in exchange repulsion, which is tempered by electrostatic effects. These electrostatic effects favour the interaction with dissected benzene for distances larger than 3.4 Å but favour benzene at closer distances. The contribution of dispersion to the difference is negligible except at small inter-monomer distances.

The long-range behaviour of the electrostatic component can be explained based on molecular quadrupole moments. Upon π-delocalization, electron density shifts towards the ring centroid (see appendix Fig. A.2), increasing the benzene quadrupole moment relative to the dissected case. This increased molecular quadrupole leads to more unfavourable quadrupole-quadrupole interactions in the benzene dimer compared to the dimer of benzene with dissected benzene. At close inter-monomer distances, there

[c] Components of the SAPT2 energy are defined as in Ref. 75.

are larger attractive electrostatic interactions for C_6H_6 interacting with benzene compared to dissected benzene, presumably due to enhanced charge interpenetration[42] in the delocalized system.

In complex molecular systems there will be other contributing factors, and non-aromatic compounds will not always engage in stronger stacking interactions than aromatic analogues. In particular, other electronic changes can overwhelm changes due to π-localization in the ring of interest. For example, SCS-MP2 predicts that the stacking interaction of benzene with the central ring of triphenylene is more favourable than with 2,3-dihydrotriphenylene, 2,3,6,7-tetrahydrotriphenylene, or 2,3,6,7,10,11-hexahydrotriphenyl-ene, despite the mild aromaticity of the central ring in triphenylene that is not present in the other systems.[67]

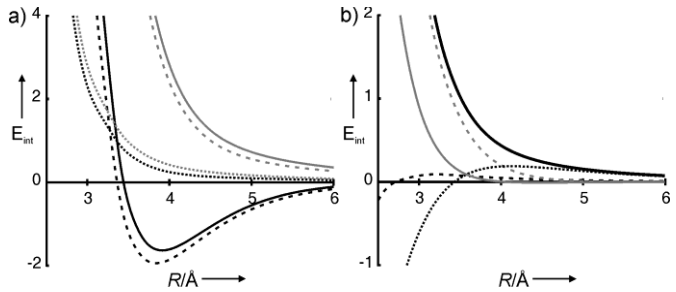

Figure 2.3: a) Estimated CCSD(T)/AVTZ (black lines) and HF/AVTZ (grey lines) interaction energies (E_{int}, kcal mol^{-1}) for benzene with benzene (solid lines) and dissected benzene (dashed lines), and the difference between the two (dotted lines). b) SAPT2 components [E_{SAPT2}, black solid line; E_{exch}, grey dashed line; E_{elec}, black dotted line; E_{ind}, grey solid line; E_{disp}, black dashed line] of the *difference* between benzene interacting with benzene and dissected benzene.

Similarly, in larger analogues of isomers **1** and **2**, the effect of disrupting aromaticity diminishes with increasing size. The result is that the stacking interaction of

benzene with methyl and methylene-substituted tetracene, for example, only differs by 0.03 kcal mol^{-1} (see SI). This attenuation of the effect of π-localization could be a manifestation of the enhanced π-π interactions involving larger acenes reported by Grimme.[60] Despite these and other exceptions, many molecules with naturally localized π-systems do exhibit enhanced stacking interactions, and should be of utility in practical applications. This includes 2,3-dimethylene-2,3-dihydronaphthalene, for which the interaction of benzene with the non-substituted ring is 0.34 kcal mol^{-1} more favourable than with naphthalene.

As noted previously by Grimme,[60] π-π interactions are not unique, and noncovalent interactions involving non-aromatic rings are often quite favourable. For example, the above computed interaction energies for model ethene-benzene and butadiene-benzene complexes are substantial (–0.85 and –1.50 kcal mol^{-1} for ethene and butadiene, respectively). In the latter case, the interaction energy is on par with that of the benzene sandwich dimer. Similarly, for sandwich complexes of cyclohexane with benzene, the interaction energy (–2.91 kcal mol^{-1}) is nearly 80% *greater* than that exhibited by the benzene sandwich dimer. This is because although the dispersion interactions in the cyclohexane-benzene complex are slightly diminished compared to those in the benzene sandwich dimer, the electrostatic interactions are far more favourable (see appendix Table A.3).

In conclusion, our main findings can be summarized as follows:

1) Monomer aromaticity is not a defining feature of "aromatic interactions", and π-stacking and anion/π interactions should be more generally defined without reference to aromaticity.
2) For small cyclic polyenes, non-aromatic systems engage in stronger π-stacking and anion/π interactions than analogous aromatic systems. The enhanced stacking interactions for non-aromatic polyenes stem from a reduction in exchange repulsion, not dispersion effects.
3) Non-covalent interactions of arenes with many non-aromatic cyclic systems are more attractive than similar arene-arene interactions, and sometimes exhibit a dependence on orientation. Consequently, these other types of interactions should be of utility in supramolecular applications.

Ramifications of these findings abound. For example, in supramolecular chemistry, it should be advantageous to incorporate interactions involving planar, non-aromatic polyenes to exploit the orientation dependence and enhanced stacking interactions provided by localized π-systems.

2.1 METHODS

Interaction energies were computed via the supramolecular approach using either SCS-MP2/TZVPP[68,69] or an estimate of CCSD(T)/AVTZ, where AV*X*Z denotes the standard aug-cc-pV*X*Z basis of Dunning.[70,71] Monomer structures were fixed at B97-D/TZV(2*d*,2*p*)[50,51] optimized geometries in the former case, and MP2/AVTZ optimized geometries in the latter. CCSD(T)/AVTZ energies were estimated by appending a

correction for basis set incompleteness (MP2/AVTZ – MP2/AVDZ) to CCSD(T)/AVDZ energies. All supramolecular interaction energies were corrected for BSSE[72] and were computed using Molpro, while B97-D geometries were optimized with Gaussian09.[73,74] Density fitting was used in all SCS-MP2 and B97-D computations. Only the 1*s* orbital was frozen on Na^+, for which the cc-pCVXZ basis sets were used. All core orbitals were frozen in the other correlated computations. SAPT2[54] computations utilized the AVDZ' basis set[75] and were executed using SAPT2008.[76] For the 1-D potential energy curves in Fig. 2.3, energies were evaluated every 0.4 Å across the full range and then every 0.1 Å surrounding the energy minimum.

CHAPTER III

PHYSICAL NATURE OF SUBSTITUENT EFFECTS IN XH/π INTERACTIONS*

3.1 INTRODUCTION

XH/π interactions (*i.e.*: CH/π, OH/π, NH/π, *etc*. See Fig. 3.1), in which an XH bond points toward the face of an aromatic ring, have proven vital in numerous chemical and biochemical contexts including the tertiary structures of proteins,[1-6] crystal packing,[7-11] and molecular recognition.[12-26] There have been many reviews covering these interactions,[22,77-80] with the bulk of previous work focusing on CH/π and OH/π interactions. As with other non-covalent interactions involving aromatic rings,[80,81] there is widespread interest in developing ways of tuning XH/π interactions through substituent effects. By understanding how simple substituents change the strength of these interactions, we can further unravel the physical nature of these interactions while also providing a potentially powerful tool for supramolecular chemistry.

There have been numerous computational studies of XH/π interactions, including many studies of the impact of substituents. We recently reviewed[80] computational studies of substituent effects in non-covalent interactions involving aromatic rings, including CH/π, OH/π, and NH/π interactions; we provide merely a summary here. Kodama *et al.*[82] introduced the concept of CH/π interactions to explain the favorable interactions between alkyl groups and phenyl rings. Subsequently, CH/π interactions,

---

* Reprinted with permission from "Physical Nature of Substituent effects in XH/π Interactions" by J. W. G. Bloom, R. K. Raju, and S. E. Wheeler, 2012. *J. Chem. Theory Comput.*, 8, 3167-3174, Copyright © 2012 American Chemical Society.

which are driven by dispersion interactions,[77,83] have been the focus of multitudinous experimental and theoretical studies, in part due to the important role that these interactions play in the recognition of carbohydrates by proteins.[84] Tsuzuki and coworkers[85,86] studied CH/π complexes of benzene with methane, ethane, ethylene, and acetylene at the CCSD(T) level, showing that the nature of the alkyl group affects the interaction energy. In particular, they showed that the interaction becomes considerably stronger as the hybridization of the carbon in the CH bond changes from sp^3 to sp^2 to sp. For example, the CH/π interaction of acetylene with benzene is an order of magnitude stronger than that of ethane with benzene.[86] This can be understood in terms of the increasing polarity of the CH bond with increasing *s*-character of the carbon.

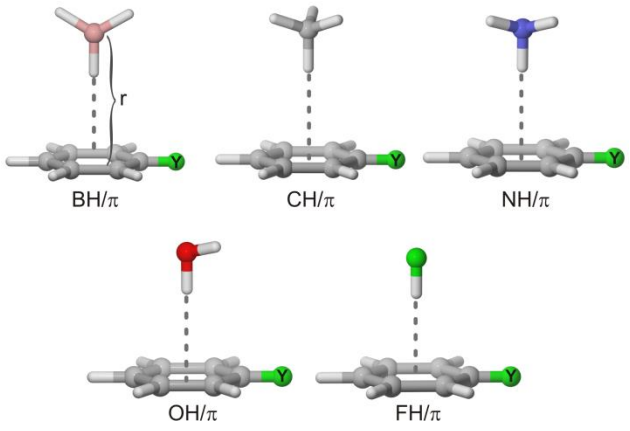

Figure 3.1: Model XH/π interactions between BH_3, CH_4, NH_3, OH_2, and FH and monosubstituted benzenes. In all cases, a single XH bond is directed towards the centroid of the phenyl ring and the interaction distance (*r*) is defined as the distance between the heavy atom of the XH group and the ring centroid.

There have been a variety of studies of aryl substituent effects on CH/π interactions.[20,87,88] Tsuzuki and coworkers[87] presented extrapolated CCSD(T) interaction

energies for the interaction of methane with toluene, π-xylene, mesitylene, and naphthalene. Their data showed a correlation between the interaction energies and the polarizabilities of the arenes, highlighting the importance of dispersion effects for these interactions. Raju *et al*.[20] analyzed the effect of aryl perfluorination on the benzene methane interaction. They showed that the effect is negligible; methane has only a slightly more favorable interaction with benzene than it has with hexafluorobenzene.

Earlier this year, Mishra *et al.*[88] analyzed the interaction of acetylene with the face of substituted benzenes using CCSD(T), several DFT functionals, and symmetry adapted perturbation theory (SAPT). This was the first systematic study of substituent effects in CH/π interactions spanning a broad range of substituents. Overall, they found that the main driver of substituent effects in these interactions was electrostatic effects, and that electron donors enhance the interaction while electron acceptors hinder the interaction. They also noted a strong correlation between the dispersion and exchange-repulsion components of these interactions, although no explanation for this finding was provided.

Several studies have examined the impact of halogen substituents on the CH-bearing group. For example, Fujii *et al.*[89] showed that although electrostatic interactions increased with the number of chlorine atoms, dispersion interactions remain the primary component of the overall interaction energies. Tsuzuki *et al.* expanded upon this with the inclusion of fluorine.[87,90] They found that both fluorine and chlorine substituted methanes interact with benzene more strongly due to enhanced electrostatic and dispersion interactions. Ugozzoli *et al.*[91] performed a more thorough DFT study of the

effect of substituents on methane, considering substitution with F, Cl, Br, I, CN, and NO_2. They found that computed interaction energies increased with increasing electron withdrawing capability of the substituent.

Several groups have also examined substituent effects in aromatic CH/π interactions, as exemplified by the T-shaped and edge-to-face configurations of the benzene dimer.[81,92-95] These include high-accuracy studies of Sherrill and co-workers[92,93] and Kim *et al.*,[44,94] as well as work by Riley and Merz[95] and Wheeler and Houk.[81] For substituents on the edge or axial ring, electron donors hinder the interaction while electron acceptors promote the interaction.

In addition to CH/π interactions, prototypical OH/π interactions (*e.g.*, $H_2O\cdots C_6H_6$ complexes) have been reported in both experimental and theoretical works.[96-104] More complex systems featuring both CH/π and OH/π interactions have also been studied. For example, Raju *et al.*[20,21,105,106] examined interactions between several types of carbohydrates and substituted benzenes, while Kumari *et al.*[107] studied simple carbohydrates paired with tryptophan.

NH/π interactions are less well studied. It has been shown that dispersion interactions constitute a large part of the overall interaction energy for these interactions while electrostatic effects impact the orientation of NH/π interactions.[86] The strength of the NH/π interaction falls between that of CH/π and OH/π interactions.[108] Kim and coworkers[109] studied dimers of several substituted benzenes with ammonia, finding a competition between an NH/π configuration and a complex in which the ammonia

interacted with the edge of the arene. The latter complexes were preferred in benzenes with electron-withdrawing substituents.

There have been previous computational studies examining a broad range of XH/π interactions with both substituted and unsubsubstituted benzenes. For example, Mishra and Sathyamurthy [110] examined dimers of CH_4, NH_3, OH_2, and FH with benzene, hexafluorobenzene, and 1,3,5-trifluorobenzene, finding that for fluorinated rings the complexes adopt structures in which the interaction is with the edge of the ring rather than the center. Similarly, Kim and coworkers[111] showed that for complexes of HF and HCl with benzene, the XH bond is directed towards the edge of the benzene rather than its center. They extended this work a few years later[112] to complexes of BH_3, CH_4, NH_3, OH_2, and FH with benzene and ethylene, showing that differences in computed binding energies among these systems were due to electrostatic effects and induction. Overall, they found that CH_4, NH_3, OH_2, and FH complexes exhibit an XH/π interaction towards the bonds and atoms of the benzene, while for the $BH_3 \cdots C_6H_6$ complex the plane of BH_3 is roughly parallel to that of the benzene. In fact, BH_3 and AlH_3 both exhibit this parallel structure as the global minimum energy configuration.[113,114] Kim and coworkers[94] subsequently examined complexes of HF, HCl, OH_2, H_2, with a range of substituted benzenes, finding that for the strongly polar species (*e.g.*: H_2O, HCl, HF) the impact of substituents on the interaction energy could be substantial due to dipole-drive electrostatic effects. These effects, along with those in substituted T-shaped benzene dimers, were captured by a Hammett-like substituent constant. Ultimately, Kim *et al.*[94] highlighted the need for future studies to elucidate the physical origin of these

interactions to aid the rational design of supramolecular systems and novel molecular devices.

Although a myriad of studies have examined XH/π interactions involving substituted arenes,[20,21,87,88,105,106,110-112] there has been only one systematic study[88] of the impact of aryl substituents on these interactions covering a broad range of substituents. Moreover, there has been no comprehensive study of substituent effects across the full range of XH/π interactions. Below we present such a systematic study quantifying the effect of aryl substituents on model XH/π interactions (X = BH_2, CH_3, NH_2, OH, and F). The physical origins of these substituent effects have been unveiled through SAPT computations and correlations with substituent constants.

3.2 THEORETICAL METHODS

Constrained optimizations were executed at the B97-D/TZV(2*d*,2*p*)[50,51] level of theory using Gaussian09[74] by fixing the XH bond over the centroid of the substituted phenyl ring, constraining this bond to remain orthogonal to the ring plane, and fixing the coordinates of all the ring atoms. All other coordinates were permitted to optimize. It should be noted that these geometries are in general not energy minima on the full potential energy surface. Instead, these model dimers are intended to permit an investigation of the impact of substituents on the strength of XH/π interactions in the absence of complicating factors from geometric changes. Throughout this work, the interaction distance (*r*) is defined as the optimized distance from the heavy atom of the XH group to the centroid of the arene.

CCSD(T)/AVTZ interaction energies, evaluated at the B97-D optimized geometries, were estimated by appending a basis set correction computed at the MP2 level to CCSD(T)/AVDZ energies, where AVXZ denotes the aug-cc-pVXZ basis set.[70-72] That is, CCSD(T)/AVTZ interaction energies were estimated via

$$\Delta E(\text{CCSD(T)/AVTZ}) \approx \Delta E(\text{CCSD(T)/AVDZ}) + \Delta E(\text{MP2/AVTZ}) - \Delta E(\text{MP2/AVDZ}).$$

To provide insight into the physical nature of substituent effects in these interactions, SAPT0/AVDZ energies[54] were computed at these same geometries using SAPT2008[76] paired with Molpro.[73] Both the B97-D and the SAPT0 interaction energies are in good agreement with the CCSD(T) data (see appendix Tables B.1 and B.2). The CCSD(T) and MP2 energies were computed using Molpro.[73] To further analyze substituent effects in XH/π interactions, multidimensional linear regression analyses were carried out comparing individual components of the interaction energies with substituent constants[115] as well as the optimized interaction distance, *r*.

3.3 RESULTS AND DISCUSSION

The prototypical XH/π interactions depicted in Fig. 3.1 were studied primarily at the estimated CCSD(T)/AVTZ and SAPT0/AVDZ levels of theory. We first consider the effect of substituents on the total interaction energies for these model systems before examining the individual energy components and correlations with substituent constants. Overall, the SAPT0 interaction energies closely follow the CCSD(T)/AVTZ data, supporting the use of SAPT0 to study individual components of these interactions. Similarly, the good performance of B97-D relative to CCSD(T)/AVTZ lends credence to

the use of B97-D optimized geometries. Comparisons of B97-D and SAPT0 data with the CCSD(T) results are shown in appendix Tables B.1 and B.2.

3.3.1 Substituent Effects on Total Interaction Energies

Computed interaction energies for the five model XH/π interactions (see Fig. 3.1) are plotted in Fig. 3.2 versus Hammett constants (σ_m) for 22 monosubstituted benzenes. The corresponding data are listed in Table 3.1. For unsubstituted benzenes (Y = H), the interaction energies increase monotonically progressing from BH to CH, NH, OH, and FH. The mean interaction energies across all 22 substituents follow this same trend. This enhanced interaction with increasing polarization of the XH bond is accompanied by an increased sensitivity to substituent effects, as indicated by the increased slope of the best-fit lines in Fig. 3.2. This is an agreement with the previous findings of Kim *et al.*[94] in their study of H_2O, HF, *etc*. complexes with substituted benzenes. This leads to stark differences in substituent effects between the nonpolar (BH and CH) and polar (NH, OH, and FH) groups. For example, the standard deviations across the set of 22 substituents for the interactions involving NH_3, OH_2, and FH range from 0.2 to 0.8 kcal mol^{-1}. For BH_3 and CH_4, computed interaction energies are essentially constant across the full range of substituted benzenes.

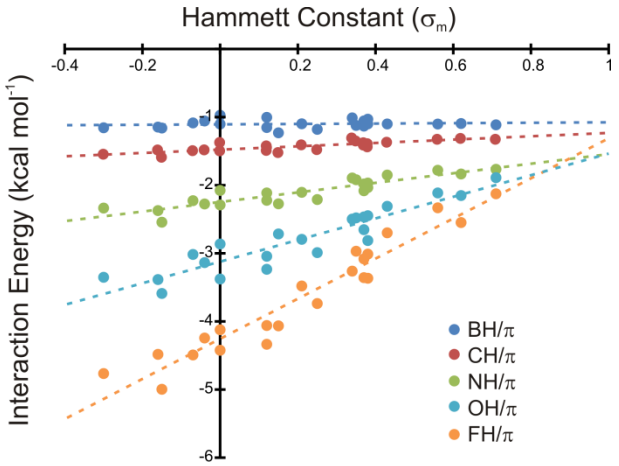

Figure 3.2: Estimated CCSD(T)/AVTZ interaction energies (kcal mol^{-1}) for prototypical XH/π interactions (See Fig. 3.1) for 22 substituted benzenes versus Hammett constants (σ_m). Dashed lines are the results of linear least-squares fits to the corresponding XH/π data.

Table 3.1: Estimated CCSD(T)/AVTZ interaction energies for prototypical XH/π interactions (See Fig. 3.1) for 22 substituted benzenes.

	σ_m	BH_3	CH_4	NH_3	OH_2	FH
H	0.00	–0.97	–1.38	–2.08	–2.86	–4.12
CCH	0.21	–1.10	–1.41	–2.11	–2.80	–3.48
CF_3	0.43	–1.10	–1.38	–1.85	–2.31	–2.70
CH_2OH	0.00	–1.10	–1.50	–2.29	–3.38	–4.42
CH_3	–0.07	–1.09	–1.50	–2.23	–3.02	–4.49
CHO	0.35	–1.12	–1.36	–1.92	–2.48	–2.97
CN	0.56	–1.10	–1.33	–1.78	–2.11	–2.33
$COCH_3$	0.38	–1.03	–1.44	–2.03	–2.81	–3.37
$COOCH_3$	0.37	–1.13	–1.42	–2.08	–2.65	–3.36
COOH	0.37	–1.06	–1.38	–1.98	–2.47	–3.08
F	0.34	–1.01	–1.31	–1.89	–2.50	–3.26
$N(CH_3)_2$	–0.15	–1.16	–1.60	–2.54	–3.59	–5.00
NH_2	–0.16	–1.15	–1.49	–2.37	–3.39	–4.48
$NHCH_3$	–0.30	–1.16	–1.55	–2.34	–3.35	–4.77
NHOH	–0.04	–1.06	–1.49	–2.28	–3.14	–4.24
NO_2	0.71	–1.11	–1.33	–1.77	–1.89	–2.13
NO	0.62	–1.10	–1.32	–1.84	–2.15	–2.55
OCF_3	0.38	–1.10	–1.40	–1.97	–2.45	–3.01
OH	0.12	–1.00	–1.43	–2.11	–3.04	–4.06
OCH_3	0.12	–1.15	–1.50	–2.22	–3.24	–4.34
SCH_3	0.15	–1.23	–1.53	–2.27	–2.72	–4.07
SH	0.25	–1.18	–1.48	–2.21	–2.99	–3.74
Min.		–0.97	–1.31	–1.77	–1.89	–2.13
Max.		–1.23	–1.60	–2.54	–3.59	–5.00
Mean		–1.10	–1.43	–2.10	–2.79	–3.63
Std. Dev.		0.06	0.08	0.21	0.47	0.84

A consequence of the increase in slope with the polarity of the XH group is that for electron-withdrawing substituents (*e.g.* NO_2, CN, *etc.*) there is only a small difference in interaction energies across the different XH/π interactions. For example, for NO_2 substituted benzene ($\sigma_m = 0.71$) the interaction with BH_3 and FH differ by only 1.0 kcal mol^{-1}, although this does represent a doubling of the BH_3 interaction energy. This can be contrasted with $NHCH_3$ ($\sigma_m = -0.30$) substituted benzene, for which the interaction is enhanced by more than a factor of four going from BH/π to FH/π. This suggests that greater differentiation between different XH/π interactions can be achieved with aryl rings bearing electron-donating groups.

Overall, electron-donating groups enhance XH/π interactions while electron-withdrawing groups hinder these interactions, as noted for acetylene-benzene dimers by Mishra *et al.*[88] This behavior, along with the SAPT0 results discussed below, indicates the importance of electrostatic interactions for each of the XH/π interaction types. However, a closer examination of the individual components of the interaction energies reveals more subtle behavior (*vide infra*). In general, the observed substituent effects in all of these XH/π interactions are consistent with popular models of substituent effects in π-stacking interactions: the π-resonance-based model of Hunter and Sanders,[36,37,116,117] the polar/π model of Cozzi and Siegel,[118,119] as well as the local, direct interaction model proposed by Wheeler[46,47,120] based on through-space effects of the substituents (*i.e.*: field effects).

3.3.2 Components of Interaction Energies

Insight into the physical nature of these substituent effects is provided by SAPT0 results, which enable the decomposition of the total interaction energies into contributions from electrostatic (Elec), exchange-repulsion (Exch), induction (Ind), and dispersion (Disp) effects. Part of our analysis of these SAPT0 data is based on a scheme recently used by Watt *et al*.[121] in their work on benzene sandwich dimer. For example, to analyze the impact of electrostatic effects on a given XH/π interaction, we add the exchange, induction, and dispersion energies together and examine the correlation of this "triply additive energy" with the total energy for each of the substituted dimers. A lack of correlation in this case indicates a balancing of the dispersion and induction energies with the exchange energy. This, in combination with a strong correlation between the electrostatic component and total energy, can indicate that electrostatic effects are the main cause of substituent effects. Such analyses have been performed for each of the four components of the total interaction energy for all five XH/π interactions.

First, however, we examine individual components of the interaction energy as well as the correlation of these individual components with the total interaction energies. Mean values and standard deviations across the set of 22 substituents are provided in Table 3.2 for the individual components of the interaction energy for each of the XH/π interactions. Mean interaction distances are also provided. On average, the electrostatic and induction components increase with increased polarity of the XH group, as expected. These enhanced electrostatic and induction effects most likely drive the concurrent decrease in interaction distances (see Table 3.2). The mean dispersion

component, on the other hand, increases going from BH to CH to NH, but then peaks and decreases going from NH to OH to FH. This can be explained in terms of competing effects of decreasing interaction distance and the decreasing polarizability of the XH group going from CH_4 to HF. The exchange-repulsion component increases with the decreasing interaction distance, as expected.

Table 3.2: Mean values and standard deviations for the interaction distance (in Å) and the electrostatic (Elec), exchange-repulsion (Exch), induction (Ind), and dispersion (Disp) components of the SAPT0 energies (kcal mol^{-1}) as well as correlation coefficients between these individual components and the total SAPT0 interaction energies for XH/π interactions.

X	r	Elec	Exch	Ind	Disp
		Mean ± standard deviation			
BH_2	3.90±0.02	–0.81±0.06	2.50±0.13	–0.28±0.05	–2.77±0.10
CH_3	3.69±0.02	–1.05±0.07	2.72±0.13	–0.30±0.05	–3.18±0.12
NH_2	3.45±0.02	–1.97±0.24	3.54±0.19	–0.59±0.07	–3.53±0.12
OH	3.30±0.01	–2.66±0.52	3.75±0.15	–1.02±0.08	–3.29±0.09
F	3.16±0.01	–3.13±0.93	3.65±0.20	–1.84±0.11	–2.74±0.09
		Correlation Coefficients with total interaction energies			
BH_2		0.63	–0.38	0.37	0.63
CH_3		0.88	–0.79	0.91	0.84
NH_2		0.97	–0.87	0.94	0.85
OH		0.99	–0.92	0.97	0.77
F		1.00	–0.95	0.98	0.87

Consideration of linear correlations between the individual energy components and the total interaction energy provides surprisingly little insight. This is because other than for the BH/π interactions, for which there are essentially no substituent effects, all four energy components are strongly correlated with the total interaction energy. Examining the standard deviations of these energy components across the set of 22 substituents does indicate that some components contribute more than others to the

overall substituent effect. Moreover, the component exhibiting the greatest change across the set of substituents varies among the XH groups. In general, increases in the electrostatic component of these interactions are accompanied by increases in its variation across the set of substituents. For example, for the FH/π interactions the standard deviation in the electrostatic component of the interactions is 0.9 kcal mol^{-1}, while the other three components have standard deviations less than 0.2 kcal mol^{-1}.

Table 3.3: Mean values and standard deviations for various sums of electrostatic (Elec), exchange-repulsion (Exch), induction (Ind), and dispersion (Disp) components of the SAPT0 energies (kcal mol^{-1}) as well as correlations between these triply-additive energies and the total SAPT0 interaction energy for XH/π interactions.

X	Exch+Ind+Disp	Elec+Ind+Disp	Elec+Exch+Disp	Elec+Exch+Ind
		Mean ± standard deviation		
BH_2	–0.55±0.06	–3.86±0.17	–1.08±0.07	1.41±0.08
CH_3	–0.77±0.05	–4.54±0.22	–1.52±0.06	1.36±0.06
NH_2	–0.58±0.06	–6.09±0.42	–1.97±0.18	0.98±0.16
OH	–0.56±0.06	–6.97±0.67	–2.20±0.45	0.07±0.46
F	–0.93±0.06	–7.70±1.12	–2.22±0.81	–1.32±0.85
		Correlation Coefficients with total interaction energies		
BH_2	0.35	0.53	0.61	0.01
CH_3	0.60	0.87	0.88	0.02
NH_2	0.02	0.95	0.98	0.83
OH	0.00	0.99	1.00	0.98
F	0.02	1.00	1.00	1.00

One difficulty with analyzing individual energy components is that they are coupled, in part, through the interaction distance. This is particularly true of the dispersion and exchange-repulsion terms. Evidence for the relative importance of the electrostatic energies in driving substituent effects for some XH/π interactions can be garnered by considering the triply additive energies discussed above and listed in Table

3.3. For the triply additive energies that exclude electrostatic effects, there is very little variation across the set of substituents, as indicated by the uniformly small standard deviations for Exch+Ind+Disp in Table 3.3. The other sums, which include electrostatic contributions, vary more considerably across the set of substituents, and this variation increases with increasing polarity of the XH group. The correlations of these triply additive energies with the total SAPT0 interaction energies tell a similar story: for NH, OH, and FH/π interactions there is no correlation between Exch+Ind+Disp and the total interaction energy, indicating that the electrostatic component is vital to describe the substituent effects. On the other hand, for the BH and CH/π interactions the triply additive energy with a low correlation is Elec+Exch+Ind. This suggests that for these two XH/π interactions the dispersion contribution is the most important.

3.3.3 Correlations with Substituent Constants

To provide additional physical insight into these interactions, we also examined correlations of the individual SAPT0 components with Hammett constants (σ_m) and molar refractivities (MR). Hammett constants are frequently used in the literature, and are intended to capture effects due to a substituent's electrostatic properties. Molar refractivities, on the other hand, are commonly used as a measure of polarizabilities.[122] We also consider correlations involving the interaction distance (r), which can be considered a property of the substituted benzene when making comparisons across different substituents for a given XH monomer. This distance is used, in part, because these non-covalent interaction energies are all dependent upon electron cloud overlap at

close range (*e.g.*: penetration effects). There is the obvious issue of using the interaction distance in linear correlations, because the components of these interaction energies should not depend linearly on *r*. However, this linear approximation should be acceptable given the narrow range of distances considered. Linear regression analyses were conducted for each of the SAPT0 energy components with the individual substituent constants as well as all pairwise combinations of these constants and the three constants together.

Before considering the correlations of interaction energies with substituent constants, we must first discern whether σ_m, MR, and *r* are independent of one another across the set of substituents (see appendix Table B.3). For these 22 substituents, the MR and σ_m values are uncorrelated, indicating a diverse sample of substituents. However, there is a strong correlation between σ_m and *r*, with the strength of the correlation increasing with increasing polarity of the XH bond. MR and *r* are only weakly correlated, and the strength of this correlation decreases with increasing XH bond polarity. These trends arise because the correlation of *r* with the other two parameters follows the extent to which those parameters describe the overall interaction (*vide infra*). Consequently, care must be exercised before conclusions are drawn regarding the correlation with any individual substituent constant.

As shown in Table 3.4, the electrostatic components of all of the XH/π interactions except BH/π are fairly well described by the Hammett constants alone. However, the strength of the correlations becomes weaker with decreased polarity of the XH group. Once the Hammett constants and the interaction distances are used in

concert, the correlations become very good, again with the exception of boron. The fact that inclusion of *r* is necessary for strong correlations is possibly due to the importance of charge penetration.

Table 3.4: Correlation coefficients for the electrostatic, exchange-repulsions, induction, and dispersion components of XH/π interactions with Hammett constants (σ_m), molar refractivity (MR), interaction distance (*r*), and combinations of these constants. The columns in bold indicate the constants or simplest combination of constants providing the best correlation across all five XH/π interactions.

X	σ_m	r	MR	(σ_m,*r*)	(MR,*r*)	(σ_m,MR)	(σ_m,MR,*r*)
				Electrostatic			
BH_2	0.04	0.18	0.20	0.48	0.25	0.28	0.51
CH_3	0.68	0.77	0.15	0.94	0.79	0.75	0.94
NH_2	0.86	0.81	0.07	0.96	0.82	0.88	0.96
OH	0.84	0.86	0.03	0.92	0.89	0.84	0.93
F	0.92	0.91	0.03	0.96	0.92	0.92	0.97
				Exchange-Repulsion			
BH_2	0.27	0.98	0.29	0.98	0.98	0.48	0.98
CH_3	0.38	0.97	0.31	0.98	0.97	0.60	0.98
NH_2	0.66	0.96	0.12	0.98	0.97	0.72	0.98
OH	0.80	0.95	0.07	0.96	0.95	0.82	0.96
F	0.82	0.99	0.04	0.99	0.99	0.83	0.99
				Induction			
BH_2	0.89	0.53	0.10	0.95	0.53	0.93	0.95
CH_3	0.88	0.55	0.10	0.96	0.57	0.92	0.96
NH_2	0.88	0.81	0.09	0.97	0.81	0.91	0.97
OH	0.90	0.87	0.09	0.96	0.87	0.93	0.96
F	0.87	0.96	0.10	0.97	0.96	0.91	0.98
				Dispersion			
BH_2	0.24	0.84	0.61	0.84	0.98	0.76	0.98
CH_3	0.25	0.86	0.62	0.86	0.96	0.78	0.97
NH_2	0.39	0.81	0.51	0.82	0.96	0.78	0.96
OH	0.44	0.78	0.48	0.81	0.95	0.81	0.95
F	0.65	0.86	0.32	0.87	0.98	0.86	0.98

The exchange-repulsion components of these interactions are strongly correlated with the interaction distance alone. This is where considering a range of XH/π

interactions proves highly useful, because r and σ_m are correlated to a different extent for the different XH groups. For example, consideration of only OH and FH/π interactions, for which σ_m and r are strongly correlated, would lead to the false conclusion that the Hammett constants provide a sound predictor of the exchange-repulsion component of XH/π interactions. This is because when electrostatic interactions are significant, the Hammett parameters indirectly capture the exchange-repulsion trends because electrostatic effects impact the overall energies and interaction distances.

The induction energy is captured mostly in the Hammett constants of the substituents. There is essentially no correlation between the induction energies and the MR values, indicating that the substituent effects on the induction component arise primarily from changes in the electrostatic properties of the substituents, not changes in their polarizabilities. That is, the changes in the induction energy arise from the different substituents polarizing the XH group. This could indicate a variety of possibilities, including that the changes in the electrostatic properties of the substituents are effectively larger than the changes in their polarizabilties. Alternatively, this could arise because the electric multipoles of the XH group are small enough that changes in the polarizabilities of the substituents result in negligible changes in the total induction energy. That the correlations of MR values with the induction energy are uniform across the different XH groups supports the former possibility. The correlation of the induction energies is significantly improved by inclusion of the interaction distance, as was observed for the electrostatic component of these interactions.

Finally, the dispersion component of these interactions is best described by a combination of *r* and MR values. Again, the correlation between the σ_m and *r* for the polar cases provides an artifactual correlation between the dispersion energies and Hammett constants for the more polar XH groups because of the correlation between σ_m and *r* for these interactions.

3.4 SUMMARY AND CONCLUDING REMARKS

We have presented a comprehensive, systematic study of substituent effects in model XH/π interactions (X = BH_3, CH_4, NH_3, OH_2, and FH) based primarily on estimated CCSD(T)/AVTZ interaction energies. Insight into the physical nature of these substituent effects was gleaned from SAPT0 computations as well as correlations with the Hammett constants (σ_m), molar refractivities (MR), and the optimized interaction distances, *r*.

Substituents can have a dramatic impact on XH/π interactions, but the magnitude of these effects as well as their physical origin depends strongly on the nature of the X group. In particular, increased polarity of the XH bond is accompanied by a substantial increase in the magnitude of substituent effects. Based on the above data we can draw the following main conclusions:

1) The electrostatic and induction components of XH/π interactions (except BH/π) are strongly correlated with σ_m and *r*. For BH/π interactions these components do not change upon substitution, so no correlation is observed.

2) Exchange-repulsion is correlated most strongly with the interaction distance, and no individual substituent constant can capture the effect of substituents on exchange-repulsion effects without explicitly accounting for the changes in interaction distance.
3) The dispersion component of the interactions is correlated with both MR and *r*. The correlation of the dispersion component with MR values alone is relatively weak.
4) The strength of XH/π interactions increases with increasing electron-donating character of the substituents, as do the differences among the different XH/π interactions.
5) The primary driver of substituent effects for the polar XH groups (NH_3, OH_2, FH) is the electrostatic energy, while dispersion effects dictate substituent effects for the non-polar monomers (BH_3, CH_4).

Overall, substituent effects in XH/π interactions are in general accord with previous work,[88,94] and follow expected trends based on simple physical models. Examining the full range of XH/π interactions has provided a comprehensive and unified view of the physical origin of substituent effects in these interactions. Although these results are based on idealized model dimers in which the X–H bond is perpendicular to the aryl ring and directed towards the ring centroid (see Fig. 3.1), they should provide a qualitative guide to XH/π interactions in more realistic supramolecular complexes.

CHAPTER IV

BROAD TRANSFERABILITY OF SUBSTITUENT EFFECTS IN π-STACKING INTERACTIONS PROVIDES NEW INSIGHTS INTO THEIR ORIGIN*

4.1 INTRODUCTION

Non-covalent interactions involving aromatic rings pervade modern chemical research.[22,56,57] Among these, π-stacking interactions play pivotal roles in a myriad of phenomena ranging from protein-DNA interactions and supramolecular self-assembly to organocatalysis.[22,56,57,123-126] Substituents are often used to tune the strength of these interactions[80] and further unraveling their physical origin will enable more refined exploitation of substituent effects in chemical applications. For example, there has been increasing interest in harnessing the effects of heteroatoms and substituents to control the molecular packing of small molecule semiconductors for the development of high-performance organic electronic materials.[127,128] Similarly, we recently demonstrated[129] that through-space substituent effects in π-stacking interactions can be used to control the local orientation of model stacked discotic systems in order to maximize charge-transfer rates.

Computational studies of π-stacking interactions typically consider three prototypical configurations of the benzene dimer, depicted in Fig. 4.1.[130] Among these, the sandwich dimer is the most extensively studied, despite this configuration being a

---

saddle point on the potential energy surface.[131] The parallel-displaced and T-shaped dimers are roughly isoenergetic and are both energy minima. We recently demonstrated[47] that substituent effects in the benzene sandwich dimer are correlated with those in the parallel-displaced dimer, supporting the use of the more symmetric sandwich dimer as a model for unraveling substituent effects in π-stacking interactions.[80]

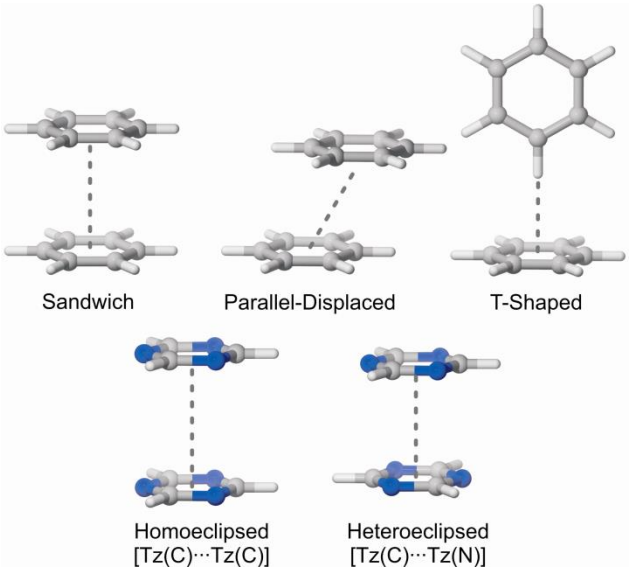

Figure 4.1: Prototypical benzene dimer configurations (top) as well as sandwich heteroeclipsed and homoeclipsed triazine dimers (bottom).

Substituent effects in π-stacking interactions have been discussed at length in recent years, and their origin is thought to be well understood.[45,47,80,120,121] Traditional conceptual models of substituent effects in π-stacking interactions, including those of Hunter and co-workers[36,37,116,117,132] and Cozzi and Siegel,[118,119,133-136] were cast primarily in terms of substituent-induced changes in the aryl π-system. In recent years, however, accurate gas-phase computational studies[44-47,81,92,93,121,130,137-142] have

pinpointed apparent flaws in these popular views.[36,37,116-119,132-136] While these conventional models posit that electron-accepting substituents enhance π-stacking interactions and donors hinder π-stacking, model gas-phase computations revealed that all substituents stabilize the benzene dimer relative to the unsubstituted case, regardless of their electron-withdrawing or -donating character.[9b,12a,12e,12i] However, in the case of monosubstituted sandwich dimers,[46] interaction energies for the substituted dimers remain correlated with Hammett σ constants, with the unsubstituted dimer being an outlier. In other words, substituent effects in gas-phase benzene sandwich dimers follow the general trend predicted by conventional models of π-stacking,[36,37,116-119,132-136] but with the caveat that the substituted dimers exhibit enhanced stabilization in the gas phase, relative to the hydrogen case, due to dispersion effects.

In 2008, Wheeler and Houk demonstrated[46] that substituent effects in the sandwich configuration of the benzene dimer are due primarily to direct, through space interactions between the substituents and the unsubstituted ring. Substituent-induced changes in the π-system of the substituted ring were shown not to contribute significantly. Such direct interactions had previously been invoked in an *ad hoc* manner by Rashkin and Waters[143] and Sherrill *et al*.[93,138] to explain unexpected substituent effects in parallel-displaced and T-shaped interactions.

More recently, we presented a new model[47] of substituent effects in π-stacking interactions in which substituent effects are dominated by local, direct interactions (*i.e.* field effects) between the substituents and the proximal vertex of the other ring. The essence of this model is that substituent effects are unchanged as long as no atomic

substitutions are made within the local environment of the substituent (see Fig. 4.2). The presumed basis of this model was that substituent effects arise primarily from the electrostatic interaction between the local dipole associated with the substituent and the local C-H dipole in the proximal vertex of the unsubstituted ring. However, concrete evidence for this presumed origin was lacking.

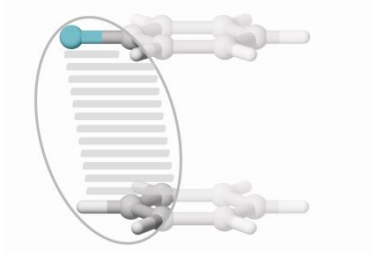

Figure 4.2: In the local, direct interaction model[47] of substituent effects in π-stacking interactions, substituent effects are predicted to be unchanged as long as the atoms present in the un-shaded region remain unchanged.

One ramification of this model[47] is that substituent effects in π-stacking interactions are expected to be highly transferable. In other words, substituent effects will be independent of the nature of the aryl ring to which the substituent is attached; instead, they will depend on the identity of the atoms in the proximal vertex of the unsubstituted ring. Such transferability of substituent effects was demonstrated for homo- and heterodimers of benzene and pyridine.[47] What remains unanswered, however, is to what extent changes can be made to both the substituted and unsubstituted ring without significantly altering substituent effects. In other words, under what circumstances will two stacked dimers exhibit the same substituent effects?

By probing the transferability of substituent effects in π-stacking interactions, we can gain new insight into the origin of these effects. Moreover, the transferability of substituent effects in aryl-aryl interactions is vital for the development of atomistic and coarse-grained molecular-mechanical force fields for applications to organic electronic materials. Such transferability would justify the development of general, transferable force-fields for substituents that are independent of the arene to which the substituents are attached.

interactions by examining sandwich dimers involving benzene (Bz), borazine (Bn), and 1,3,5-triazine (Tz) (see Fig. 4.3). These systems exhibit drastically different electronic character, and provide a means of probing the transferability of substituent effects across diverse stacked systems. Moreover, all three of these systems are planar and aromatic, and there has been growing interest in the use of B- and N-heterocycles in organic electronic materials,[144-151] in materials for gas-storage and separation,[152-159] and even as enzyme inhibitors.[160-163] All of these applications will benefit from refined control over π-stacking interactions involving N- and B-heterocycles.

In the present work, we probe the transferability of substituent effects in π-stacking Anand and co-workers[164] reported that many substituted borazines exhibit π-stacking interactions in the solid state, although in some cases other interactions dominate. There have been a limited number of computational studies[165,166] of π-stacking interactions involving borazine and no computational studies of substituent effects in these dimers. In 2003, Kawahara *et al*.[165] presented MP2 and CCSD(T) results for sandwich, parallel-displaced, and T-shaped borazine dimers, finding that the

heteroeclipsed borazine sandwich dimer (see Fig. 4.1 for analogous triazine dimer) was the most strongly interacting. More recently, Bettinger *et al.*[166] studied homo- and heterodimers of benzene and borazine.

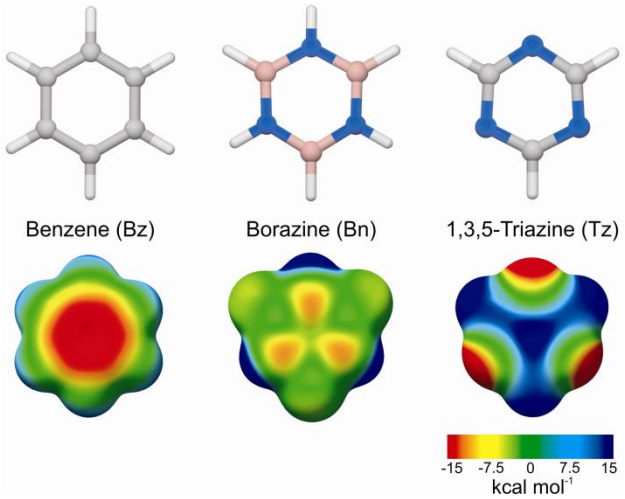

Figure 4.3: Structures and molecular electrostatic potentials (ESPs) of benzene, borazine, and triazine.

There have been a number of computational studies[167-173] of stacked triazine dimers over the last decade, but, as with the borazine dimers, there have been no systematic studies of substituent effects. In 2005, Ugozzoli and Massera[167] examined stacked dimers of benzene and triazine, predicting a strong interaction between benzene and triazine in a parallel-displaced configuration. Three years later, Tschumper *et al.*[168] studied the effects of heterogeneity on π-stacking interactions, including those in parallel-displaced benzene and triazine homo- and heterodimers. They found that, for the parallel-displaced dimers, the interaction energy in the mixed triazine-benzene dimer (–3.8 kcal mol^{-1}) was more favorable than that of homodimers of either benzene (–2.8 kcal

mol^{-1}) or triazine (–3.0 kcal mol^{-1}). A correlation was reported between the electrostatic component of these interactions, as predicted by second-order symmetry-adapted perturbation theory (SAPT2), and the total interaction energies.[168] Also in 2008, Wang and Hobza studied[169] π-stacking interactions of several N-heterocycles with benzene. In contrast to Tschumper *et al*.,[168] they attributed the stronger interaction of triazine with benzene, relative to the benzene homodimer, to dispersion effects based on the higher polarizability of triazine. More recently, Mishra *et al*. studied[170] both stacking and edge-to-face interactions for a range of N-heterocyclic dimers, finding that the strength of these interactions were comparable. Kim and co-workers[171,172] employed both spectroscopic and computational techniques to study non-covalent interactions of phenylacetylene with triazine, pyrazine, and pyridine, reporting that parallel-displaced π-stacking configurations are preferentially formed over other arrangements. Finally, in 2012, Sütay *et al*. studied[173] various pyrazine and triazine homodimers using a range of computational methods, reporting that either parallel-displaced or hydrogen-bonded dimers are the most favorable, depending on the level of theory employed.

Below, we systematically study substituent effects in stacked homo- and heterodimers of benzene, borazine, and triazine. The primary aim is to probe the extent to which substituent effects in π-stacking interactions are transferable among these diverse stacked systems. The results indicate that substituent effects do not depend on the ring to which the substituent is attached, but are instead determined by the identity of the unsubstituted ring. Moreover, unexpected correlations among substituent effects in disparate stacked dimers provide new insight into the origin of substituent effects in π-

stacking interactions. These correlations are explained based on computed electric fields for the unsubstituted arenes, which supports the view that substituent effects in π-stacking interactions are dominated by the electrostatic interaction of the local dipole associated with the substituent and the other ring.

4.2 THEORETICAL METHODS

Interaction energies for a wide range of eclipsed sandwich dimers were evaluated at the CCSD(T), SAPT0, and B97-D levels of theory.[50,51,53,54,70,174-178] For the unsubstituted dimers, counterpoise-corrected[72] CCSD(T)/AVTZ interaction energies were estimated by appending a basis set correction evaluated at the MP2 level onto CCSD(T)/AVDZ energies:

CCSD(T)/AVTZ ≈ CCSD(T)/AVDZ + [MP2/AVTZ – MP2/AVDZ],

where AVXZ denotes the aug-cc-pVXZ basis set of Dunning and co-workers.[70,71] To locate the equilibrium inter-ring separation (R_e) for each dimer, a series of single point energies were evaluated at this level of theory at 0.1 Å increments near the minima. A simple quadratic function was fit to the 3-4 lowest-lying points to interpolate the R_e value and interaction energy. These computations utilized fixed monomer geometries optimized at the MP2/AVTZ level of theory. To gain additional insight into the interaction of these non-substituted dimers, SAPT0 interaction energies[53,54,176,177] were evaluated at the CCSD(T) predicted equilibrium separations using the jun-cc-pVDZ basis set.[179] The jun-cc-pVDZ basis set comprises the standard Dunning aug-cc-pVDZ basis set, but without diffuse functions on hydrogen and without diffuse *f*

functions on non-hydrogen atoms (*i.e.* the aug-cc-pVDZ′ used by Sherrill and co-workers[75,130]). SAPT predicts accurate intermolecular interaction energies, while also providing a rigorous decomposition of these interaction energies into physically meaningful components ($E_{int} = E_{elec} + E_{exch} + E_{ind} + E_{disp}$).

To examine the impact of substituents on these stacked dimers, we considered a diverse set of 22 substituents: BF_2, CCH, CF_3, CH_2OH, CH_3, CHO, CN, $COCH_3$, $COOCH_3$, COOH, F, NH_2, $NHCH_3$, NO_2, NO, OCF_3, OH, OCH_3, SCH_3, SH, SiF_3 and SiH_3. This set of substituents provides a representative sample, and ranges from strong electon-donors (*e.g.* $NHCH_3$) to strong electron-acceptors (*e.g.* NO_2). For each substituted arene, monomers were optimized at the B97-D/TZV(2*p*,2*d*) level of theory.[50,51,70,178] For many substituents there are multiple low-lying rotamers. For substituted borazines and triazines, the substituent rotamer that is equivalent to the lowest lying for substituted benzene was used.

Geometries of all possible eclipsed monosubstituted sandwich dimers of benzene, borazine, and triazine (460 dimers total) were optimized with fixed monomer geometries at the B97-D/TZV(2*d*,2*p*) level of theory.[50,51,70,178] For the asymmetric substituents, the arene faces will be unique, so there are two ways of forming the stacked sandwich dimers. We determined the most favorable arrangement for the benzene dimer and replicated this alignment for the other dimers. This facilitated direct comparisons of substituent effects across the different substituted dimers. Given the relatively poor performance of B97-D for many of the unsubstituted dimers (*vide infra*), SAPT0/jun-cc-pVDZ interaction energies were computed for all substituted dimers at the B97-D

optimized equilibrium separations. SAPT0 energies were also evaluated at inter-ring separations of 3.5 and 4.0 Å for all dimers.

Borazine and triazine have only three-fold symmetry, and borazines can be substituted at either the boron or nitrogen positions. To distinguish among the different sites of substitution, and to denote which atoms are eclipsed in the stacked dimers, we have adopted the following naming scheme. Bn(N)-X and Bn(B)-X denote borazines substituted at the N and B sites, respectively. For dimers in which borazine is unsubstituted, Bn(N) and Bn(B) indicate that the substituted atom of the other ring is aligned with the N and B of borazine, respectively. Similarly, for dimers in which triazine is the unsubstituted ring, Tz(N) and Tz(C) indicate that the N and C-H of triazine are eclipsed with the substituted atom of the other ring, respectively (see later figures for examples). Throughout this work, A, B, C, *etc*. are used to denote any of Bz, Bn(N), Bn(B), Tz(C), or Tz(N).

Molecular electrostatic potential (ESP) maps (Fig. 4.3) were created using UCSF Chimera[180] by mapping the electrostatic potential, computed at the B97/TZV(2*d*,2*p*) level of theory, onto an electron-density isosurface ($\rho = 0.001$ *e*/bohr^3). B97/TZV(2*d*,2*p*) electrostatic potentials and electric fields were also computed in the plane bisecting benzene, borazine, and triazine. All DFT computations were carried out using Gaussian09,[74] while Molpro[73] was employed to evaluate MP2 and CCSD(T) energies. SAPT0 energies were computed using Psi4.[181] Throughout this work, slopes between two sets of interaction energies were analyzed in terms of total least squares (orthogonal regression), rather than the more common ordinary linear least squares. Such analyses

are more appropriate in this case, as the aim is to describe the linear correlation between two equivalent sets of data.

4.3 RESULTS AND DISCUSSION

4.3.1 Unsubstituted Dimers of Benzene, Borazine, and Triazine

First, we consider unsubstituted sandwich dimers of benzene, borazine, and triazine. This will provide a baseline against which substituent effects can be compared, and will enable us to gauge the accuracy of B97-D and SAPT0 for these stacked dimers. Table 4.1 shows estimated CCSD(T)/AVTZ interaction energies for all unique sandwich dimers involving these three arenes. Heterodimers of triazine and borazine with benzene interact more strongly than the benzene homodimer, as previously noted;[166,168] the strongest interactions are predicted for heteroeclipsed borazine and triazine homodimers. That is, Bn(B)···Bn(N) interacts more strongly than Bn(B)···Bn(B) or the dimers of borazine with either triazine or benzene. The most favorable sandwich dimer is Tz(C)···Tz(N). The Tz(C)···Tz(N) sandwich dimer is more favorable than the parallel displaced configuration (as reported by Tschumper *et al*.[168]), as previously noted by Fowler and Buckingham[39] based on distributed multipole analyses and as predicted by venerable rules for aromatic interactions from Hunter and Sanders.[36] The data in Table 4.1 also underscore our previous finding that monomer aromaticity is not a prerequisite for strong stacking interactions.[182] For example, borazine is typically considered to be

significantly less aromatic than benzene,[166,183] yet borazine stacks at least as strongly as benzene.

The origin of the observed trends in interaction energies are clarified by the SAPT0 components listed in Table 4.1. The electrostatic component of the interaction energies correlate strongly (correlation coefficient r = 0.95) with the total CCSD(T) interaction energies. The other SAPT0 components are also correlated with the total interaction energy, but this presumably is due to the coupling of effects through the interaction distance (as observed recently for XH/π interactions).[184] Comparing Bn(B)···Bn(B) with Bn(B)···Bn(N), for example, the electrostatic component is strongly favorable for the more stable heteroeclipsed dimer, yet mildly unfavorable for the homoeclipsed dimer. This follows the findings of Tschumper and co-workers[168] regarding the impact of heterogeneity on π-stacking interactions.

Table 4.1: Estimated CCSD(T)/AVTZ and B97-D/TZV(2*d*,2*p*) interaction energies (E_{int}) and equilibrium inter-ring separations (R_e, in Å), SAPT0 energy components and total SAPT0 interaction energies (E_{int}) for dimers of benzene (Bz), borazine (Bn), and triazine (Tz).[a]

		CCSD(T)		B97-D		SAPT0//CCSD(T)					SAPT0//B97-D
		R_e	E_{int}	R_e	E_{int}	E_{elec}	E_{exch}	E_{ind}	E_{disp}	E_{int}	E_{int}
Bz	Bz	3.92	–1.6	3.90	–1.8	0.4	3.3	–0.2	–4.8	–1.4	–1.4
	Bn	3.79	–2.2	3.69	–3.1	–0.6	3.6	–0.3	–4.6	–1.9	–1.9
	Tz	3.67	–3.1	3.69	–3.2	–2.0	4.6	–0.3	–5.4	–3.2	–3.2
Bn(B)	Bn(B)	3.89	–1.8	3.65	–3.3	0.1	2.0	–0.1	–3.2	–1.2	–0.6
	Bn(N)	3.52	–3.3	3.28	–5.9	–3.0	5.7	–0.4	–5.4	–3.1	–3.1
	Tz(C)	3.68	–2.7	3.59	–3.7	–0.8	3.1	–0.2	–4.2	–2.1	–1.9
Tz(C)	Bn(N)	3.56	–3.1	3.48	–4.0	–2.2	4.4	–0.3	–5.0	–3.1	–3.2
	Tz(C)	3.74	–1.5	3.97	–1.8	0.9	2.1	–0.1	–3.8	–1.0	–1.0
	Tz(N)	3.46	–3.8	3.50	–3.9	–3.3	5.3	–0.4	–5.8	–4.2	–4.2

[a] All energies in kcal mol^{-1}. E_{elec} = electrostatic, E_{exch} = exchange-repulsions, E_{ind} = induction, E_{disp} = dispersion.

First, we consider unsubstituted sandwich dimers of benzene, borazine, and triazine. This will provide a baseline against which substituent effects can be compared, and will enable us to gauge the accuracy of B97-D and SAPT0 for these stacked dimers. Table 4.1 shows estimated CCSD(T)/AVTZ interaction energies for all unique sandwich dimers involving these three arenes. Heterodimers of triazine and borazine with benzene interact more strongly than the benzene homodimer, as previously noted;[166,168] the strongest interactions are predicted for heteroeclipsed borazine and triazine homodimers. That is, Bn(B)···Bn(N) interacts more strongly than Bn(B)···Bn(B) or the dimers of borazine with either triazine or benzene. The most favorable sandwich dimer is Tz(C)···Tz(N). The Tz(C)···Tz(N) sandwich dimer is more favorable than the parallel displaced configuration (as reported by Tschumper *et al*.[168]), as previously noted by Fowler and Buckingham[39] based on distributed multipole analyses and as predicted by venerable rules for aromatic interactions from Hunter and Sanders.[36] The data in Table 4.1 also underscore our previous finding that monomer aromaticity is not a prerequisite for strong stacking interactions.[182] For example, borazine is typically considered to be significantly less aromatic than benzene,[166,183] yet borazine stacks at least as strongly as benzene.

The origin of the observed trends in interaction energies are clarified by the SAPT0 components listed in Table 4.1. The electrostatic component of the interaction energies correlate strongly (correlation coefficient r = 0.95) with the total CCSD(T) interaction energies. The other SAPT0 components are also correlated with the total interaction energy, but this presumably is due to the coupling of effects through the

interaction distance (as observed recently for XH/π interactions).[184] Comparing Bn(B)···Bn(B) with Bn(B)···Bn(N), for example, the electrostatic component is strongly favorable for the more stable heteroeclipsed dimer, yet mildly unfavorable for the homoeclipsed dimer. This follows the findings of Tschumper and co-workers[168] regarding the impact of heterogeneity on π-stacking interactions.

Overall, the total SAPT0 interaction energies are strongly correlated with the reference CCSD(T) data (r = 0.97), although SAPT0 generally underestimates the CCSD(T) interaction energies. On the other hand, the agreement between the B97-D/TZV(2*d*,2*p*) interaction energies and the CCSD(T) data is rather poor. In particular, B97-D overestimates the interaction energies, relative to CCSD(T), by anywhere from 2% to 85%. However, SAPT0 energies evaluated at the B97-D optimized structures are in agreement with the CCSD(T) data, with the exception of Bn(B)···Bn(B). Consequently, SAPT0 interaction energies for the substituted dimers are considered below for the substituted dimers.

4.3.2 Substituent Effects in Sandwich Dimers of Benzene, Borazine, and Triazine

Next, we consider the impact of substituents on the 20 possible sandwich dimers of benzene, borazine, and triazine. As noted above, substituent effects in most of these dimers have not previously been examined. The range of interaction energies for each dimer is plotted in Fig. 4.4, along with interaction energies for X = H, CN, and NH_2 (see SI for data). For many of the dimers, substituents enhance the strength of the interaction regardless of their electron-withdrawing or donating character (*i.e.* X = H leads to the

weakest interaction), in accord with previous observations for the benzene sandwich dimer.[45,46,137,140] However, in general, substituents lead to both enhanced and diminished π-stacking interactions, relative to the unsubstituted case. That is, for many of these dimers the unsubstituted case (X = H) is not the weakest interacting. Moreover, in many of these dimers the substituent effects follow drastically different trends than in the benzene dimer. For example, in the benzene sandwich dimer, CN leads to strongly enhanced interactions relative to X = H, while NH_2 substituents provide only modest stabilization. This reflects differences in the electrostatic contributions to the interactions, which are highly favorable for X = CN, but not for X = NH_2. This can be contrasted with the A-X···Tz(N) dimers. In these cases, the impact of CN substituents is very weak, while X = NH_2 leads to substantial stabilization compared to X = H. This again reflects the underlying electrostatic component of these interactions: X = NH_2 leads to significant favorable electrostatic interactions, while CN substitution results in electrostatic interactions that are slightly less favorable than for X = H.

Overall, substituent and heteroatom effects provide powerful means of tuning the strength of π-stacking interactions, and the predicted interaction energies range from –0.6 kcal mol^{-1} for the Bn(N)-H···Bn(N) dimer to –5.70 kcal mol^{-1} for the Tz-NO_2···Bz dimer. Perhaps more importantly, as shown below, the impact of substituents and heteroatoms for a given unsubstituted ring are largely independent of one another, providing nearly orthogonal means of tuning the strength of π-stacking interactions.

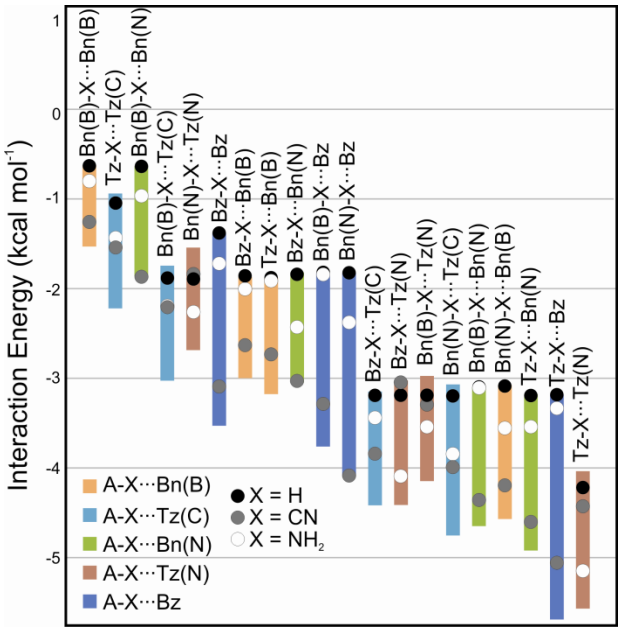

Figure 4.4: Span of interaction energies over all substituents (filled rectangles) of SAPT0 interaction energies for substituted sandwich dimers of benzene, borazine, and triazine.

4.3.3 Transferability of Substituent Effects

Next, we compare substituent effect trends across hetero- and homodimers of benzene, borazine, and triazine. In Fig. 4.5a, we see that substituent effects in Bz-X···Tz(C) dimers are completely uncorrelated with those in Bz-X···Tz(N) dimers (r = 0.04). That is, rotating triazine by 60° completely alters the substituent effects in substituted benzene-triazine dimers. This behavior is observed in general; regardless of the identity of the substituted ring, changing the unsubstituted ring from Tz(C) to Tz(N) drastically alters the impact of substituents. This seems to be in conflict with expectations based on resonance-based views of substituent effects in π-stacking interactions. For example, in popular models,[36,37,116,117,132] substituent effects should depend only on the overall electron-rich or electron-poor character of the interacting

rings, which is clearly independent of their relative orientation. Similarly, in the polar/π model of Cozzi and Siegel,[118,119,133-136] substituent effects should be unaltered as long as the quadrupole moment of the unsubstituted ring remains constant. Instead, we see that aligning either the C-H or nitrogen vertex of triazine with the substituent on the other ring leads to drastically different substituent effects. Due to the symmetry of triazine, molecular quadrupole moments alone do not distinguish between the two types of vertices, and any substituent effect model cast in terms of quadrupole moments will be unable to predict the lack of correlation in Fig. 4.5a.

Table 4.2: Slopes and correlation coefficients (r) for total least squares analyses of SAPT0 interaction energies for substituted dimers of the type B-X···A vs A-X···A.

		R = 3.5 Å		R = R_e		R = 4.0 Å	
A	B-X	Slope	r	Slope	r	Slope	r
Bz	Bn(B)-X	0.94	0.96	1.01	0.98	0.96	0.98
	Bn(N)-X	1.05	0.98	1.10	0.98	1.01	0.98
	Tz(C)-X	1.03	0.96	1.18	0.98	1.04	0.96
Bn(B)	Bz-X	1.40	0.93	1.34	0.95	1.14	0.98
	Bn(N)-X	1.08	0.95	1.54	0.89	1.03	0.97
	Tz(C)-X	1.29	0.94	1.34	0.95	1.21	0.97
Bn(N)	Bz-X	0.85	0.87	0.95	0.86	0.85	0.96
	Bn(B)-X	0.84	0.91	1.39	0.92	0.92	0.94
	Tz(C)-X	0.88	0.91	1.30	0.94	0.99	0.91
Tz(C)	Bz-X	0.91	0.92	1.05	0.97	0.92	0.94
	Bn(B)-X	0.99	0.94	1.08	0.97	1.00	0.94
	Bn(N)-X	1.01	0.94	1.47	0.95	0.99	0.94

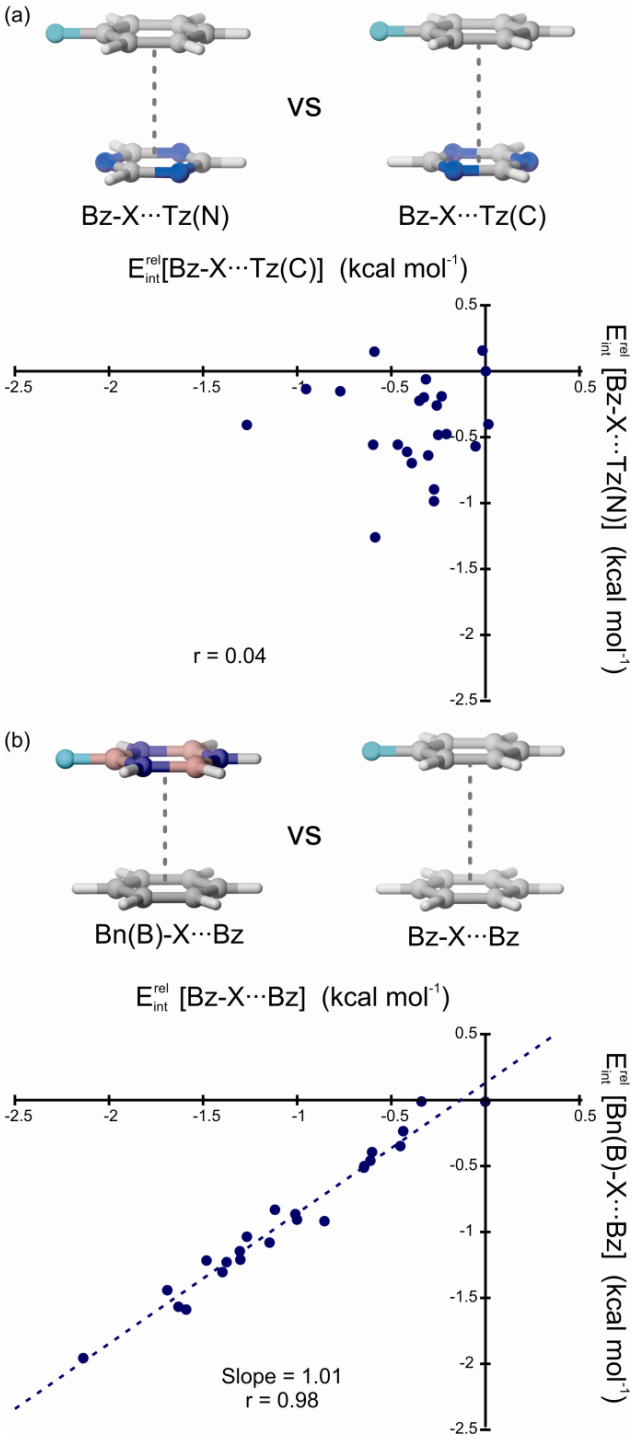

Figure 4.5: Relative SAPT0 interaction energies (kcal mol^{-1}) for sandwich dimers of (a) Bz-X···Tz(C) versus Bz-X···Tz(N) and (b) Bz-X···Bz versus Bn(N)-X···Bz.

Fig. 4.5a can be contrasted with Fig. 4.5b, in which relative interaction energies for Bn(B)-X···Bz dimers are plotted against those for Bz-X···Bz. Despite the different electronic character of the substituted Bn(B) and Bz rings, we see a strong linear correlation ($r = 0.98$) between substituent effects in these two dimers, with a best-fit line with slope near unity. Correlation coefficients and the slopes of total least squares lines for all possible pairs of dimers of the type B-X···A vs A-X···A are listed in Table 4.2. For any pair of dimers for which the unsubstituted ring is the same, substituents effects are correlated ($0.86 < r < 0.98$). That is, substituent effects in π-stacking interactions are dictated by the identity of the unsubstituted ring, with the substituted ring having no direct impact.[d]

The deviations from unity of the best-fit line slopes in Table 4.2 arise in many cases from differences in the equilibrium inter-ring separations among the different sandwich dimers. For example, substituent effects in the Tz-X···Bz dimers are on average greater than those in the Bz-X···Bz dimers because of the smaller average inter-ring separation for benzene-triazine heterodimers compared to benzene homodimers. In this and many other cases, evaluating interaction energies at fixed inter-ring separations of either 3.5 Å or 4.0 Å ameliorates this problem to a large extent, leading to generally stronger correlations and slopes closer to unity (see Table 4.2).

Curiously, for some of the dimer pairs, evaluating the interaction energy at fixed inter-ring separations leads to best-fit lines with slopes slightly farther from one. For

[d] The unsubstituted ring can alter the substituent effects in an indirect way, for example, by altering the inter-ring separation of the dimer.

example, the slopes of the best-fit line is close to unity when comparing Bz-X···Bn(N) versus Bn(N)-X···Bn(N) at their corresponding R_e values, yet deviate from one when evaluating interaction energies at inter-ring separations of either 3.5 or 4.0 Å. This potentially arises from differences in the ring geometries and the lengths of the bonds connecting the substituents with the rings, both of which affect the position of the substituent relative to the unsubstituted ring, despite the fixed inter-ring separation. Regardless, the overall trend is clear: as long as the unsubstituted dimer remains unchanged, substituent effect trends are transferable, even if the strength of the substituent effects shows some slight variability.

To quantify the extent of transferability of individual contributions to the interaction energies, we have also considered correlations among individual components of the SAPT0 interaction energies (see appendix Table C.2). Comparing dimers of the type A-X···A with B-X···A, the data show that the electrostatic and dispersion components are each correlated. The correlations for the exchange components are slightly weaker. The induction components, which are admittedly small, show very weak (or even negative) correlations for many of the pairs of dimers. Regardless, the primary components of these interaction energies (electrostatic, dispersion, and exchange-repulsion effects) are all individually transferable among dimers in which the unsubstituted ring is held constant. This transferability of the individual components of these interaction energies is much stronger at fixed inter-ring separations, and justifies the development of classical potentials for substituents that are independent of the nature of the ring to which they are attached.

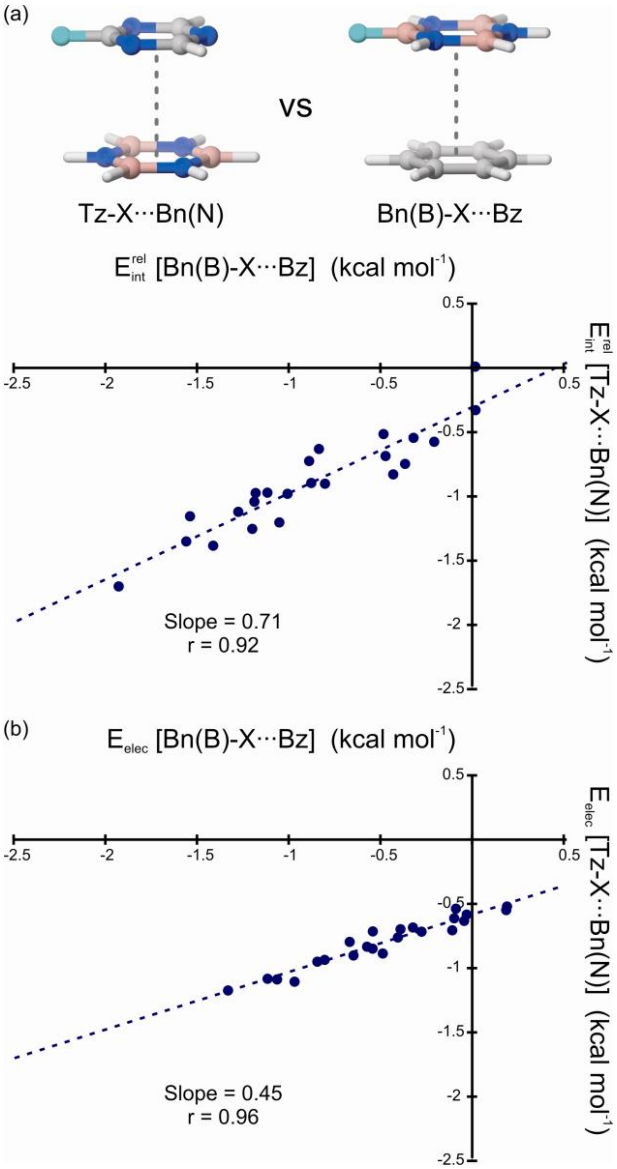

Figure 4.6: (a) Relative SAPT0 interaction energies (R = R_e) and (b) electrostatic components of the interaction energies (R = 4.0 Å) for sandwich dimers of Bn(B)-X···Bz versus Tz-X···Bn(N).

We also considered possible correlations between all pairs of dimers. Unexpectedly, in addition to the cases listed in Table 4.2, there are many pairs of dimers for which substituent effects are similar. In general, substituent effects are correlated

between any two dimers in which the unsubstituted ring is Bz, Bn(N), or Bn(B), regardless of the identity of the substituted ring (see Table 4.3). For example, relative interaction energies for Tz-X···Bn(N) dimers are plotted against Bn(B)-X···Bz in Fig. 4.6a. Substituent effects in these dimers are correlated (r = 0.92), despite none of the rings being in common between the two dimers. Despite the correlations displayed in Table 4.3, the slopes of the best-fit lines deviate from one. This is particularly pronounced when comparing A-X···Bz dimers with either C-X···Bn(N) or C-X···Bn(B) dimers, for which substituent effects in the former case are consistently about twice as strong as those in the latter two dimers. These trends are also present for fixed inter-ring distances of 3.5 and 4.0 Å, and are not simply the result of cancelation of effects occurring at equilibrium distances (see appendix Table C.3 for data at R = 3.5 and 4.0 Å). Instead, these correlations arise from some intrinsic similarity of benzene and borazine (*vide infra*). For all other dimers, linear correlations are weak or nonexistent, apart from a few aberrant cases (see appendix Table C.4 for full correlation matrix). Apparently, substituent effects in π-stacking interactions are not only transferable in cases in which the unsubstituted ring remains constant, but also in select cases in which the substituted rings differ markedly in electronic character.

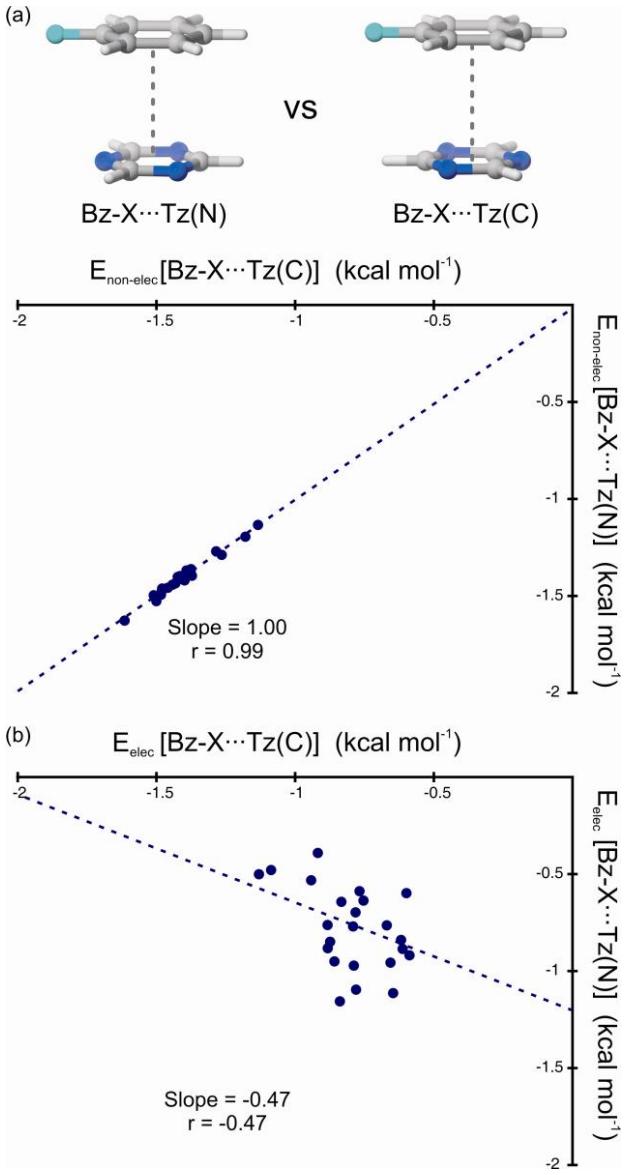

Figure 4.7: (a) Non-electrostatic and (b) electrostatic components of the interaction energies for sandwich dimers of Bz-X···Tz(N) versus Bz-X···Tz(C), at R = 4.0 Å.

Table 4.3: Slopes and correlation coefficients (r) for total least squares analyses of SAPT0 interaction energies for A-X···B vs C-X···D.[a]

		C-X···Bn(N)							
		Bz-X		Bn(B)-X		Bn(N)-X		Tz-X	
B	A-X	Slope	r	Slope	r	Slope	r	Slope	r
Bz	Bz-X	0.45	0.74	0.75	0.92	0.55	0.93	0.72	0.94
	Bn(B)-X	0.44	0.70	0.75	0.93	0.53	0.90	0.71	0.92
	Bn(N)-X	0.41	0.75	0.68	0.89	0.51	0.96	0.65	0.93
	Tz-X	0.35	0.67	0.62	0.89	0.44	0.88	0.60	0.92
		C-X···Bn(B)							
Bz	Bz-X	0.58	0.90	0.43	0.90	0.64	0.86	0.59	0.95
	Bn(B)-X	0.57	0.90	0.43	0.92	0.62	0.81	0.59	0.95
	Bn(N)-X	0.52	0.87	0.38	0.88	0.58	0.87	0.53	0.93
	Tz-X	0.47	0.86	0.35	0.87	0.52	0.82	0.50	0.94
		C-X···Bn(N)							
Bn(B)	Bz-X	0.84	0.61	1.33	0.84	0.92	0.83	1.25	0.81
	Bn(B)-X	1.28	0.67	1.82	0.84	1.28	0.85	1.70	0.85
	Bn(N)-X	0.71	0.62	1.18	0.76	0.81	0.83	1.10	0.80
	Tz-X	0.85	0.67	1.31	0.89	0.93	0.88	1.23	0.89

[a] SAPT0 interaction energies evaluated at B97-D/TZV(2d,2p) optimized dimer geometries.

We again consider correlations of the individual components of the interaction energies, this time to determine which components of these interactions control whether substituent effects are correlated between two dimers. This was done at an inter-ring separation of 4.0 Å, to remove complications from varying inter-ring separations. The non-electrostatic component of the SAPT0 interaction energies (*i.e.* $E_{non\text{-}elec} = E_{exch} + E_{ind} + E_{disp}$) is very strongly correlated between *all pairs of dimers* (see Fig. 4.7a, for example, and appendix Table C.7). That is, the impact of substituents on the non-electrostatic part of the interaction energy is the same regardless of the identity of the substituted or unsubstituted ring. As a result, whether two dimers will exhibit the same substituent effects hinges entirely on electrostatic effects. For pairs of dimers for which

the electrostatic components are correlated, the total interaction energies are also correlated. In particular, the electrostatic components of the SAPT0 interaction energies are strongly correlated for all dimers in which the unsubstituted rings are Bz, Bn(N), or Bn(B). Moreover, the slopes of the best-fit lines are close to one half when comparing the electrostatic components of the interaction energies in A-X···Bn(N) and A-X···Bn(B) dimers with B-X···Bz dimers, indicating that the electrostatic effects in the former two dimers are about half the strength of those in B-X···Bz dimers (*e.g.* see Fig. 4.6b). This explains the non-unit slopes in Table 4.3.

Similarly, for pairs of dimers that exhibit uncorrelated electrostatic interactions, the total interactions are also uncorrelated. For example, Fig. 4.7b shows the electrostatic components of the interaction energies of Bz-X···Tz(C) versus Bz-X···Tz(N) dimers. The lack of correlation between the total interaction energies (Fig. 4.5a) stems primarily from the scatter in the electrostatic components of the interaction energies. In this and other cases, the electrostatic interactions are, to some extent, anti-correlated between the two dimers. In these cases, the total interaction energies are uncorrelated, because of the correlated non-electrostatic components and anti-correlated electrostatic components.

That the correlation of substituent effects between two dimers depend solely on the electrostatic components of the interaction energies provides a physical justification for the local, direct interaction model of substituent effects in π-stacking interactions.[47] In particular, it corroborates the supposition that substituent effects derive from the

electrostatic interaction of the local multipole (dominated by the local dipole) associated with the substituent with the other ring. To understand why these electrostatic interactions are similar in seemingly disparate dimers, we need to examine the electric fields of the unsubstituted arenes.

4.3.4 Substituent Effects and Electric Fields

The electrostatic interaction of a dipole with a molecule depends on the dot product of the dipole with the molecular electric field. In Fig. 4.8, electric fields in the plane perpendicular to the molecular planes and bisecting the rings are plotted for benzene, borazine, and triazine. Also plotted are the electrostatic potentials in this plane, for reference. In the region of the substituents, the electric field above both ends of borazine is similar in direction, but about half the magnitude, to that of benzene. The similarity of electric field direction above borazine and benzene can be seen in Fig. 4.9a, in which we plot the dot product of the normalized electric field surrounding borazine with the electric field of benzene at each point. The strength of the borazine electric field, relative to that of benzene, is plotted in Fig. 4.9b. Hence, the local dipole of the substituents will result in similar electrostatic interactions with either vertex of borazine as it will with benzene, yet with about half the strength. This is in accord with the electrostatic data (see Fig. 4.6b, for example), which showed that the electrostratic component of the substituent effects in A-X$^{\cdots}$Bn(N) dimers is about half that of B-X$^{\cdots}$Bz dimers. In other words, the correlation of substituent effects in A-X$^{\cdots}$Bn(N) and A-

X···Bn(B) dimers with those in B-X···Bz dimers arises because the electric fields above the vertices of Bz, Bn(N), and Bn(B) are similar in direction. The non-unit slopes arise from the differences in the strengths of the electric fields.

This can be contrasted with the electric fields above either vertex of triazine. In this case, the electric field is nearly orthogonal to that above benzene. Again, this can be seen in Fig. 4.9a, which shows that in the region of the substituents the component of the triazine electric field along the benzene electric field is near zero. Thus, triazine and benzene will interact with different components of the local dipole associated with the substituent, giving rise to qualitatively different substituent trends. This explains the seemingly odd effects of NH_2 and CN substituents discussed in Sec. B. In particular, for A-X···Tz(N) dimers, X = NH_2 leads to highly favorable electrostatic interactions while for X = CN the electrostatic interactions are less favorable than in the unsubstituted dimers, in stark contrast to dimes in which benzene is the unsubstituted ring. The local dipole of CN is aligned with the electric field above benzene, while it is perpendicular to the field above triazine. Similarly, the local dipole of NH_2 is more closely aligned with the electric field of triazine than that of benzene.

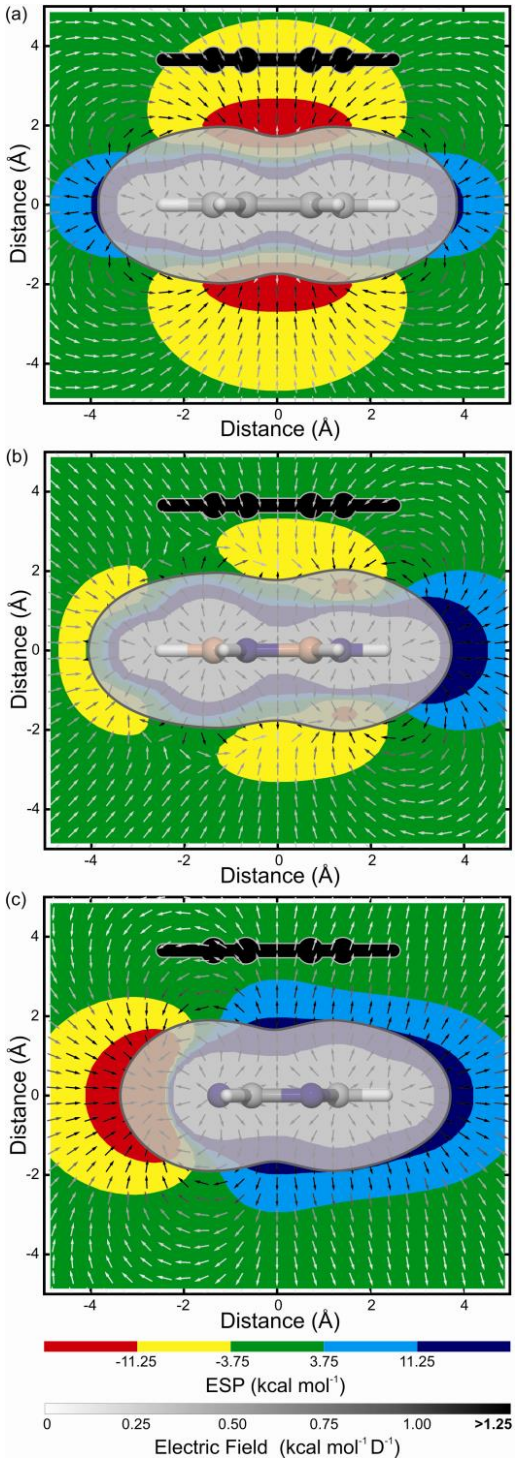

Figure 4.8: Electrostatic potential (solid colors, kcal mol^{-1}) and electric field (arrows, kcal mol^{-1} D^{-1}) in the plane perpendicular to and bisecting the molecular plane of (a) benzene, (b) borazine, and (c) triazine. For reference, the gray shaded region is an electron density isosurface (ρ = 0.001 *e*/bohr^3) and the black silhouette is of a sandwich stacked benzene at *R* = 3.65 Å.

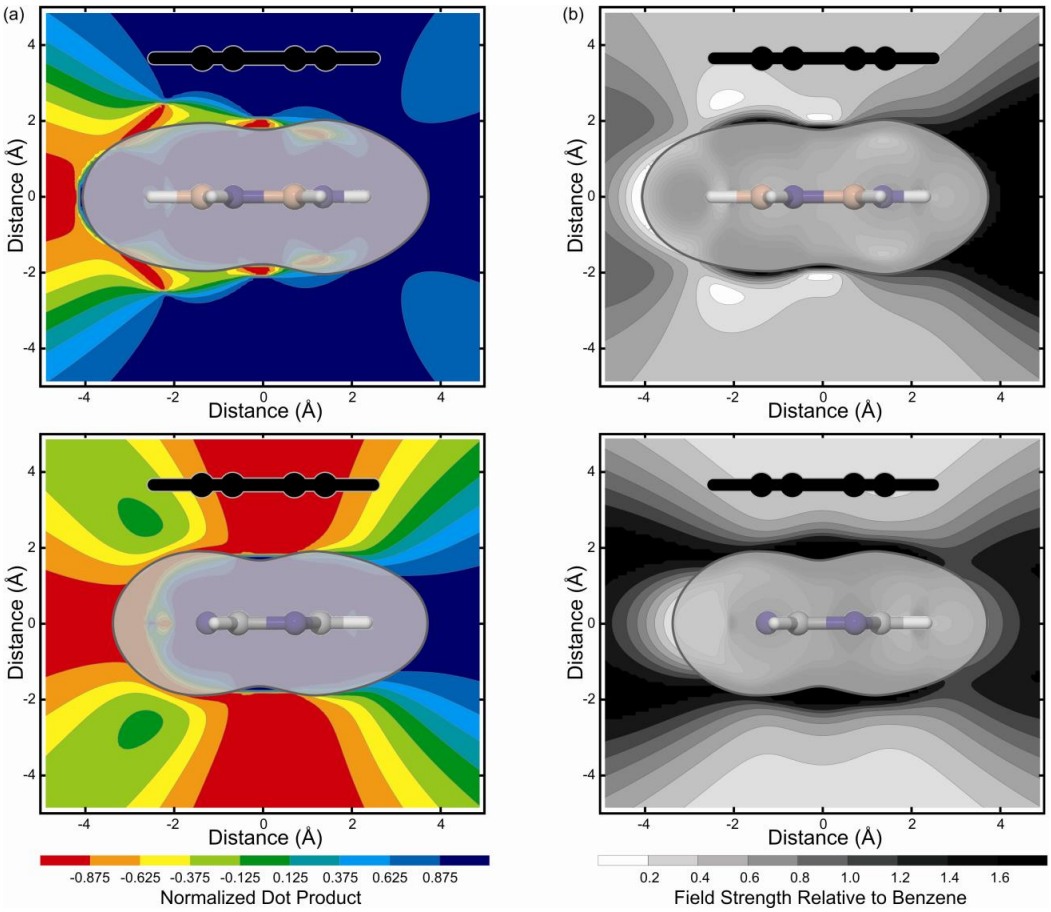

Figure 4.9: (a) Dot product of normalized electric field vectors of benzene with those of borazine (top) and triazine (bottom). In these plots, blue indicates the electric field is aligned with that of benzene, while red signifies anti-alignment. Green indicates that the electric field is orthogonal to that of benzene. (b) Strength of the electric field for borazine (top) and triazine (bottom) relative to the electric field of benzene. In both (a) and (b), the gray shaded region is an electron density isosurface (ρ = 0.001 *e*/bohr^3) and the black silhouette is of a sandwich stacked benzene at *R* = 3.65 Å.

Of course, the electric field is simply the negative gradient of the electrostatic potential, so the electric fields plotted in Fig. 4.8 are obtainable visually, although indirectly, from electrostatic potential plots themselves. The key, however, is not to consider the sign of the ESP, but to focus on the *gradient of the ESP* in the region of the substituent. In this context, the customary practice of plotting ESPs on electron density

isosurfaces (*e.g*. Fig. 4.3) will generally not be helpful, as the electric field at points on these surfaces are not always representative of the electric field in the region of a substituent on a stacked ring. Two-dimensional plots of the ESP more readily provide information about the ESP, and, indirectly, the electric field, in the proximity of the substituent.

In summary, the previously published local, direct interaction model (Fig. 4.2)[47] is a special case for the transferability of substituent effects in π-stacking interactions. In addition to cases in which the atoms in the local environment of the substituent are unchanged, substituent effects will remain unaltered as long as changes to the unsubstituted ring *do not significantly alter the electric field surrounding the unsubstituted ring*. Unfortunately, such cases cannot be determined simply by examining the identity of the atoms in the local environment of the substituent (as indicated in Fig. 4.2), but instead require examinations of computed electric fields (or ESPs). Once these fields have been computed for a set of unsubstituted arenes, they can be used to qualitatively determine substituent effects for the corresponding dimers. Regardless, the transferability of substituent effects among diverse stacked dimers can be explained based on the interaction of the local dipole moment associated with the substituent and the electric field of the unsubstituted arene. This provides significant new insight into the origin of substituent effects in π-stacking interactions, and emphasizes that electric fields can prove valuable in analyses of many non-covalent interactions in which local dipole moments are prevalent. Finally, we note that the electric fields displayed in Fig. 4.8 are in a single plane bisecting the aryl rings. However, many substituents will have local

dipoles located out of this plane, and the overall substituent effect will also depend on the electric field in these regions.

4.4 SUMMARY AND CONCLUDING REMARKS

We have presented gas-phase interaction energies for substituted homo- and heterodimers of benzene, borazine, and triazine computed primarily at the SAPT0/jun-cc-pVDZ level of theory. Four main conclusions can be drawn from the data:

1) In general, the interaction energies of stacked sandwich dimers can be both enhanced or diminished by substituents, and for many dimers the substituent effects exhibit trends markedly different from those in the benzene sandwich dimer. Whether a given substituent leads to strongly enhanced stacking interactions does not depend on its electron donating or accepting character, but instead depends on the orientation of its local dipole moment relative to the electric field of the unsubstituted ring.
2) Substituent effects in π-stacking interactions are broadly transferable, and remain unchanged as long as the electric field of the unsubstituted ring in the vicinity of the substituent is unchanged. A special case of this occurs when the identity of the unsubstituted ring remains unchanged (*i.e.* the local, direct interaction model depicted in Fig. 4.2).[47]
3) The transferability of substituent effects in π-stacking interactions extends to the main components of these interactions (electrostatic, dispersion, and exchange-repulsion effects), which portends the development of molecular

mechanics force fields that will accurately capture substituent effects in π-stacking interactions.

4) Whether substituent effects are correlated between two dimers hinges entirely on the electrostatic components of the interactions. This supports the concept that substituent effects in π-stacking arise from the electrostatic interaction of the local dipole associated with the substituent and the electric field of the unsubstituted ring.

The broad transferability of substituent effects in π-stacking interactions provides new insight into their origin, with important implications for qualitative models of these effects. First, the correlation of substituent effects in sandwich dimers in which the unsubstituted ring is unchanged bolsters the local, direct interaction model of substituent effects in π-stacking interactions.[47] Moreover, the existence of additional correlations between substituent effects in diverse stacked dimers revealed that the local, direct interaction model is a special case of a broader understanding of substituent effects in π-stacking interactions based on the electric fields of the unsubstituted rings.

However, we note here that the above results are for highly constrained model dimers in which the stacked rings are perfectly aligned, and perfectly parallel. Such arrangements are rare in molecular systems, although they do occur.[142] As such, the observed trends might not be fully applicable to more common, parallel-displaced configurations. In particular, the unexpected correlations between substituent effects in diverse stacked dimers are in part due to coincidental similarities of the electric fields above benzene and borazine. Regardless, that substituent effect trends in these model

dimers can be explained in terms of electric fields provides a potentially powerful tool for analyzing substituent effects in π-stacking interactions. For example, work by Arnstein and Sherrill[138] revealed that substituent effects in parallel displaced benzene dimers vary significantly as a function of displacement distance. Although possible qualitative explanations of observed trends were provided in that work, the present results suggest that consideration of electric fields could provide a more precise explanation. Future analyses of more diverse systems in terms of computed electric fields should move us one step closer to a comprehensive understanding of substituent effects in π-stacking interactions.

CHAPTER V

ORIGIN OF ANION/π INTERACTIONS INVOLVING N-HETEROCYCLES

Anion/π interactions,[185-187] which have been defined as attractive non-covalent interactions between anions and faces of π-acidic rings,[22,58,188-193] are among a bevy of recent additions to the supramolecular toolkit.[100,194-196] Anion/π interactions often involve azabenzenes (azines) such as s-triazine and s-tetrazine, and can provide a powerful tool for anion binding, recognition, transport, *etc*.[197-201]

Despite growing interest in anion/π interactions, there is no general model of their origin. Most authors[188,192] ascribe the interactions to a combination of electrostatic and induction effects (anion-induced polarization of the arene),[202,203] although there have been conflicting reports regarding the importance of dispersion interactions.[22,188,192,204] The electrostatic component of these interactions is often characterized by the Q_{zz} component of the molecular quadrupole moment of the arene. In particular, favourable anion/π interactions arise in cases where Q_{zz} is positive, although examples exist of favourable anion/π interactions involving arenes for which Q_{zz} is near zero or even slightly negative.[188,192,205-208] The electrostatic component of anion/π interactions can be described more rigorously in terms of electrostatic potentials (ESPs), which provide a measure of the net electrostatic interaction that a positive test charge would experience at a given point in space in the presence of a molecule. ESPs implicitly include the effects of all orders of electric multipoles, and provide a sound descriptor of the electrostatic components of anion/π interactions when evaluated at the position of the anion. In

general, strong anion/π interactions arise for arenes in which the ESP above the ring is positive. But, what is the origin of these positive ESP and Q_{zz} values?

Wheeler and Houk[139] showed that changes in the ESPs above substituted arenes are dominated by through-space effects of the substituents, not changes in the aryl π-electron-density. Similarly, they described[66] anion/π interactions involving substituted benzenes using a simple model in which the unfavourable interaction of the anion with the phenyl ring remains unchanged, and binding arises from the favourable electrostatic interactions between the anion and the local dipoles associated with the substituents. This view is analogous to our local, direct interaction model of substituent effects in π-stacking interactions.[47,80,120,209] But, what about anion/π interactions involving *N*-heterocycles? Are these interactions attractive because of the depletion of π-electron density, as is often assumed, or from other effects?

Complicating these questions is the fact that ESPs and molecular quadrupole moments reflect the distribution of positive and negative charge throughout the molecule. For example, Q_{zz} measures the relative distribution of charge located away from the *xy*-plane to charge located away from the *z*-axis. Consequently, a positive Q_{zz} for an arene can indicate the depletion of negative charge above and below the ring (*i.e.*, reduction of the π-electron-density) or the net build-up of negative charge around the periphery of the ring. This distinction is rarely made in discussions of anion/π interactions,[58,185-193] in which changes in Q_{zz} are attributed to the former effect.

Here, we explain the favourable interactions of anions with *N*-heterocycles based on a simple physical model. First, we show that anion/π interactions involving azines

are more favourable than those involving benzene solely because of electrostatic effects. Moreover, these enhanced electrostatic interactions result from changes in the σ-systems of these arenes, where "σ-system" refers to the neutral system comprising the σ-electrons and associated components of the nuclear charges. The data show that anions are repelled by the π-systems regardless of the number of nitrogens in the ring.[e] Indeed, the electrostatic interaction of the anion with the π-electron-density is even more unfavourable for the azines than it is for benzene. That is, anion/π interactions involving *N*-heterocycles are attractive despite changes in the π-system, not because of it.

The azines pyridine, pyrazine, s-triazine, and s-tetrazine provide a convenient platform for understanding the origin of anion/π interactions. Together with benzene, these systems provide a linear progression from unfavourable anion/π interactions (for benzene), to strongly attractive interactions for s-tetrazine. In Table 5.1, we provide accurate interaction energies of Cl^- with these five aromatic rings at the corresponding equilibrium distances, computed at the CCSD(T)/aug-cc-pVTZ level of theory. Interaction energies are plotted in Fig. 5.1a as a function of the distance of the anion above the ring centroid. The data show that, beginning with pyridine, each additional nitrogen atom enhances the anion/π interaction by 2.8 ± 0.2 kcal mol^{-1}.

[e] The term "π-system" is rarely defined explicitly when used in the literature, which often leads to confusion when discussing the nature of anion/π interactions. For example, "π-system" can refer to the entire arene or the π-electrons of the arene, etc., leaving phrases such as "electron-deificient π-system" ill-defined. Here, "π-system" is used strictly to refer to the π-electrons and associated nuclear charges.

Table 5.1: CCSD(T) and SAPT2 interaction energies [$E_{CCSD(T)}$ and E_{SAPT2}, respectively] and SAPT2 energy components for Cl^- interacting with benzene and four azines at the corresponding equilibrium distances (in Angstroms) and at R = 3.5 Å.[a]

	R	$E_{CCSD(T)}$	E_{SAPT2}	E_{elec}	E_{exch}	E_{ind}	E_{disp}
benzene	3.88	0.9	0.0	4.2	2.5	–3.7	–3.0
pyridine	3.59	–1.3	–2.6	1.0	5.1	–4.5	–4.2
pyrazine	3.39	–4.0	–5.8	–3.5	8.1	–5.0	–5.4
s-triazine	3.26	–7.0	–8.6	–8.2	10.8	–5.2	–5.9
s-tetrazine	3.17	–9.7	–11.9	–12.6	13.1	–5.6	–6.7
benzene	3.50	1.2	3.1	3.1	6.6	–5.1	–5.0
pyridine	3.50	–1.2	0.4	0.4	6.4	–4.8	–4.8
pyrazine	3.50	–4.0	–2.5	–2.5	6.1	–4.5	–4.6
s-triazine	3.50	–6.6	–5.2	–5.2	5.9	–4.2	–4.2
s-tetrazine	3.50	–8.8	–7.6	–7.6	5.7	–4.2	–4.1

[a] All energies in kcal mol^{-1}. E_{elec} = Electrostatic, E_{exch} = exchange-repulsion, E_{ind} = induction, and E_{disp} = dispersion.

The contributions of electrostatic, exchange-repulsion, induction, and dispersion effects to these interactions, as predicted by second-order symmetry-adapted perturbation theory (SAPT2),[53,54,176,177] are also listed in Table 5.1. At first glance, these data appear to show that electrostatics, dispersion, and induction all contribute to the enhanced anion/π interactions exhibited by the azines, relative to benzene. However, this is an artifact of the decreasing anion-arene distance that accompanies the increasing number of nitrogen atoms. At a given anion-arene separation (*e.g.*, 3.5 Å, see Table 5.1), the enhanced anion/π interactions involving azines are due almost exclusively to electrostatic effects, which are significantly larger than exchange-repulsion, induction, or dispersion effects. At any given distance, dispersion and induction effects favour interactions with benzene over the azines (see Supporting Information).

Table 5.2: ESP values, along with σ- and π-components of the ESP, 3.5 Å above the centroids of benzene and four azines, as well as the Q_{zz} values and σ- and π-components of Q_{zz}.

	ESP	ESP(σ)	ESP(π)	Q_{zz}	$Q_{zz}(\sigma)$	$Q_{zz}(\pi)$
benzene	–8.2	6.7	–14.9	–8.9	5.4	–14.3
pyridine	–5.2	9.6	–14.8	–5.9	7.8	–13.8
pyrazine	–2.0	12.5	–14.5	–2.9	10.3	–13.2
s-triazine	1.4	15.4	–14.1	0.3	12.8	–12.4
s-tetrazine	3.6	17.8	–14.2	2.5	14.9	–12.4

[a] ESP values are in kcal mol^{-1}; Q_{zz} values are in Buckinghams.

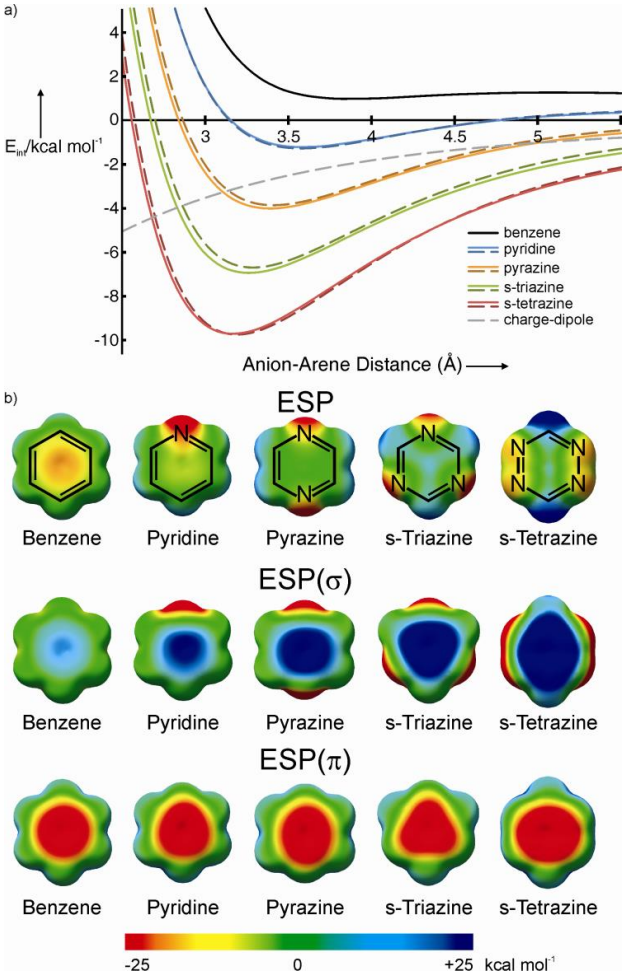

Figure 5.1: a) CCSD(T) interaction energies (solid lines) of Cl^- with five arenes as a function of the anion-centroid distance, the interaction of a negative charge with a radial point dipole of 1.2 D located 2 Å from the origin (grey dashed line), and potentials arising from the addition of one, two, three, *etc*. charge-dipole interactions to the benzene interaction potential (coloured dashed lines). (b) ESPs of benzene and four azines, as well as the σ- and π-components of these ESPs, all mapped onto total electron density isosurfaces.

In Table 5.2, we provide the ESP 3.5 Å above the centroids of benzene and the four azines. These ESP values are very strongly anti-correlated with the computed electrostatic components of the interaction energies (r = –0.9996), as well as the CCSD(T) interaction energies (r = –0.9997). The Q_{zz} values (see Table 5.2) of the arenes are similarly correlated with the total interaction energies.

Because both Q_{zz} and ESPs reflect the distribution of charges throughout the molecule, it is difficult to untangle the effects of the σ- and π-systems from these data alone. However, by exploiting the symmetry of molecular orbitals associated with the σ- and π-electrons, one can dissect the electron density into σ- and π-components. By analogously partitioning the nuclear charges into σ- and π-components,[f] we can decompose the total ESP into contributions describing the electrostatic interaction of a positive test charge with the σ-system [ESP(σ)] and the π-system [ESP(π)]. Q_{zz} values can be similarly partitioned into $Q_{zz}(\sigma)$ and $Q_{zz}(\pi)$. Such decompositions of ESP and Q_{zz} values are provided in Table 5.2. Strikingly, the ESP(π) values exhibit negligible variation across all five arenes, while the σ-components of these ESPs change dramatically. In other words, the vast majority of the change in ESPs above the rings is due to changes in the σ-system, and the trend in anion/π interactions across the azines is similarly due to the redistribution of charges in the molecular plane. The electrostatic interaction of the anion with the π-system is almost as unfavourable for s-tetrazine as it

[f] The nuclear charges are partitioned based on the number of electrons that a given nucleus contributes to the σ- and π-system. For the azines, the σ-nuclear charges for both carbons and nitrogens is 5, while the π-nuclear charges are 1 and 2, respectively. In all cases, the entire nuclear charge for hydrogen contributes to the σ-system.

is for benzene or any of the other azines. Similar trends are observed for Q_{zz}. The swing in Q_{zz} from –8.9 B for benzene to 3.6 B for s-tetrazine is due primarily to changes in the σ-system. The π-components of Q_{zz} change very little across these arenes, although the changes are slightly larger than observed for the ESPs.

More qualitatively, the σ- and π-contributions to ESP maps, which can provide additional insight into anion/π interactions, can also be examined. ESP maps for benzene and the four azines are depicted in Fig. 5.1b, as well as the σ- and π-components of these ESP maps. In accord with the behaviour of the ESP values at a single point above the ring centroids, the π-components of the ESP maps show little variation across these five diverse arenes. Instead, the significant differences among the ESP maps arise from changes in ESP(σ). Undoubtedly, there are differences in the distribution of π-electron density among these molecules. However, there is little net effect of these changes on the total ESP above these rings, or on interactions of these rings with anions.

But, what changes in the σ-system are driving these drastic differences in ESPs and Q_{zz} values? The most significant effect of replacing a CH with a nitrogen atom is the consolidation of the hydrogen and carbon nuclei into a single nitrogen nucleus. This redistribution of nuclear charges results in substantial changes to the nuclear components of the ESP and Q_{zz} (see Table 5.3). For example, the nuclear contribution to the ESP above s-triazine is 54.1 kcal mol^{-1} greater than above benzene, whereas the total ESP values at these positions differ by only 9.6 kcal mol^{-1}. This is because the reorganization of electron density going from benzene to triazine partially counteracts the change in nuclear positions. The electrostatic interactions of the anion with both the σ- and π-

electron densities are less favourable for the azines than they are for benzene. In other words, the π-electron-densities of the azines actually repel anions even more strongly than the π-electron-density of benzene! The same conclusions are reached by examining the nuclear and electronic contributions to Q_{zz} (see Supporting Information).

Table 5.3: ESP values 3.5 Å above the azines (ΔESP), as well as the nuclear (ΔESP_N), σ-electronic [$\Delta ESP_e(\sigma)$] and π-electronic [$\Delta ESP_e(\pi)$] contributions, all relative to benzene.[a]

	ΔESP	ΔESP_N	ΔESP_e	$\Delta ESP_e(\sigma)$	$\Delta ESP_e(\pi)$
pyridine	3.0	18.0	–15.0	–14.2	–0.8
pyrazine	6.2	35.2	–29.1	–27.6	–1.5
s-triazine	9.5	54.1	–44.6	–42.4	–2.2
s-tetrazine	11.8	64.4	–52.6	–50.3	–2.3

[a] ESP values are in kcal mol^{-1}.

The net effect of introducing nitrogen atoms into these rings is a change in the radial distribution of charge in the plane of the ring, with significantly more positive charge near the ring centroid. This net migration of positive charge towards the ring centroid leads to the positive ESPs and Q_{zz} values of the azines. One can describe this redistribution of charge as a change in the local dipole at the position of each nitrogen atom around the ring. In particular, the lone pair on the nitrogens in the azines leads to a significant radial dipole that is oriented opposite to that of the small local C-H dipoles of benzene (see Fig. 5.2). The favourable electrostatic interactions between anions and the azines arise from the interactions of the anion with the positive end of the radial, in-plane dipoles associated with each nitrogen atom. This can be seen more quantitatively in Fig. 5.1, in which we plot the classical electrostatic interaction of a negative charge

with a radial point dipole of 1.2 D located 2 Å from the origin in the molecular plane.[g] If this charge-dipole interaction is added to the interaction potential for Cl^- with benzene, the resulting potential energy curve matches that for Cl^- interacting with pyridine. Similarly, if twice this charge-dipole interaction is added to the benzene potential, then the pyrazine potential is reproduced, *etc*. Indeed, the interaction potential of Cl^- with all of the azines can be accurately reproduced by this simple charge-dipole model (see Fig. 5.1).

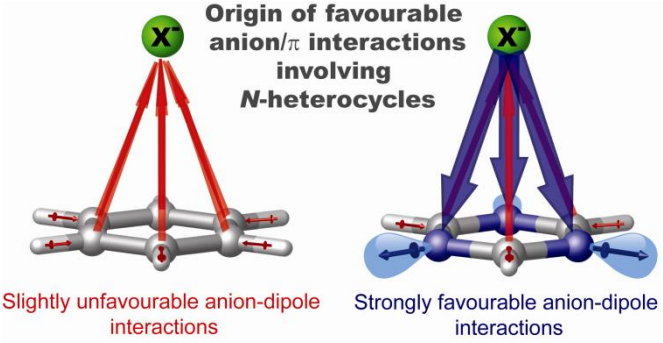

Figure 5.2: The enhanced binding of anions by azines, relative to benzene, arise because of electrostatic interactions of the anion with the in-plane, radial dipoles associated with each nitrogen; the interaction of the anion with the π-system is at least as unfavourable for the azines as it is for benzene.

In conclusion, we have shown that *N*-heterocyclic azines bind anions more strongly than benzene primarily because of the redistribution of charge within the molecular plane. The dominant effect is the movement of nuclear charges accompanying the replacement of CH moieties with nitrogen atoms, which is incompletely

[g] This position is roughly midway along the C-H bond, and the magnitude of the dipole moment is derived from distributed multipole analyses of triazine using six equally-spaced expansion centers 2Å from the ring centroid.

compensated by the redistribution of σ-electron density. The π-electrons of the azines actual repel anions more strongly than the π-electrons of benzene. Overall, the binding of anions by any of the azines can be modelled by a classical charge-dipole interaction appended to an accurate interaction potentials for Cl^- with benzene. That this charge-dipole model works so well precludes any significant role of charge-transfer or orbital interactions on the strength of anion/π interactions involving azines.[188] Together, these results provide a sound understanding of the origin of anion/π interactions, and also shed considerable light on the nature of π-acidic arenes.

5.1 THEORETICAL METHODS

Non-covalent complexes of Cl^- with benzene, pyridine, pyrazine (1,2-diazine), s-triazine (1,3,5-triazine), and s-tetrazine (1,2,4,5-tetrazine) were studied primarily at the CCSD(T)/aug-cc-pVTZ and SAPT2/aug-cc-pVTZ levels of theory. Counterpoise-corrected CCSD(T)/aug-cc-pVTZ quilibrium geometries for model complexes were computed within the frozen-monomer approximation by computing single point energies with Cl^- located above the ring centroid at 0.1 Å increments. The equilibrium distance of the anion above the ring centroid and the corresponding interaction energy were found by fitting a second-order polynomial to the points surrounding the lowest-energy point along these one-dimensional scans. SAPT2/aug-cc-pVTZ energies[53,54,176,177] were also evaluated for each point along these scans. All computations used frozen monomers optimized at the MP2/aug-cc-pVTZ level of theory. ESPs and Q_{zz}, as well as the σ- and π-contributions to ESPs and Q_{zz}, were computed at the HF/aug-cc-pVTZ level of theory

using a locally modified version of Psi3.[210] Details regarding the computation of ESP(σ), ESP(π), $Q_{zz}(\sigma)$, and $Q_{zz}(\pi)$ are available in Supporting Information. For pyridine, Q_{zz} was computed relative to the center of mass. ESP maps were constructed by mapping the ESP onto an electron density isosurface ($\rho = 0.001$ *e*/au^3) using UCSF Chimera.[180] CCSD(T) computations were performed using Molpro,[73] while Psi4[181] was used for the SAPT2 computations. The SAPT2 computations employed density fitting techniques, and all correlated computations utilized the frozen-core approximation.

CHAPTER VI

CONCLUSIONS

For too long, the subfield of π-interactions has been governed by false assumptions. Often these interactions were referred to as aromatic interactions solely for the fact that the majority of π-interactions involved aromatic rings. This could easily have been an accident of nature as aromatic molecules provide significantly greater monomer stability than their nonaromatic cousins. Since the publication of "Taking the Aromaticity out of Aromatic Interactions" found in Chapter II, there has been a several examples of nonaromatic π-stacking. These newfound nonaromatic π-interactions should yield new routes toward even stronger interactions in biological and organic electronic systems. Additionally, it prevents an artificial limitation in our understanding of chemistry.

The other main assumption surrounds the well-known Hunter-Sanders model and its derivatives. This model has been shown by countless other works to be inferior to the newer local direct interaction model of substituent effects. The local direct interaction model,as originally conceived, stated that π-stacking was driven by an interaction of the local dipole of a substituent with the near apex of the other ring. Chapter III expands this model to the much lesser studied XH/π interactions, showing a similar trend for polar XH groups. The nonpolar groups warrant further investigation as they are dispersion driven, which is not explained with the current local direct interaction model. Chapter IV broadened the local direct interaction model to include not just substituents,

but also heteroatom substitutions in the ring. These interactions can be well predicted through the use of electric fields of an unchanging ring and dipoles. Finally, Chapter V extended the local direct interaction model to anion/π interactions. In doing so, a last vestige of the Hunter-Sanders models was shown inaccurate. The culmination of these works helps reconcile the models used in π-interactions with more physically sound concepts for better exploitation of these interactions in real systems.

REFERENCES

(1) Muktha, B.; Srinivas, O.; Amresh, M. R.; Guru Row, T. N.; Jayaraman, N.; Sekar, K. *Carbohydr. Res.* **2003**, *338*, 2005.

(2) Quiocho, F. A.; Vyas, N. K. *Nature* **1984**, *310*, 381.

(3) Spiwok, V.; Lipovová, P.; Skálová, T.; Buchtelová, E.; Hašek, J.; Králová, B. *Carbohydr. Res.* **2004**, *339*, 2275.

(4) Tatko, C. D.; Waters, M. L. *J. Am. Chem. Soc.* **2004**, *126*, 2028.

(5) Vyas, N. K.; Vyas, M. N.; Quiocho, F. A. *Nature* **1987**, *327*, 635.

(6) Jiten Singh, N.; Shin, D.; Lee, H. M.; Kim, H. T.; Chang, H.-J.; Cho, J. M.; Kim, K. S.; Ro, S. *J. Struct. Biol.* **2011**, *174*, 173.

(7) Matsumoto, A.; Tanaka, T.; Tsubouchi, T.; Tashiro, K.; Saragai, S.; Nakamoto, S. *J. Am. Chem. Soc.* **2002**, *124*, 8891.

(8) Nagahama, S.; Inoue, K.; Sada, K.; Miyata, M.; Matsumoto, A. *Cryst. Growth Des.* **2003**, *3*, 247.

(9) Saigo, K.; Kobayashi, Y. *Chem. Rec.* **2007**, *7*, 47.

(10) Umezawa, Y.; Tsuboyama, S.; Honda, K.; Uzawa, J.; Nishio, M. *Bull. Chem. Soc. Jpn.* **1998**, *71*, 1207.

(11) Umezawa, Y.; Tsuboyama, S.; Takahashi, H.; Uzawa, J.; Nishio, M. *Tetrahedron* **1999**, *55*, 10047.

(12) Amabilino, D. B.; Ashton, P. R.; Brown, C. L.; Córdova, E.; Godínez, L. A.; Goodnow, T. T.; Kaifer, A. E.; Newton, S. P.; Pietraszkiewicz, M.; Philp, D.; Raymo, F. M.; Reder, A. S.; Rutland, M. T.; Slawin, A. M. Z.; Spencer, N.; Stoddart, J. F.; Williams, D. J. *J. Am. Chem. Soc.* **1995**, *117*, 1271.

(13) Frontera, A.; Garau, C.; Quiñonero, D.; Ballester, P.; Costa, A.; Deyà, P. M. *Org. Lett.* **2003**, *5*, 1135.

(14) Kobayashi, K.; Asakawa, Y.; Kato, Y.; Aoyama, Y. *J. Am. Chem. Soc.* **1992**, *114*, 10307.

(15) Lakshminarayanan, P. S.; Kumar, D. K.; Ghosh, P. *J. Am. Chem. Soc.* **2006**, *128*, 9600.

(16) Sozzani, P.; Comotti, A.; Bracco, S.; Simonutti, R. *Chem, Commun.* **2004**, *10*, 768.

(17) Tóth, G.; Köver, K. E.; Murphy, R. F.; Lovas, S. *J. Phys. Chem. B* **2004**, *108*, 9287.

(18) Yamamoto, Y.; Yamamoto, A.; Furuta, S. Y.; Horie, M.; Kodama, M.; Sato, W.; Akiba, K. Y.; Tsuzuki, S.; Uchimaru, T.; Hashizume, D.; Iwasaki, F. *J. Am. Chem. Soc.* **2005**, *127*, 14540.

(19) Raju, R. K.; Burton, N. A.; Hillier, I. H. *Phys. Chem. Chem. Phys.* **2010**, *12*, 7117.

(20) Raju, R. K.; Hillier, I. H.; Burton, N. A.; Vincent, M. A.; Doudou, S.; Bryce, R. A. *Phys. Chem. Chem. Phys.* **2010**, *12*, 7959.

(21) Raju, R. K.; Ramraj, A.; Vincent, M. A.; Hillier, I. H.; Burton, N. A. *Phys. Chem. Chem. Phys.* **2008**, *10*, 6500.

(22) Salonen, L. M.; Ellermann, M.; Diederich, F. *Angew. Chem. Int. Ed.* **2011**, *50*, 4808.

(23) Müller-Dethlefs, K.; Hobza, P. *Chem. Rev.* **2000**, *100*, 143.

(24) Kwon, J. Y.; Singh, N. J.; Kim, H. N.; Kim, S. K.; Kim, K. S.; Yoon, J. *J. Am. Chem. Soc.* **2004**, *126*, 8892.

(25) Barwell, N. P.; Davis, A. P. *J. Org. Chem.* **2011**, *76*, 6548.

(26) Kozmon, S.; Matuska, R.; Spiwok, V.; Koca, J. *Phys. Chem. Chem. Phys.* **2011**, *13*, 14215.

(27) Jorgensen, W. L. *Science* **2004**, *303*, 1813.

(28) Sontz, P. A.; Muren, N. B.; Barton, J. K. *Acc. Chem. Res.* **2012**, *45*, 1792.

(29) Coropceanu, V.; Cornil, J.; da Silva Filho, D. A.; Olivier, Y.; Silbey, R.; Brédas, J.-L. *Chem. Rev.* **2007**, *107*, 926.

(30) Brédas, J.-L.; Norton, J. E.; Cornil, J.; Coropceanu, V. *Acc. Chem. Res.* **2009**, *42*, 1691.

(31) Zade, S. S.; Bendikov, M. *Chem. Eur. J.* **2007**, *13*, 3688.

(32) Chen, A.-J.; Hsu, I. J.; Wu, W.-Y.; Su, Y.-T.; Tsai, F.-Y.; Mou, C.-Y. *Langmuir* **2013**, *29*, 2580.

(33) Copeland, K. L.; Tschumper, G. S. *J. Chem. Theory Comput.* **2012**, *8*, 4279.

(34) Economopoulos, S. P.; Chochos, C. L.; Ioannidou, H. A.; Neophytou, M.; Charilaou, C.; Zissimou, G. A.; Frost, J. M.; Sachetan, T.; Shahid, M.; Nelson, J.; Heeney, M.; Bradley, D. D. C.; Itskos, G.; Koutentis, P. A.; Choulis, S. A. *Rsc Advances* **2013**, *3*, 10221.

(35) Perdih, F. *Acta Crystallographica Section C-Crystal Structure Communications* **2012**, *68*, M64.

(36) Hunter, C. A.; Sanders, J. K. M. *J. Am. Chem. Soc.* **1990**, *112*, 5525.

(37) Hunter, C. A.; Lawson, K. R.; Perkins, J.; Urch, C. J. *J. Chem. Soc., Perkin Trans. 2* **2001**, 651.

(38) Battaglia, M. R.; Buckingham, A. D.; Williams, J. H. *Chem. Phys. Lett.* **1981**, *78*, 421.

(39) Fowler, P. W.; Buckingham, A. D. *Chem. Phys. Lett.* **1991**, *176*, 11.

(40) Stone, A. J.; Alderton, M. *Mol. Phys.* **1985**, *56*, 1065.

(41) Vigné-Maeder, F.; Claverie, P. *J. Chem. Phys.* **1988**, *88*, 4934.

(42) Stone, A. J. *The Theory of Intermolecular Forces*; Oxford University Press: Oxford, 1996.

(43) Beg, S.; Waggoner, K.; Ahmad, Y.; Watt, M.; Lewis, M. *Chem. Phys. Lett.* **2008**, *455*, 98.

(44) Lee, E. C.; Kim, D.; Jurečka, P.; Tarakeshwar, P.; Hobza, P.; Kim, K. S. *J. Phys. Chem. A* **2007**, *111*, 3446.

(45) Hohenstein, E. G.; Duan, J.; Sherrill, C. D. *J. Am. Chem. Soc.* **2011**, *133*, 13244.

(46) Wheeler, S. E.; Houk, K. N. *J. Am. Chem. Soc.* **2008**, *130*, 10854.

(47) Wheeler, S. E. *J. Am. Chem. Soc.* **2011**, *133*, 10262.

(48) Argaman, N.; Makov, G. *Am. J. Phys.* **2000**, *68*, 69.

(49) Becke, A. D. *J. Chem. Phys.* **1992**, *96*, 2155.

(50) Becke, A. *J. Chem. Phys.* **1997**, *107*, 8554.

(51) Grimme, S. *J. Comput. Chem.* **2006**, *27*, 1787.

(52) Grimme, S. *WIREs Comp. Mol. Sci.* **2011**, *1*, 211.

(53) Szalewicz, K. *WIREs Comp. Mol. Sci.* **2012**, *2*, 254.

(54) Jeziorski, B.; Moszyński, R.; Szalewicz, K. *Chem. Rev.* **1994**, *94*, 1887.

(55) Waters, M. L. *Curr. Opin. Chem. Biol.* **2002**, *6*, 736.

(56) Schneider, H.-J. *Angew. Chem. Int. Ed.* **2009**, *48*, 3924.

(57) Meyer, E. A.; Castellano, R. K.; Diederich, F. *Angew. Chem. Int. Ed.* **2003**, *42*, 1210.

(58) Schottel, B. L.; Chifotides, H. T.; Dunbar, K. R. *Chem. Soc. Rev.* **2008**, *37*, 68.

(59) Ma, J. C.; Dougherty, D. A. *Chem. Rev.* **1997**, *97*, 1303.

(60) Grimme, S. *Angew. Chem. Int. Ed.* **2008**, *47*, 3430.

(61) Schleyer, P. v. R.; Puhlhofer, F. *Org. Lett.* **2002**, *4*, 2873.

(62) Wheeler, S. E.; Houk, K. N.; Schleyer, P. v. R.; Allen, W. D. *J. Am. Chem. Soc.* **2009**, *131*, 2547.

(63) George, P.; Trachtman, M.; Bock, C. W.; Brett, A. M. *Theor. Chem. Acc.* **1975**, *38*, 121.

(64) George, P.; Trachtman, M.; Bock, C. W.; Brett, A. M. *J. Chem. Soc., Perkin Trans. 2* **1976**, 1222.

(65) Chen, Z.; Wannere, C. S.; Corminboeuf, C.; Puchta, R.; Schleyer, P. v. R. *Chem. Rev.* **2005**, *105*, 3842.

(66) Wheeler, S. E.; Houk, K. N. *J. Phys. Chem. A* **2010**, *114*, 8658.

(67) Schleyer, P. v. R.; Maerker, C.; Dransfeld, A.; Jiao, H.; van Eikema Hommes, J. R. *J. Am. Chem. Soc.* **1996**, *118*, 6317.

(68) Grimme, S. *J. Chem. Phys.* **2003**, *118*, 9095.

(69) Schafer, A.; Huber, C.; Ahlrichs, R. *J. Chem. Phys.* **1994**, *100*, 5829.

(70) Dunning, T. H., Jr. *J. Chem. Phys.* **1989**, *90*, 1007.

(71) Kendall, R. A.; Dunning, T. H., Jr.; Harrison, R. J. *J. Chem. Phys.* **1992**, *96*, 6796.

(72) Boys, S. F.; Bernardi, F. *Mol. Phys.* **1970**, *19*, 553.

(73) MOLPRO is a package of ab initio programs written by H.-J. Werner, P. J. Knowles, G. Knizia, F. R. Manby, M. Schütz, P. Celani, T. Korona, R. Lindh, A. Mitrushenkov, G. Rauhut, K. R. Shamasundar, T. B. Adler, R. D. Amos, A. Bernhardsson, A. Berning, D. L. Cooper, M. J. O. Deegan, A. J. Dobbyn, F. Eckert, E. Goll, C. Hampel, A. Hesselmann, G. Hetzer, T. Hrenar, G. Jansen, C. Köppl, Y. Liu, A. W. Lloyd, R. A. Mata, A. J. May, S. J. McNicholas, W. Meyer, M. E. Mura, A. Nicklaß, D. P. O'Neill, P. Palmieri, K. Pflüger, R. Pitzer, M. Reiher, T. Shiozaki, H. Stoll, A. J. Stone, R. Tarroni, T. Thorsteinsson, M. Wang, A. Wolf . .

(74) Gaussian 09, Revision B.01, M. J. Frisch, G. W. Trucks, H. B. Schlegel, G. E. Scuseria, M. A. Robb, J. R. Cheeseman, G. Scalmani, V. Barone, B. Mennucci, G. A. Petersson, H. Nakatsuji, M. Caricato, X. Li, H. P. Hratchian, A. F. Izmaylov, J. Bloino, G. Zheng, J. L. Sonnenberg, M. Hada, M. Ehara, K. Toyota, R. Fukuda, J. Hasegawa, M. Ishida, T. Nakajima, Y. Honda, O. Kitao, H. Nakai, T. Vreven, J. A. Montgomery, Jr., J. E. Peralta, F. Ogliaro, M. Bearpark, J. J. Heyd, E. Brothers, K. N. Kudin, V. N. Staroverov, R. Kobayashi, J. Normand, K. Raghavachari, A. Rendell, J. C. Burant, S. S. Iyengar, J. Tomasi, M. Cossi, N. Rega, J. M. Millam, M. Klene, J. E. Knox, J. B. Cross, V. Bakken, C. Adamo, J. Jaramillo, R. Gomperts, R. E. Stratmann, O. Yazyev, A. J. Austin, R. Cammi, C. Pomelli, J. W. Ochterski, R. L. Martin, K. Morokuma, V. G. Zakrzewski, G. A. Voth, P. Salvador, J. J. Dannenberg, S. Dapprich, A. D. Daniels, Ö. Farkas, J. B. Foresman, J. V. Ortiz, J. Cioslowski, and D. J. Fox, Gaussian, Inc., Wallingford CT, 2010.

(75) Sinnokrot, M. O.; Sherrill, C. D. *J. Phys. Chem. A* **2006**, *110*, 10656.

(76) SAPT2008: "An Ab Initio Program for Many-Body Symmetry-Adapted Perturbation Theory Calculations of Intermolecular Interaction Energies" by R. Bukowski, W. Cencek, P. Jankowski, B. Jeziorski, M. Jeziorska, S. A. Kucharski, V. F. Lotrich, A. J. Misquitta, R. Moszynski, K. Patkowski, R. Podeszwa, S. Rybak, K. Szalewicz, H. L. Williams, R. J. Wheatley, P. E. S. Wormer, and P. S. Żuchowski.

(77) Tsuzuki, S.; Fujii, A. *Phys. Chem. Chem. Phys.* **2008**, *10*, 2584.

(78) Tsuzuki, S.; Uchimaru, T. *Curr. Org. Chem.* **2006**, *10*, 745.

(79) Takahashi, O.; Kohno, Y.; Nishio, M. *Chem. Rev.* **2010**, *110*, 6049.

(80) Raju, R. K.; Bloom, J. W. G.; An, Y.; Wheeler, S. E. *ChemPhysChem* **2011**, *12*, 3116.

(81) Wheeler, S. E.; Houk, K. N. *Mol. Phys.* **2009**, *107*, 749.

(82) Kodama, Y.; Nishihata, K.; Nishio, M.; Nakagawa, N. *Tetrahedron Lett.* **1977**, *18*, 2105.

(83) Tsuzuki, S.; Uchimaru, T.; Mikami, M. *J. Phys. Chem. A* **2011**, *115*, 11256.

(84) Asensio, J. L.; Ardá, A.; Cañada, F. J.; Jiménez-Barbero, J. *Acc. Chem. Res.* **2013**, *46*, 946.

(85) Shibasaki, K.; Fujii, A.; Mikami, N.; Tsuzuki, S. *J. Phys. Chem. A* **2006**, *110*, 4397.

(86) Tsuzuki, S.; Honda, K.; Uchimaru, T.; Mikami, M.; Tanabe, K. *J. Am. Chem. Soc.* **2000**, *122*, 3746.

(87) Morita, S.-i.; Fujii, A.; Mikami, N.; Tsuzuki, S. *J. Phys. Chem. A* **2006**, *110*, 10583.

(88) Mishra, B. K.; Karthikeyan, S.; Ramanathan, V. *J. Chem. Theory Comput.* **2012**, *8*, 1935.

(89) Fujii, A.; Shibasaki, K.; Kazama, T.; Itaya, R.; Mikami, N.; Tsuzuki, S. *Phys. Chem. Chem. Phys.* **2008**, *10*, 2836.

(90) Tsuzuki, S.; Honda, K.; Uchimaru, T.; Mikami, M.; Tanabe, K. *J. Phys. Chem. A* **2002**, *106*, 4423.

(91) Ugozzoli, F.; Arduini, A.; Massera, C.; Pochini, A.; Secchi, A. *New J. Chem.* **2002**, *26*, 1718.

(92) Sinnokrot, M. O.; Sherrill, C. D. *J. Am. Chem. Soc.* **2004**, *126*, 7690.

(93) Ringer, A. L.; Sinnokrot, M. O.; Lively, R. P.; Sherrill, C. D. *Chem. Eur. J.* **2006**, *12*, 3821.

(94) Lee, E. C.; Hong, B. H.; Lee, J. Y.; Kim, J. C.; Kim, D.; Kim, Y.; Tarakeshwar, P.; Kim, K. S. *J. Am. Chem. Soc.* **2005**, *127*, 4530.

(95) Riley, K. E.; Merz, K. M., Jr. *J. Phys. Chem. B* **2006**, *109*, 17752.

(96) Tarakeshwar, P.; Choi, H. S.; Lee, S. J.; Lee, J. Y.; Kim, K. S.; Ha, T. K.; Jang, J. H.; Lee, J. G.; Lee, H. *J. Chem. Phys.* **1999**, *111*, 5838.

(97) Reimann, B.; Buchhold, K.; Barth, H. D.; Brutschy, B.; Tarakeshwar, P.; Kim, K. S. *J. Chem. Phys.* **2002**, *117*, 8805.

(98) Riehn, C.; Reimann, B.; Buchhold, K.; Vaupel, S.; Barth, H. D.; Brutschy, B.; Tarakashwar, P.; Kim, K. S. *J. Chem. Phys.* **2001**, *115*, 10045.

(99) Buchhold, K.; Reimann, B.; Djafari, S.; Barth, H. D.; Brutschy, B.; Tarakeshwar, P.; Kim, K. S. *J. Chem. Phys.* **2000**, *112*, 1844.

(100) Gallivan, J. P.; Dougherty, D. A. *Org. Lett.* **1999**, *1*, 103.

(101) Danten, Y. *J. Phys. Chem. A* **1999**, *103*, 3530.

(102) Scheiner, S.; Kar, T.; Pattanayak, J. *J. Am. Chem. Soc.* **2002**, *124*, 13257.

(103) Tarakeshwar, P.; Kim, K. S.; Brutschy, B. *J. Chem. Phys.* **1999**, *110*, 8501.

(104) Riehn, C.; Buchhold, K.; Reimann, B.; Djafari, S.; Barth, H. D.; Brutschy, B.; Tarakeshwar, P.; Kim, K. S. *J. Chem. Phys.* **2000**, *112*, 1170.

(105) Raju, R. K.; Ramraj, A.; Hillier, I. H.; Vincent, M. A.; Burton, N. A. *Phys. Chem. Chem. Phys.* **2009**, *11*, 3411.

(106) Ramraj, A.; Raju, R. K.; Wang, Q.; Hillier, I. H.; Bryce, R. A.; Vincent, M. A. *J. Mol. Graphics Modell.* **2010**, *29*, 321.

(107) Kumari, M.; Balaji, P. V.; Sunoj, R. B. *Phys. Chem. Chem. Phys.* **2011**, *13*, 6517.

(108) Jurečka, P.; Šponer, J.; Černý, J.; Hobza, P. *Phys. Chem. Chem. Phys.* **2006**, *8*, 1985.

(109) Vaupel, S.; Brutschy, B.; Tarakeshwar, P.; Kim, K. S. *J. Am. Chem. Soc.* **2006**, *128*, 5416.

(110) Mishra, B. K.; Sathyamurthy, N. *J. Phys. Chem. A* **2007**, *111*, 2139.

(111) Tarakeshwar, P.; Lee, S. J.; Lee, J. Y.; Kim, K. S. *J. Chem. Phys.* **1998**, *108*, 7217.

(112) Tarakeshwar, P.; Choi, H. S.; Kim, K. S. *J. Am. Chem. Soc.* **2001**, *123*, 3323.

(113) Tarakeshwar, P.; Kim, K. S. *J. Phys. Chem. A* **1999**, *103*, 9116.

(114) Tarakeshwar, P.; Lee, S. J.; Lee, J. Y.; Kim, K. S. *J. Phys. Chem. B* **1998**, *103*, 184.

(115) Hansch, C.; Leo, A.; Taft, R. W. *Chem. Rev.* **1991**, *91*, 165.

(116) Cockroft, S. L.; Hunter, C. A.; Lawson, K. R.; Perkins, J.; Urch, C., J. *J. Am. Chem. Soc.* **2005**, *127*, 8594.

(117) Cockroft, S. L.; Perkins, J.; Zonta, C.; Adams, H.; Spey, S. E.; Low, C. M. R.; Vinter, J. G.; Lawson, K. R.; Urch, C. J.; Hunter, C. A. *Org. Biomol. Chem.* **2007**, *5*, 1062.

(118) Cozzi, F.; Cinquini, M.; Annunziata, R.; Siegel, J. S. *J. Am. Chem. Soc.* **1993**, *115*, 5330.

(119) Cozzi, F.; Cinquini, M.; Annunziata, R.; Dwyer, T.; Siegel, J. S. *J. Am. Chem. Soc.* **1992**, *114*, 5729.

(120) Wheeler, S. E. *Acc. Chem. Res.* **2013**, *46*, 1029.

(121) Watt, M.; Hardebeck, L. K. E.; Kirkpatrick, C. C.; Lewis, M. *J. Am. Chem. Soc.* **2011**, *133*, 3854.

(122) Hansch, C.; Leo, A.; Unger, S. H.; Kim, K. H.; Nikaitani, D.; Lien, E. J. *J. Med. Chem.* **1973**, *16*, 1207.

(123) Zürcher, M.; Diederich, F. *J. Org. Chem.* **2008**, *73*, 4345.

(124) Knowles, R. R.; Jacobsen, E. N. *Proc. Natl. Acad. Sci. U. S. A.* **2010**, *107*, 20678.

(125) Takenaka, N.; Chen, J. S.; Captain, B. *Org. Lett.* **2011**, *13*, 1654.

(126) Lu, T.; Zhu, R.; An, Y.; Wheeler, S. E. *J. Am. Chem. Soc.* **2012**, *134*, 3095.

(127) Hains, A. W.; Liang, Z.; Woodhouse, M. A.; Gregg, B. A. *Chem. Rev.* **2010**, *110*, 6689.

(128) Bassani, D. M.; Jonusauskaite, L.; Lavie-Cambot, A.; McClenaghan, N. D.; Pozzo, J.-L.; Ray, D.; Vives, G. *Coord. Chem. Rev.* **2010**, *254*, 2429.

(129) Wheeler, S. E. *CrystEngComm* **2012**, *14*, 6140.

(130) Sherrill, C. D. Computations of Noncovalent pi interactions. In *Rev. Comput. Chem.*; Lipkowitz, K. B., Cundari, T. R., Eds.; Wiley-VCH: New York, 2009; Vol. 26; pp 1.

(131) Sinnokrot, M. O.; Valeev, E. F.; Sherrill, C. D. *J. Am. Chem. Soc.* **2002**, *124*, 10887.

(132) Cockroft, S. L.; Hunter, C. A. *Chem. Soc. Rev.* **2007**, *36*, 172.

(133) Cozzi, F.; Ponzini, F.; Annunziata, R.; Cinquini, M.; Siegel, J. S. *Angew. Chem. Int. Ed.* **1995**, *34*, 1019.

(134) Cozzi, F.; Siegel, J. S. *Pure Appl. Chem.* **1995**, *67*, 683.

(135) Cozzi, F.; Annunziata, R.; Benaglia, M.; Cinquini, M.; Raimondi, L.; Baldridge, K. K.; Siegel, J. S. *Org. Biomol. Chem.* **2003**, *1*, 157.

(136) Cozzi, F.; Annunziata, R.; Benaglia, M.; Baldridge, K. K.; Aguirre, G.; Estrada, J.; Sritana-Anant, Y.; Siegel, J. S. *Phys. Chem. Chem. Phys.* **2008**, *10*, 2686.

(137) Sinnokrot, M. O.; Sherrill, C. D. *J. Phys. Chem. A* **2003**, *107*, 8377.

(138) Arnstein, S. A.; Sherrill, C. D. *Phys. Chem. Chem. Phys.* **2008**, *10*, 2646.

(139) Wheeler, S. E.; Houk, K. N. *J. Chem. Theory Comput.* **2009**, *5*, 2301.

(140) Ringer, A. L.; Sherrill, C. D. *J. Am. Chem. Soc.* **2009**, *131*, 4574.

(141) Seo, J.-I.; Kim, I.; Lee, Y. S. *Chem. Phys. Lett.* **2009**, *474*, 101.

(142) Wheeler, S. E.; McNeil, A. J.; Müller, P.; Swager, T. M.; Houk, K. N. *J. Am. Chem. Soc.* **2010**, *132*, 3304.

(143) Rashkin, M. J.; Waters, M. L. *J. Am. Chem. Soc.* **2002**, *124*, 1860.

(144) Sham, I. H. T.; Kwok, C.-C.; Che, C.-M.; Zhu, N. *Chem. Commun.* **2005**, 3547.

(145) Yamaguchi, S.; Wakamiya, A. *Pure Appl. Chem.* **2006**, *78*, 1413.

(146) Anthony, J. E. *Chem. Rev.* **2006**, *106*, 5028.

(147) Bunz, U. H. F. *Chem. Eur. J.* **2009**, *15*, 6780.

(148) Bunz, U. H. F. *Pure Appl. Chem.* **2010**, *82*, 953.

(149) Bunz, U. H. F.; Engelhart, J. U.; Lindner, B. D.; Schaffroth, M. *Angew. Chem. Int. Ed.* **2013**, *52*, 3810.

(150) Zhong, H.; Lai, H.; Fang, Q. *J. Phys. Chem. C* **2010**, *115*, 2423.

(151) Luechai, A.; Gasiorowski, J.; Petsom, A.; Neugebauer, H.; Sariciftci, N. S.; Thamyongkit, P. *J. Mater. Chem.* **2012**, *22*, 23030.

(152) Kuhn, P.; Antonietti, M.; Thomas, A. *Angew. Chem. Int. Ed.* **2008**, *47*, 3450.

(153) Jackson, K. T.; Rabbani, M. G.; Reich, T. E.; El-Kaderi, H. M. *Polym. Chem.* **2011**, *2*, 2775.

(154) Reich, T. E.; Jackson, K. T.; Jena, P.; El-Kaderi, H. M. *J. Mater. Chem.* **2011**, *10629-10632*

(155) Reich, T. E.; Behera, S.; Jackson, K. T.; Jena, P.; El-Kaderi, H. M. *J. Mater. Chem.* **2012**, *22*, 13524.

(156) Jackson, K. T.; Reich, T. E.; El-Kaderi, H. M. *Chem. Commun.* **2012**, *48*, 8823.

(157) Luo, W.; Neiner, D.; Karkamkar, A.; Parab, K.; Garner, E. B.; Dixon, D. A.; Matson, D.; Autrey, T.; Liu, S.-Y. *Dalton Trans.* **2013**, *42*, 611.

(158) Luo, W.; Campbell, P. G.; Zakharov, L. N.; Liu, S.-Y. *J. Am. Chem. Soc.* **2011**, *133*, 19326.

(159) Campbell, P. G.; Zakharov, L. N.; Grant, D.; Dixon, D. A.; Liu, S.-Y. *J. Am. Chem. Soc.* **2010**, *132*, 3289.

(160) Abbey, E. R.; Liu, S.-Y. *Org. Biomol. Chem.* **2013**, *11*, 2060.

(161) Knack, D. H.; Marshall, J. L.; Harlow, G. P.; Dudzik, A.; Szaleniec, M.; Liu, S.-Y.; Heider, J. *Angew. Chem. Int. Ed.* **2013**, *52*, 2599.

(162) Campbell, P. G.; Marwitz, A. J. V.; Liu, S.-Y. *Angew. Chem. Int. Ed.* **2012**, *51*, 6074.

(163) Liu, L.; Marwitz, A. J. V.; Matthews, B. W.; Liu, S.-Y. *Angew. Chem. Int. Ed.* **2009**, *48*, 6817.

(164) Anand, B.; Nöth, H.; Schwenk-Kircher, H.; Troll, A. *Eur. J. Inorg. Chem.* **2008**, *2008*, 3186.

(165) Kawahara, S.; Tsuzuki, S.; Uchimaru, T. *J. Chem. Phys.* **2003**, *119*, 10081.

(166) Bettinger, H. F.; Kar, T.; Sánchez-García, E. *J. Phys. Chem. A* **2009**, *113*, 3353.

(167) Ugozzoli, F.; Massera, C. *CrystEngComm* **2005**, *7*, 121.

(168) Bates, D. M.; Anderson, J. A.; Oloyede, P.; Tschumper, G. S. *Phys. Chem. Chem. Phys.* **2008**, *10*, 2775.

(169) Wang, W.; Hobza, P. *ChemPhysChem* **2008**, *9*, 1003.

(170) Mishra, B. K.; Arey, J. S.; Sathyamurthy, N. *J. Phys. Chem. A* **2010**, *114*, 9606.

(171) Guin, M.; Patwari, G. N.; Karthikeyan, S.; Kim, K. S. *Phys. Chem. Chem. Phys.* **2011**, *13*, 5514.

(172) Guin, M.; Patwari, G. N.; Karthikeyan, S.; Kim, K. S. *Phys. Chem. Chem. Phys.* **2009**, *11*, 11207.

(173) Sütay, B.; Tekin, A.; Yurtsever, M. *Theor. Chem. Acc.* **2012**, *131*, 1120.

(174) Hampel, C.; Peterson, K. A.; Werner, H.-J. *Chem. Phys. Lett.* **1992**, *190*, 1.

(175) Raghavachari, K.; Trucks, G. W.; Pople, J. A.; Head-Gordon, M. *Chem. Phys. Lett.* **1989**, *157*, 479.

(176) Hohenstein, E. G.; Sherrill, C. D. *J. Chem. Phys.* **2010**, *133*, 014101.

(177) Hohenstein, E. G.; Sherrill, C. D. *J. Chem. Phys.* **2010**, *132*, 184111.

(178) Schafer, A.; Huber, C.; Ahlrichs, R. *J. Chem. Phys.* **1994**, *100*, 5829.

(179) Papajak, E.; Truhlar, D. G. *J. Chem. Theory Comput.* **2011**, *7*, 10.

(180) Pettersen, E. F.; Goddard, T. D.; Huang, C. C.; Couch, G. S.; Greenblatt, D. M.; Meng, E. C.; Ferrin, T. E. *J. Comput. Chem.* **2004**, *25*, 1605.

(181) Turney, J. M.; Simmonett, A. C.; Parrish, R. M.; Hohenstein, E. G.; Evangelista, F. A.; Fermann, J. T.; Mintz, B. J.; Wilke, J. J.; Abrams, M. L.; Russ, N. J.; Leininger, M. L.; Janssen, C. L.; Seidl, E. T.; Allen, W. D.; Schaefer, H. F.; King, R. A.; Valeev, E. F.; Sherrill, C. D.; Crawford, T. D. *WIREs Comp. Mol. Sci.* **2012**, *2*, 556.

(182) Bloom, J. W. G.; Wheeler, S. E. *Angew. Chem. Int. Ed.* **2011**, *50*, 7847.

(183) Islas, R.; Chamorro, E.; Robles, J.; Heine, T.; Santos, J. C.; Merino, G. *Struct. Chem.* **2007**, *18*, 833.

(184) Bloom, J. W. G.; Raju, R. K.; Wheeler, S. E. *J. Chem. Theory Comput.* **2012**, *8*, 3167.

(185) Alkorta, I.; Rozas, I.; Elguero, J. *J. Am. Chem. Soc.* **2002**, *124*, 8593.

(186) Mascal, M.; Armstrong, A.; Bartberger, M. D. *J. Am. Chem. Soc.* **2002**, *124*, 6274.

(187) Quiñonero, D.; Garau, C.; Rotger, C.; Frontera, A.; Ballester, P.; Costa, A.; Deyà, P. M. *Angew. Chem. Int. Ed.* **2002**, *41*, 3389.

(188) Frontera, A.; Gamez, P.; Mascal, M.; Mooibroek, T. J.; Reedijk, J. *Angew. Chem. Int. Ed.* **2011**, *50*, 9564.

(189) Gamez, P.; Mooibroek, T. J.; Teat, S. J.; Reedijk, J. *Acc. Chem. Res.* **2007**, *40*, 435.

(190) Mooibroek, T. J.; Black, C. A.; Gamez, P.; Reedijk, J. *Cryst. Growth Des.* **2008**, *8*, 1082.

(191) Berryman, O. B.; Johnson, D. W. *Chem. Commun.* **2009**, 3143.

(192) Frontera, A.; Quiñonero, D.; Deyà, P. M. *WIREs Comp. Mol. Sci.* **2011**, *1*, 440.

(193) Wang, D.-X.; Wang, M.-X. *J. Am. Chem. Soc.* **2013**, *135*, 892.

(194) Egli, M.; Sarkhel, S. *Acc. Chem. Res.* **2007**, *40*, 197.

(195) Mooibroek, T. J.; Gamez, P.; Reedijk, J. *CrystEngComm* **2008**, *10*, 1501.

(196) Spruell, J. M.; Coskun, A.; Friedman, D. C.; Forgan, R. S.; Sarjeant, A. A.; Trabolsi, A.; Fahrenbach, A. C.; Barin, G.; Paxton, W. F.; Dey, S. K.; Olson, M. A.; Benítez, D.; Tkatchouk, E.; Colvin, M. T.; Carmielli, R.; Caldwell, S. T.; Rosair, G. M.; Gunatilaka Hewage, S.; Duclairoir, F.; Seymour, J. L.; Slawin, A. M. Z.; Goddard, W. A., III; Waielewski, M. R.; Cooke, G.; Stoddart, J. F. *Nature Chem.* **2010**, *2*, 870.

(197) Chifotides, H. T.; Dunbar, K. R. *Acc. Chem. Res.* **2013**, *46*, 894.

(198) Zhao, Y.; Domoto, Y.; Orentas, E.; Beuchat, C.; Emery, D.; Mareda, J.; Sakai, N.; Matile, S. *Angew. Chem. Int. Ed.* **2013**, *52*, 9940.

(199) Mareda, J.; Matile, S. *Chem. Eur. J.* **2009**, *15*, 28.

(200) Dawson, R. E.; Hennig, A.; Weimann, D. P.; Emery, D.; Ravikumar, V.; Montenegro, J.; Takeuchi, T.; Gabutti, S.; Mayor, M.; Mareda, J.; Schalley, C. A.; Matile, S. *Nature Chem.* **2010**, *2*, 533.

(201) Chifotides, H. T.; Giles, I. D.; Dunbar, K. R. *J. Am. Chem. Soc.* **2013**, *135*, 3039.

(202) Garau, C.; Frontera, A.; Quiñonero, D.; Ballester, P.; Costa, A.; Deyà, P. M. *ChemPhysChem* **2003**, *4*, 1344.

(203) Quiñonero, D.; Garau, C.; Frontera, A.; Ballester, P.; Costa, A.; Deyà, P. M. *Chem. Phys. Lett.* **2002**, *359*, 486.

(204) Kim, D.; Tarakeshwar, P.; Kim, K. S. *J. Phys. Chem. A* **2004**, *108*, 1250.

(205) Clements, A.; Lewis, M. *J. Phys. Chem. A* **2006**, *110*, 12705.

(206) Garau, C.; Quiñonero, D.; Frontera, A.; Ballester, P.; Costa, A.; Deyà, P. M. *Org. Lett.* **2003**, *5*, 2227.

(207) Garau, C.; Frontera, A.; Quiñonero, D.; Ballester, P.; Costa, A.; Deyà, P. M. *Chem. Phys. Lett.* **2004**, *392*, 85.

(208) Geronimo, I.; Singh, N. J.; Kim, K. S. *J. Chem. Theory Comput.* **2011**, *7*, 825.

(209) Raju, R. K.; Bloom, J. W. G.; Wheeler, S. E. *J. Chem. Theory Comput.* **2013**, *9*, 3479.

(210) Crawford, T. D.; Sherrill, C. D.; Valeev, E. F.; Fermann, J. T.; King, R. A.; Leininger, M. L.; Brown, S. T.; Janssen, C. L.; Seidl, E. T.; Kenny, J. P.; Allen, W. D. *J. Comput. Chem.* **2007**, *28*, 1610.

APPENDIX A

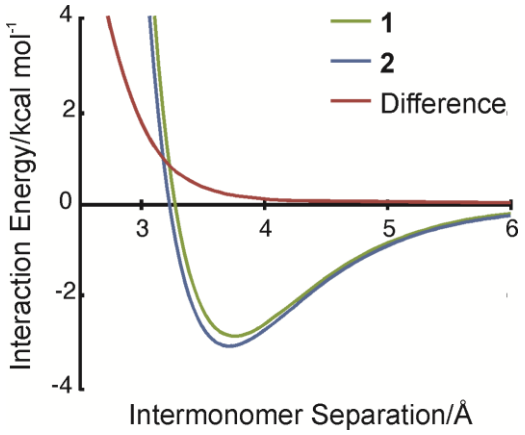

Figure A.1: SCS-MP2 interaction energies for the sandwich dimers of benzene with isomers 1 and 2, and the difference between the two, as a function of the inter-monomer distance *R*.

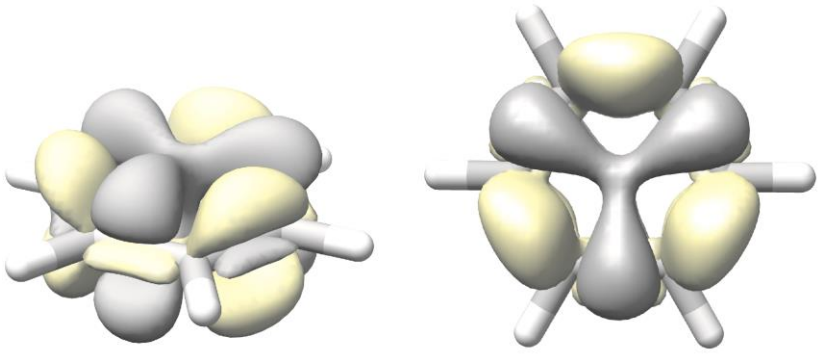

Figure A.2: Electron density difference isosurface ($\Delta\rho$ = 0.002 *e*/au^3) between benzene and dissected benzene. Grey indicates regions where the density is greater in benzene than in dissected benzene, while yellow indicates regions where the density in the dissected system is greater than in benzene (*i.e.*: location of the localized double bonds). Aromatic π-delocalization leads to a net shift of electron density towards the centre of the ring.

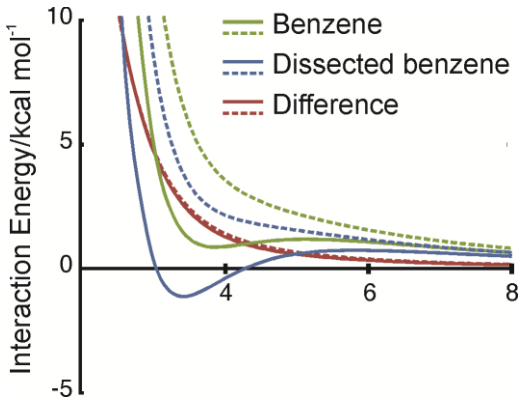

Figure A.3: CCSD(T) (solid lines) and HF (dashed lines) interaction energies for Cl^- interacting with benzene and dissected benzene, and the difference between the two, as a function of the inter-monomer distance *R*.

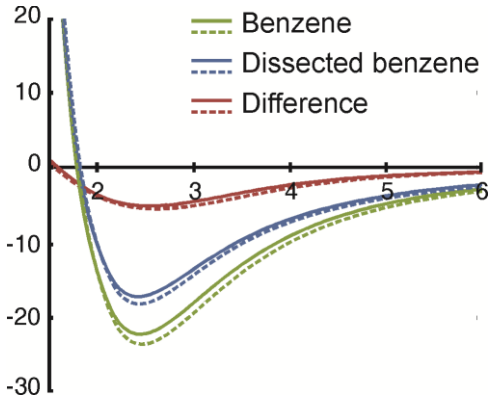

Figure A.4: CCSD(T) (solid lines) and HF (dashed lines) interaction energies for Na^+ interacting with benzene and dissected benzene, and the difference between the two, as a function of the inter-monomer distance *R*.

Table A.1: SAPT2 energy components (kcal mol^{-1}) for the interaction of benzene with dissected benzene.

	Butadiene					Ethene					Dissected Benzene				
R	Eelec	Eexch	Eind	Edisp	Etotal	Eelec	Eexch	Eind	Edisp	Etotal	Eelec	Eexch	Eind	Edisp	Etotal
2.0	-213.57	492.36	-35.01	-76.97	166.82	-119.20	278.85	-19.85	-42.85	96.95	-283.11	640.54	-45.46	-102.34	209.63
2.4	-69.93	170.78	-8.60	-36.66	55.59	-39.76	97.30	-6.35	-20.20	31.00	-90.51	220.44	-6.78	-49.38	73.77
2.8	-21.73	57.54	-3.34	-18.54	13.93	-12.59	33.05	-2.41	-10.13	7.92	-27.44	73.49	-2.78	-25.24	18.03
3.2	-6.23	18.91	-1.34	-9.90	1.45	-3.64	10.98	-0.94	-5.36	1.04	-7.77	23.81	-1.21	-13.60	1.23
3.4	-3.10	10.74	-0.84	-7.34	-0.53	-1.80	6.27	-0.58	-3.96	-0.07	-3.88	13.40	-0.77	-10.14	-1.38
3.6	-1.37	6.07	-0.52	-5.50	-1.31	-0.78	3.57	-0.36	-2.96	-0.52	-1.76	7.51	-0.48	-7.62	-2.35
3.7	-0.83	4.56	-0.41	-4.77	-1.44	-0.46	2.69	-0.28	-2.56	-0.61	-1.11	5.62	-0.38	-6.62	-2.49
3.8	-0.44	3.42	-0.32	-4.15	-1.48	-0.23	2.02	-0.22	-2.22	-0.65	-0.63	4.20	-0.30	-5.77	-2.51
3.9	-0.16	2.57	-0.26	-3.61	-1.46	-0.06	1.52	-0.18	-1.94	-0.65	-0.29	3.14	-0.24	-5.03	-2.43
4.0	0.04	1.93	-0.21	-3.15	-1.39	0.06	1.15	-0.14	-1.69	-0.62	-0.05	2.34	-0.20	-4.40	-2.30
4.2	0.27	1.08	-0.14	-2.42	-1.20	0.20	0.65	-0.09	-1.29	-0.54	0.23	1.31	-0.14	-3.38	-1.98
4.4	0.37	0.61	-0.10	-1.87	-0.99	0.25	0.37	-0.06	-1.00	-0.44	0.35	0.73	-0.10	-2.62	-1.63
4.8	0.38	0.19	-0.05	-1.14	-0.62	0.26	0.11	-0.03	-0.61	-0.27	0.39	0.22	-0.05	-1.61	-1.05
5.2	0.33	0.06	-0.03	-0.72	-0.37	0.22	0.03	-0.02	-0.38	-0.15	0.33	0.07	-0.03	-1.02	-0.65
5.6	0.26	0.02	-0.02	-0.47	-0.21	0.17	0.01	-0.01	-0.25	-0.08	0.27	0.02	-0.02	-0.67	-0.40
6.0	0.21	0.00	-0.01	-0.31	-0.11	0.14	0.00	-0.01	-0.16	-0.03	0.22	0.00	-0.01	-0.45	-0.24

Table A.2: SAPT2 energy components (kcal mol^{-1}) for the interaction of benzene with benzene, dissected benzene, and the difference between the two.

	Benzene					Dissected Benzene					Difference				
R	Eelec	Eexch	Eind	Edisp	Etotal	Eelec	Eexch	Eind	Edisp	Etotal	Eelec	Eexch	Eind	Edisp	Etotal
2.0	-289.86	668.73	-21.45	-104.70	252.72	-283.11	640.54	-45.46	-102.34	209.63	-6.75	28.19	24.01	-2.36	43.09
2.4	-93.69	231.73	0.85	-49.84	89.06	-90.51	220.44	-6.78	-49.38	73.77	-3.18	11.29	7.63	-0.46	15.29
2.8	-28.60	77.92	-0.99	-25.21	23.13	-27.44	73.49	-2.78	-25.24	18.03	-1.16	4.43	1.80	0.03	5.10
3.2	-8.01	25.47	-0.78	-13.51	3.17	-7.77	23.81	-1.21	-13.60	1.23	-0.24	1.66	0.43	0.09	1.95
3.4	-3.91	14.40	-0.57	-10.05	-0.13	-3.88	13.40	-0.77	-10.14	-1.38	-0.02	1.00	0.20	0.08	1.26
3.6	-1.66	8.10	-0.40	-7.55	-1.51	-1.76	7.51	-0.48	-7.62	-2.35	0.10	0.59	0.08	0.07	0.84
3.7	-0.97	6.07	-0.33	-6.56	-1.79	-1.11	5.62	-0.38	-6.62	-2.49	0.14	0.45	0.05	0.06	0.70
3.8	-0.47	4.54	-0.28	-5.71	-1.91	-0.63	4.20	-0.30	-5.77	-2.51	0.16	0.35	0.03	0.06	0.59
3.9	-0.12	3.40	-0.23	-4.98	-1.93	-0.29	3.14	-0.24	-5.03	-2.43	0.18	0.26	0.01	0.05	0.51
4.0	0.13	2.55	-0.20	-4.35	-1.87	-0.05	2.34	-0.20	-4.40	-2.30	0.19	0.20	0.00	0.05	0.44
4.2	0.42	1.42	-0.14	-3.34	-1.64	0.23	1.31	-0.14	-3.38	-1.98	0.19	0.11	-0.01	0.04	0.34
4.4	0.53	0.80	-0.10	-2.59	-1.37	0.35	0.73	-0.10	-2.62	-1.63	0.18	0.06	-0.01	0.03	0.27
4.8	0.53	0.24	-0.06	-1.59	-0.87	0.39	0.22	-0.05	-1.61	-1.05	0.15	0.02	-0.01	0.02	0.18
5.2	0.45	0.07	-0.04	-1.00	-0.52	0.33	0.07	-0.03	-1.02	-0.65	0.12	0.00	0.00	0.02	0.13
5.6	0.36	0.02	-0.02	-0.65	-0.30	0.27	0.02	-0.02	-0.67	-0.40	0.09	0.00	0.00	0.01	0.10
6.0	0.28	0.00	-0.01	-0.44	-0.16	0.22	0.00	-0.01	-0.45	-0.24	0.07	0.00	0.00	0.01	0.08

Table A.3: SAPT2 energy components (kcal mol^{-1}) for the interaction of cyclohexane with benzene.

R	Eelec	Eexch	Eind	Edisp	Etotal
2.8	-97.77	273.00	-41.85	-50.00	83.38
3.2	-34.02	93.01	-11.33	-23.94	23.72
3.6	-11.19	30.12	-3.36	-12.19	3.38
3.8	-6.40	16.87	-1.88	-8.91	-0.32
4	-3.67	9.37	-1.07	-6.60	-1.98
4.1	-2.79	6.96	-0.82	-5.71	-2.35
4.2	-2.13	5.16	-0.63	-4.95	-2.53
4.3	-1.62	3.83	-0.48	-4.30	-2.58
4.4	-1.24	2.83	-0.37	-3.75	-2.53
4.5	-0.96	2.09	-0.29	-3.27	-2.43
4.6	-0.74	1.54	-0.23	-2.87	-2.29
4.7	-0.58	1.14	-0.18	-2.52	-2.14
4.8	-0.45	0.83	-0.14	-2.21	-1.98
5	-0.29	0.45	-0.09	-1.73	-1.66
5.2	-0.19	0.24	-0.06	-1.36	-1.37
5.6	-0.10	0.07	-0.03	-0.86	-0.92
6	-0.06	0.02	-0.02	-0.56	-0.62
6.4	-0.04	0.00	-0.01	-0.38	-0.43
6.8	-0.03	0.00	-0.01	-0.26	-0.30

Table A.4: Interaction energies (kcal mol^{-1}) for the sandwich dimer of benzene with benzene and dissected benzene

R	Benzene	Dissected Benzene	Difference
2.0	257.21	176.07	81.14
2.4	96.82	82.67	14.15
2.8	25.01	20.63	4.38
3.2	3.96	2.47	1.49
3.4	0.46	-0.43	0.89
3.6	-1.06	-1.61	0.55
3.7	-1.41	-1.85	0.44
3.8	-1.58	-1.94	0.36
3.9	-1.63	-1.93	0.29
4.0	-1.61	-1.86	0.25
4.2	-1.43	-1.62	0.19
4.4	-1.19	-1.34	0.15
4.8	-0.73	-0.84	0.11
5.2	-0.41	-0.50	0.09
5.6	-0.22	-0.29	0.07
6.0	-0.10	-0.16	0.05

Table A.5: Absolute energies (hartree) and interaction energies (kcal mol^{-1}) for the benzene sandwich dimer.

R	AVTZ dimer	AVTZ monA	AVTZ monB	AVDZ dimer	AVDZ monA	AVDZ monB	CCSD(T) dimer	CCSD(T) monA	CCSD(T) monB	Eint
2.0	-463.155672	-231.750740	-231.750740	-462.733856	-231.554154	-231.554154	-462.822296	-231.630414	-231.630414	257.21
2.4	-463.359112	-231.748576	-231.748576	-462.950025	-231.549302	-231.549302	-463.086312	-231.625570	-231.625570	96.82
2.8	-463.464183	-231.747135	-231.747135	-463.056885	-231.545609	-231.545609	-463.199488	-231.621793	-231.621793	25.01
3.2	-463.491910	-231.746257	-231.746257	-463.083538	-231.542876	-231.542876	-463.229982	-231.618950	-231.618950	3.96
3.4	-463.495564	-231.745966	-231.745966	-463.086421	-231.541899	-231.541899	-463.234119	-231.617932	-231.617932	0.46
3.6	-463.496535	-231.745743	-231.745743	-463.086706	-231.541165	-231.541165	-463.235365	-231.617171	-231.617171	-1.06
3.7	-463.496482	-231.745649	-231.745649	-463.086375	-231.540878	-231.540878	-463.235431	-231.616875	-231.616875	-1.41
3.8	-463.496225	-231.745564	-231.745564	-463.085888	-231.540636	-231.540636	-463.235288	-231.616627	-231.616627	-1.58
3.9	-463.495840	-231.745484	-231.745484	-463.085316	-231.540432	-231.540432	-463.235018	-231.616417	-231.616417	-1.63
4.0	-463.495382	-231.745411	-231.745411	-463.084707	-231.540257	-231.540257	-463.234672	-231.616237	-231.616237	-1.61
4.2	-463.494397	-231.745284	-231.745284	-463.083486	-231.539971	-231.539971	-463.233877	-231.615939	-231.615939	-1.43
4.4	-463.493458	-231.745179	-231.745179	-463.082360	-231.539739	-231.539739	-463.233068	-231.615696	-231.615696	-1.19
4.8	-463.491946	-231.745018	-231.745018	-463.080630	-231.539420	-231.539420	-463.231764	-231.615361	-231.615361	-0.73
5.2	-463.490932	-231.744901	-231.744901	-463.079580	-231.539256	-231.539256	-463.230984	-231.615196	-231.615196	-0.41
5.6	-463.490312	-231.744828	-231.744828	-463.078860	-231.539118	-231.539118	-463.230429	-231.615058	-231.615058	-0.22
6.0	-463.489954	-231.744790	-231.744790	-463.078300	-231.538971	-231.538971	-463.229964	-231.614907	-231.614907	-0.10

Table A.6: Absolute energies (hartree) and interaction energies (kcal mol^{-1}) for the benzene-butadiene dimer.

R	AVTZ dimer	AVTZ monA	AVTZ monB	AVDZ dimer	AVDZ monA	AVDZ monB	CCSD(T) dimer	CCSD(T) monA	CCSD(T) monB	Eint
2.0	-387.144774	-155.621476	-231.749881	-386.790130	-155.484689	-231.551537	-386.903366	-155.554007	-231.627835	162.50
2.4	-387.287177	-155.619986	-231.748015	-386.939789	-155.481147	-231.547593	-387.072804	-155.550496	-231.623867	58.63
2.8	-387.350368	-155.619015	-231.746793	-387.004458	-155.478591	-231.544570	-387.142875	-155.547901	-231.620751	14.13
3.2	-387.366177	-155.618416	-231.746025	-387.019498	-155.476763	-231.542252	-387.160818	-155.546012	-231.618322	1.42
3.4	-387.367893	-155.618210	-231.745769	-387.020638	-155.476118	-231.541401	-387.162855	-155.545342	-231.617429	-0.55
3.6	-387.368046	-155.618050	-231.745571	-387.020284	-155.475631	-231.540762	-387.163175	-155.544838	-231.616763	-1.32
3.7	-387.367823	-155.617983	-231.745487	-387.019859	-155.475440	-231.540515	-387.163023	-155.544641	-231.616507	-1.46
3.8	-387.367495	-155.617922	-231.745410	-387.019363	-155.475278	-231.540308	-387.162766	-155.544474	-231.616293	-1.50
3.9	-387.367106	-155.617867	-231.745341	-387.018838	-155.475141	-231.540133	-387.162451	-155.544333	-231.616112	-1.47
4.0	-387.366690	-155.617817	-231.745277	-387.018312	-155.475023	-231.539984	-387.162106	-155.544212	-231.615959	-1.40
4.2	-387.365860	-155.617730	-231.745167	-387.017311	-155.474831	-231.539742	-387.161398	-155.544014	-231.615706	-1.19
4.4	-387.365108	-155.617660	-231.745078	-387.016425	-155.474678	-231.539548	-387.160732	-155.543855	-231.615504	-0.97
4.8	-387.363938	-155.617549	-231.744948	-387.015095	-155.474466	-231.539282	-387.159695	-155.543634	-231.615225	-0.58
5.2	-387.363175	-155.617468	-231.744860	-387.014287	-155.474349	-231.539139	-387.159072	-155.543515	-231.615081	-0.33
5.6	-387.362714	-155.617419	-231.744805	-387.013735	-155.474250	-231.539020	-387.158633	-155.543417	-231.614962	-0.17
6.0	-387.362445	-155.617392	-231.744774	-387.013317	-155.474151	-231.538900	-387.158281	-155.543317	-231.614838	-0.09

Table A.7: Absolute energies (hartree) and interaction energies (kcal mol^{-1}) for the benzene-ethene dimer.

R	AVTZ dimer	AVTZ monA	AVTZ monB	AVDZ dimer	AVDZ monA	AVDZ monB	CCSD(T) dimer	CCSD(T) monA	CCSD(T) monB	Eint
2.0	-309.997591	-78.403143	-231.748036	-309.714424	-78.331967	-231.546731	-309.819828	-78.372972	-231.622978	103.81
2.4	-310.106189	-78.402359	-231.746795	-309.826550	-78.330133	-231.544176	-309.937230	-78.371167	-231.620374	31.07
2.8	-310.139802	-78.401845	-231.746007	-309.861109	-78.328842	-231.542274	-309.974741	-78.369871	-231.618384	7.25
3.2	-310.148033	-78.401521	-231.745517	-309.868978	-78.327930	-231.540837	-309.984068	-78.368941	-231.616861	0.60
3.4	-310.148880	-78.401406	-231.745351	-309.869526	-78.327613	-231.540303	-309.985051	-78.368615	-231.616297	-0.41
3.6	-310.148909	-78.401317	-231.745220	-309.869290	-78.327375	-231.539899	-309.985138	-78.368370	-231.615871	-0.79
3.7	-310.148769	-78.401279	-231.745165	-309.869046	-78.327282	-231.539742	-309.985025	-78.368275	-231.615707	-0.84
3.8	-310.148576	-78.401247	-231.745114	-309.868769	-78.327204	-231.539611	-309.984862	-78.368195	-231.615571	-0.85
3.9	-310.148354	-78.401218	-231.745069	-309.868482	-78.327140	-231.539503	-309.984676	-78.368129	-231.615459	-0.83
4.0	-310.148121	-78.401192	-231.745028	-309.868199	-78.327085	-231.539412	-309.984480	-78.368073	-231.615366	-0.78
4.2	-310.147663	-78.401149	-231.744961	-309.867670	-78.326997	-231.539271	-309.984094	-78.367983	-231.615221	-0.65
4.4	-310.147254	-78.401115	-231.744908	-309.867207	-78.326926	-231.539163	-309.983738	-78.367909	-231.615109	-0.52
4.8	-310.146628	-78.401064	-231.744834	-309.866491	-78.326812	-231.539009	-309.983164	-78.367789	-231.614949	-0.30
5.2	-310.146227	-78.401027	-231.744787	-309.866028	-78.326730	-231.538914	-309.982786	-78.367705	-231.614852	-0.16
5.6	-310.145986	-78.401001	-231.744758	-309.865725	-78.326671	-231.538841	-309.982536	-78.367645	-231.614778	-0.08
6.0	-310.145844	-78.400985	-231.744739	-309.865509	-78.326625	-231.538773	-309.982352	-78.367599	-231.614707	-0.03

Table A.8: Absolute energies (hartree) and interaction energies (kcal mol^{-1}) for the benzene-cyclohexane dimer.

R	AVTZ dimer	AVTZ monA	AVTZ monB	AVDZ dimer	AVDZ monA	AVDZ monB	CCSD(T) dimer	CCSD(T) monA	CCSD(T) monB	Eint
2.8	-466.960119	-231.751132	-235.349074	-466.530349	-231.553216	-235.127134	-466.700675	-231.629524	-235.235153	96.69
3.2	-467.065085	-231.749029	-235.348212	-466.636855	-231.548863	-235.124932	-466.814271	-231.625206	-235.232953	24.54
3.6	-467.094728	-231.747621	-235.347711	-466.666726	-231.546089	-235.123333	-466.847610	-231.622385	-235.231349	2.53
3.8	-467.098740	-231.747073	-235.347521	-466.670433	-231.544873	-235.122735	-466.852253	-231.621127	-235.230752	-1.06
4	-467.099792	-231.746610	-235.347363	-466.671048	-231.543791	-235.122266	-466.853486	-231.619994	-235.230283	-2.53
4.1	-467.099726	-231.746414	-235.347294	-466.670732	-231.543298	-235.122071	-466.853395	-231.619475	-235.230090	-2.81
4.2	-467.099439	-231.746243	-235.347230	-466.670180	-231.542834	-235.121900	-466.853024	-231.618983	-235.229919	-2.91
4.3	-467.099018	-231.746095	-235.347171	-466.669483	-231.542396	-235.121748	-466.852475	-231.618517	-235.229769	-2.89
4.4	-467.098521	-231.745967	-235.347116	-466.668710	-231.541985	-235.121613	-466.851823	-231.618079	-235.229635	-2.78
4.5	-467.097989	-231.745856	-235.347063	-466.667910	-231.541603	-235.121494	-466.851122	-231.617673	-235.229517	-2.63
4.6	-467.097449	-231.745756	-235.347014	-466.667119	-231.541255	-235.121388	-466.850415	-231.617302	-235.229413	-2.45
4.7	-467.096919	-231.745665	-235.346968	-466.666364	-231.540943	-235.121295	-466.849730	-231.616971	-235.229320	-2.26
4.8	-467.096409	-231.745581	-235.346925	-466.665660	-231.540670	-235.121212	-466.849086	-231.616680	-235.229238	-2.07
5	-467.095483	-231.745430	-235.346850	-466.664433	-231.540233	-235.121072	-466.847959	-231.616219	-235.229100	-1.70
5.2	-467.094699	-231.745305	-235.346788	-466.663446	-231.539923	-235.120963	-466.847052	-231.615894	-235.228991	-1.39
5.6	-467.093524	-231.745106	-235.346700	-466.662039	-231.539537	-235.120805	-466.845763	-231.615494	-235.228834	-0.91
6	-467.092748	-231.744958	-235.346645	-466.661116	-231.539294	-235.120689	-466.844916	-231.615245	-235.228718	-0.60
6.4	-467.092260	-231.744872	-235.346609	-466.660481	-231.539121	-235.120588	-466.844332	-231.615070	-235.228617	-0.41
6.8	-467.091946	-231.744822	-235.346583	-466.660031	-231.538994	-235.120499	-466.843915	-231.614940	-235.228528	-0.28

Table A.9: Interaction energies (kcal mol^{-1}) for Na^+ with benzene and dissected benzene.

R	Benzene	Dissected Benzene	Difference
1.2	140.99	137.33	3.67
1.6	23.10	23.92	-0.82
2.0	-16.16	-12.15	-4.01
2.2	-21.96	-17.10	-4.86
2.3	-23.09	-17.99	-5.11
2.4	-23.46	-18.21	-5.25
2.5	-23.26	-17.96	-5.30
2.6	-22.67	-17.39	-5.28
2.7	-21.83	-16.63	-5.19
2.8	-20.81	-15.76	-5.05
2.9	-19.70	-14.84	-4.87
3.2	-16.28	-12.11	-4.17
3.6	-12.28	-9.11	-3.16
4.0	-9.25	-6.94	-2.31
4.4	-7.05	-5.37	-1.68
4.8	-5.47	-4.24	-1.23
5.2	-4.32	-3.39	-0.93
5.6	-3.46	-2.75	-0.71
6.0	-2.82	-2.26	-0.56
6.4	-2.32	-1.88	-0.44
6.8	-1.94	-1.58	-0.36

Table A.10: Absolute energies (hartree) and interaction energies (kcal mol^{-1}) for the Na^{+}-benzene dimer.

R	AVTZ dimer	AVTZ monA	AVTZ monB	AVDZ dimer	AVDZ monA	AVDZ monB	CCSD(T) dimer	CCSD(T) monA	CCSD(T) monB	Eint
1.2	-393.465367	-231.746669	-161.941574	-393.158786	-231.542573	-161.861588	-393.238202	-231.618647	-161.866743	140.99
1.6	-393.651423	-231.746144	-161.940802	-393.353022	-231.541544	-161.859901	-393.432894	-231.617672	-161.864941	23.10
2.0	-393.712364	-231.745752	-161.940163	-393.419657	-231.541100	-161.858251	-393.500048	-231.617230	-161.863206	-16.16
2.2	-393.721055	-231.745604	-161.939919	-393.429864	-231.540881	-161.857582	-393.510362	-231.616995	-161.862505	-21.96
2.3	-393.722654	-231.745544	-161.939816	-393.431974	-231.540760	-161.857307	-393.512498	-231.616865	-161.862216	-23.09
2.4	-393.723050	-231.745492	-161.939723	-393.432763	-231.540635	-161.857071	-393.513298	-231.616729	-161.861968	-23.46
2.5	-393.722582	-231.745445	-161.939638	-393.432597	-231.540505	-161.856871	-393.513134	-231.616589	-161.861757	-23.26
2.6	-393.721510	-231.745402	-161.939559	-393.431758	-231.540372	-161.856702	-393.512291	-231.616444	-161.861579	-22.67
2.7	-393.720030	-231.745360	-161.939487	-393.430460	-231.540235	-161.856561	-393.510984	-231.616294	-161.861430	-21.83
2.8	-393.718296	-231.745318	-161.939420	-393.428863	-231.540095	-161.856442	-393.509377	-231.616140	-161.861304	-20.81
2.9	-393.716418	-231.745275	-161.939360	-393.427088	-231.539953	-161.856342	-393.507591	-231.615984	-161.861197	-19.70
3.2	-393.710649	-231.745149	-161.939209	-393.421473	-231.539540	-161.856111	-393.501949	-231.615531	-161.860948	-16.28
3.6	-393.703925	-231.744993	-161.939063	-393.414772	-231.539131	-161.855885	-393.495244	-231.615084	-161.860708	-12.28
4.0	-393.698832	-231.744883	-161.938958	-393.409676	-231.538945	-161.855732	-393.490180	-231.614884	-161.860549	-9.25
4.4	-393.695147	-231.744818	-161.938882	-393.405986	-231.538886	-161.855624	-393.486530	-231.614826	-161.860435	-7.05
4.8	-393.692489	-231.744776	-161.938828	-393.403266	-231.538843	-161.855511	-393.483845	-231.614785	-161.860315	-5.47
5.2	-393.690559	-231.744750	-161.938795	-393.401228	-231.538790	-161.855398	-393.481833	-231.614730	-161.860199	-4.32
5.6	-393.689142	-231.744738	-161.938777	-393.399704	-231.538740	-161.855311	-393.480328	-231.614676	-161.860111	-3.46
6.0	-393.688076	-231.744730	-161.938766	-393.398565	-231.538702	-161.855257	-393.479206	-231.614635	-161.860057	-2.82
6.4	-393.687255	-231.744721	-161.938758	-393.397705	-231.538675	-161.855229	-393.478360	-231.614606	-161.860029	-2.32
6.8	-393.686609	-231.744711	-161.938748	-393.397045	-231.538655	-161.855216	-393.477709	-231.614585	-161.860017	-1.94

Table A.11: Absolute energies (hartree) and interaction energies (kcal mol^{-1}) for the Na^{+}-butadiene dimer.

R	AVTZ dimer	AVTZ monA	AVTZ monB	AVDZ dimer	AVDZ monA	AVDZ monB	CCSD(T) dimer	CCSD(T) monA	CCSD(T) monB	Eint
1.2	-317.394144	-155.618574	-161.941304	-317.153633	-155.476437	-161.860851	-317.227532	-155.545664	-161.865950	104.27
1.6	-317.534306	-155.618229	-161.940591	-317.300208	-155.475701	-161.859358	-317.373821	-155.544975	-161.864368	15.80
2.0	-317.579523	-155.618003	-161.939971	-317.349958	-155.475452	-161.857932	-317.423580	-155.544734	-161.862864	-13.15
2.2	-317.585973	-155.617913	-161.939753	-317.357585	-155.475324	-161.857321	-317.431196	-155.544597	-161.862223	-17.41
2.3	-317.587155	-155.617875	-161.939665	-317.359158	-155.475250	-161.857060	-317.432759	-155.544518	-161.861950	-18.23
2.4	-317.587433	-155.617841	-161.939585	-317.359739	-155.475173	-161.856834	-317.433328	-155.544436	-161.861714	-18.48
2.5	-317.587056	-155.617810	-161.939513	-317.359601	-155.475095	-161.856642	-317.433177	-155.544351	-161.861514	-18.31
2.6	-317.586215	-155.617780	-161.939446	-317.358953	-155.475016	-161.856482	-317.432518	-155.544263	-161.861347	-17.85
2.7	-317.585059	-155.617752	-161.939384	-317.357955	-155.474935	-161.856351	-317.431509	-155.544174	-161.861211	-17.18
2.8	-317.583702	-155.617724	-161.939327	-317.356726	-155.474852	-161.856244	-317.430271	-155.544083	-161.861099	-16.38
2.9	-317.582229	-155.617697	-161.939274	-317.355357	-155.474767	-161.856157	-317.428895	-155.543989	-161.861006	-15.52
3.2	-317.577676	-155.617620	-161.939139	-317.350990	-155.474519	-161.855967	-317.424525	-155.543716	-161.860802	-12.81
3.6	-317.572308	-155.617524	-161.939003	-317.345696	-155.474266	-161.855783	-317.419268	-155.543440	-161.860603	-9.64
4.0	-317.568212	-155.617451	-161.938910	-317.341600	-155.474141	-161.855644	-317.415238	-155.543308	-161.860457	-7.22
4.4	-317.565248	-155.617406	-161.938849	-317.338618	-155.474096	-161.855545	-317.412324	-155.543264	-161.860353	-5.47
4.8	-317.563120	-155.617376	-161.938808	-317.336442	-155.474065	-161.855454	-317.410201	-155.543234	-161.860258	-4.22
5.2	-317.561586	-155.617359	-161.938783	-317.334827	-155.474029	-161.855364	-317.408627	-155.543198	-161.860165	-3.31
5.6	-317.560463	-155.617350	-161.938768	-317.333627	-155.473995	-161.855292	-317.407457	-155.543162	-161.860092	-2.64
6.0	-317.559624	-155.617343	-161.938758	-317.332737	-155.473969	-161.855246	-317.406591	-155.543136	-161.860046	-2.14
6.4	-317.558981	-155.617336	-161.938750	-317.332072	-155.473952	-161.855222	-317.405945	-155.543118	-161.860022	-1.76
6.8	-317.558480	-155.617330	-161.938742	-317.331565	-155.473941	-161.855212	-317.405453	-155.543106	-161.860012	-1.46

Table A.12: Absolute energies (hartree) and interaction energies (kcal mol^{-1}) for the Na^+-ethene dimer.

R	AVTZ dimer	AVTZ monA	AVTZ monB	AVDZ dimer	AVDZ monA	AVDZ monB	CCSD(T) dimer	CCSD(T) monA	CCSD(T) monB	Eint
1.2	-240.248903	-78.401596	-161.940459	-240.082910	-78.327749	-161.858992	-240.128817	-78.368724	-161.863984	58.49
1.6	-240.329110	-78.401441	-161.939893	-240.166711	-78.327365	-161.857871	-240.212391	-78.368374	-161.862797	7.83
2.0	-240.355655	-78.401342	-161.939471	-240.195735	-78.327239	-161.856917	-240.241289	-78.368259	-161.861791	-9.10
2.2	-240.359674	-78.401302	-161.939344	-240.200437	-78.327182	-161.856528	-240.245941	-78.368199	-161.861383	-11.71
2.3	-240.360461	-78.401281	-161.939295	-240.201472	-78.327148	-161.856364	-240.246953	-78.368163	-161.861214	-12.24
2.4	-240.360689	-78.401259	-161.939251	-240.201907	-78.327112	-161.856224	-240.247368	-78.368125	-161.861068	-12.41
2.5	-240.360498	-78.401236	-161.939210	-240.201895	-78.327077	-161.856105	-240.247338	-78.368087	-161.860945	-12.33
2.6	-240.360003	-78.401214	-161.939173	-240.201557	-78.327042	-161.856007	-240.246984	-78.368050	-161.860844	-12.05
2.7	-240.359294	-78.401192	-161.939137	-240.200985	-78.327008	-161.855928	-240.246399	-78.368012	-161.860762	-11.63
2.8	-240.358440	-78.401172	-161.939102	-240.200250	-78.326973	-161.855863	-240.245654	-78.367974	-161.860695	-11.13
2.9	-240.357496	-78.401154	-161.939070	-240.199409	-78.326938	-161.855810	-240.244805	-78.367936	-161.860639	-10.57
3.2	-240.354494	-78.401108	-161.938983	-240.196617	-78.326836	-161.855693	-240.242009	-78.367824	-161.860514	-8.78
3.6	-240.350832	-78.401059	-161.938892	-240.193062	-78.326725	-161.855570	-240.238488	-78.367704	-161.860381	-6.60
4.0	-240.347970	-78.401022	-161.938832	-240.190193	-78.326659	-161.855466	-240.235682	-78.367634	-161.860272	-4.91
4.4	-240.345881	-78.400996	-161.938794	-240.188061	-78.326623	-161.855391	-240.233617	-78.367598	-161.860195	-3.68
4.8	-240.344389	-78.400979	-161.938769	-240.186522	-78.326597	-161.855335	-240.232131	-78.367573	-161.860137	-2.81
5.2	-240.343326	-78.400969	-161.938755	-240.185410	-78.326576	-161.855285	-240.231058	-78.367551	-161.860086	-2.18
5.6	-240.342557	-78.400963	-161.938747	-240.184603	-78.326558	-161.855244	-240.230279	-78.367533	-161.860044	-1.72
6.0	-240.341989	-78.400959	-161.938741	-240.184017	-78.326545	-161.855218	-240.229712	-78.367520	-161.860018	-1.39
6.4	-240.341558	-78.400955	-161.938734	-240.183584	-78.326537	-161.855205	-240.229295	-78.367512	-161.860005	-1.13
6.8	-240.341226	-78.400953	-161.938728	-240.183258	-78.326531	-161.855200	-240.228980	-78.367506	-161.860000	-0.94

Table A.13: Interaction energies (kcal mol^{-1}) for Cl^- with benzene and dissected benzene.

R	Benzene	Dissected Benzene	Difference
2.0	96.60	73.42	23.18
2.4	32.22	19.84	12.38
2.8	9.46	3.08	6.39
3.0	4.94	0.31	4.64
3.2	2.60	-0.82	3.42
3.3	1.92	-1.04	2.96
3.4	1.47	-1.10	2.57
3.5	1.18	-1.07	2.25
3.6	1.00	-0.98	1.98
3.7	0.90	-0.85	1.75
3.8	0.86	-0.70	1.56
3.9	0.86	-0.54	1.39
4.0	0.88	-0.38	1.26
4.2	0.95	-0.09	1.04
4.4	1.03	0.15	0.87
4.8	1.14	0.49	0.65
5.2	1.17	0.66	0.51
5.6	1.13	0.72	0.41
6.0	1.06	0.72	0.33
6.4	0.97	0.70	0.28
6.8	0.88	0.65	0.23
7.2	0.80	0.60	0.20
7.6	0.72	0.55	0.17
8.0	0.64	0.49	0.15

Table A.14: Absolute energies (hartree) and interaction energies (kcal mol^{-1}) for the Cl$^-$-benzene dimer.

R	AVTZ dimer	AVTZ monA	AVTZ monB	AVDZ dimer	AVDZ monA	AVDZ monB	CCSD(T) dimer	CCSD(T) monA	CCSD(T) monB	Eint
2.0	-691.388000	-231.746095	-459.784778	-691.117079	-231.542736	-459.729617	-691.199145	-231.618866	-459.746621	96.60
2.4	-691.483341	-231.745636	-459.783118	-691.217106	-231.541366	-459.726761	-691.303670	-231.617459	-459.743166	32.22
2.8	-691.515488	-231.745326	-459.782198	-691.250613	-231.540287	-459.724891	-691.339581	-231.616320	-459.740873	9.46
3.0	-691.521403	-231.745216	-459.781912	-691.256607	-231.539832	-459.724303	-691.346309	-231.615832	-459.740153	4.94
3.2	-691.524177	-231.745122	-459.781688	-691.259348	-231.539453	-459.723895	-691.349577	-231.615424	-459.739657	2.60
3.3	-691.524863	-231.745079	-459.781593	-691.260012	-231.539297	-459.723745	-691.350448	-231.615256	-459.739475	1.92
3.4	-691.525249	-231.745039	-459.781509	-691.260389	-231.539167	-459.723623	-691.351002	-231.615115	-459.739330	1.47
3.5	-691.525424	-231.745001	-459.781433	-691.260573	-231.539062	-459.723525	-691.351337	-231.615003	-459.739214	1.18
3.6	-691.525454	-231.744965	-459.781366	-691.260635	-231.538982	-459.723447	-691.351527	-231.614917	-459.739122	1.00
3.7	-691.525389	-231.744931	-459.781307	-691.260621	-231.538924	-459.723385	-691.351624	-231.614855	-459.739049	0.90
3.8	-691.525265	-231.744899	-459.781253	-691.260564	-231.538885	-459.723333	-691.351662	-231.614814	-459.738988	0.86
3.9	-691.525108	-231.744870	-459.781206	-691.260485	-231.538858	-459.723289	-691.351663	-231.614787	-459.738937	0.86
4.0	-691.524935	-231.744843	-459.781164	-691.260395	-231.538841	-459.723251	-691.351641	-231.614771	-459.738892	0.88
4.2	-691.524593	-231.744800	-459.781092	-691.260208	-231.538819	-459.723183	-691.351556	-231.614751	-459.738811	0.95
4.4	-691.524299	-231.744769	-459.781035	-691.260033	-231.538798	-459.723123	-691.351449	-231.614732	-459.738739	1.03
4.8	-691.523918	-231.744736	-459.780955	-691.259774	-231.538752	-459.723025	-691.351260	-231.614686	-459.738620	1.14
5.2	-691.523774	-231.744722	-459.780907	-691.259663	-231.538712	-459.722954	-691.351173	-231.614645	-459.738534	1.17
5.6	-691.523773	-231.744713	-459.780875	-691.259666	-231.538683	-459.722902	-691.351182	-231.614613	-459.738471	1.13
6.0	-691.523847	-231.744705	-459.780852	-691.259736	-231.538658	-459.722863	-691.351250	-231.614587	-459.738424	1.06
6.4	-691.523957	-231.744699	-459.780834	-691.259839	-231.538639	-459.722833	-691.351347	-231.614566	-459.738387	0.97
6.8	-691.524081	-231.744694	-459.780822	-691.259956	-231.538624	-459.722810	-691.351458	-231.614550	-459.738358	0.88
7.2	-691.524207	-231.744690	-459.780812	-691.260076	-231.538613	-459.722793	-691.351573	-231.614539	-459.738338	0.80
7.6	-691.524327	-231.744687	-459.780806	-691.260194	-231.538606	-459.722782	-691.351686	-231.614532	-459.738324	0.72
8.0	-691.524438	-231.744686	-459.780801	-691.260305	-231.538601	-459.722775	-691.351794	-231.614527	-459.738315	0.64

Table A.15: Absolute energies (hartree) and interaction energies (kcal mol^{-1}) for the Cl^{-}-butadiene dimer.

R	AVTZ dimer	AVTZ monA	AVTZ monB	AVDZ dimer	AVDZ monA	AVDZ monB	CCSD(T) dimer	CCSD(T) monA	CCSD(T) monB	Eint
2.0	-615.312799	-155.618235	-459.784154	-615.105371	-155.476630	-459.728425	-615.183126	-155.545913	-459.745211	61.44
2.4	-615.374001	-155.617925	-459.782739	-615.170708	-155.475724	-459.726155	-615.252118	-155.544987	-459.742442	19.33
2.8	-615.393694	-155.617722	-459.781953	-615.191685	-155.475033	-459.724623	-615.274866	-155.544256	-459.740553	4.99
3.0	-615.397083	-155.617653	-459.781712	-615.195187	-155.474740	-459.724120	-615.278866	-155.543942	-459.739936	2.27
3.2	-615.398527	-155.617597	-459.781526	-615.196626	-155.474492	-459.723759	-615.280646	-155.543677	-459.739494	0.94
3.3	-615.398821	-155.617572	-459.781448	-615.196907	-155.474389	-459.723621	-615.281057	-155.543567	-459.739328	0.58
3.4	-615.398937	-155.617547	-459.781378	-615.197015	-155.474302	-459.723509	-615.281273	-155.543474	-459.739192	0.37
3.5	-615.398929	-155.617523	-459.781316	-615.197011	-155.474231	-459.723417	-615.281361	-155.543398	-459.739082	0.25
3.6	-615.398840	-155.617500	-459.781260	-615.196939	-155.474175	-459.723344	-615.281367	-155.543340	-459.738995	0.19
3.7	-615.398700	-155.617477	-459.781211	-615.196832	-155.474134	-459.723285	-615.281325	-155.543297	-459.738925	0.19
3.8	-615.398531	-155.617456	-459.781167	-615.196708	-155.474104	-459.723237	-615.281256	-155.543267	-459.738869	0.21
3.9	-615.398351	-155.617436	-459.781128	-615.196580	-155.474084	-459.723198	-615.281176	-155.543247	-459.738823	0.25
4.0	-615.398170	-155.617418	-459.781094	-615.196455	-155.474070	-459.723165	-615.281090	-155.543234	-459.738784	0.31
4.2	-615.397833	-155.617390	-459.781035	-615.196226	-155.474052	-459.723110	-615.280921	-155.543217	-459.738720	0.42
4.4	-615.397553	-155.617370	-459.780989	-615.196032	-155.474036	-459.723064	-615.280764	-155.543202	-459.738665	0.53
4.8	-615.397183	-155.617350	-459.780924	-615.195752	-155.474003	-459.722987	-615.280518	-155.543170	-459.738573	0.68
5.2	-615.397018	-155.617339	-459.780886	-615.195608	-155.473976	-459.722927	-615.280381	-155.543142	-459.738501	0.74
5.6	-615.396977	-155.617332	-459.780861	-615.195565	-155.473956	-459.722882	-615.280334	-155.543122	-459.738446	0.74
6.0	-615.397003	-155.617327	-459.780842	-615.195584	-155.473942	-459.722848	-615.280346	-155.543107	-459.738405	0.71
6.4	-615.397063	-155.617323	-459.780828	-615.195637	-155.473931	-459.722822	-615.280391	-155.543096	-459.738373	0.66
6.8	-615.397140	-155.617321	-459.780817	-615.195707	-155.473923	-459.722803	-615.280454	-155.543087	-459.738350	0.60
7.2	-615.397221	-155.617319	-459.780809	-615.195783	-155.473917	-459.722790	-615.280525	-155.543082	-459.738333	0.55
7.6	-615.397300	-155.617318	-459.780804	-615.195861	-155.473913	-459.722780	-615.280597	-155.543078	-459.738322	0.50
8.0	-615.397375	-155.617317	-459.780800	-615.195935	-155.473911	-459.722774	-615.280667	-155.543075	-459.738314	0.45

Table A.16: Absolute energies (hartree) and interaction energies (kcal mol^{-1}) for the Cl$^-$-ethene dimer.

R	AVTZ dimer	AVTZ monA	AVTZ monB	AVDZ dimer	AVDZ monA	AVDZ monB	CCSD(T) dimer	CCSD(T) monA	CCSD(T) monB	Eint
2.0	-538.128989	-78.401433	-459.782904	-537.992289	-78.327806	-459.726089	-538.046057	-78.368819	-459.742400	36.96
2.4	-538.164584	-78.401268	-459.781999	-538.030623	-78.327386	-459.724772	-538.086056	-78.368399	-459.740772	12.72
2.8	-538.176994	-78.401153	-459.781491	-538.044044	-78.327067	-459.723901	-538.100161	-78.368065	-459.739688	3.96
3.0	-538.179409	-78.401113	-459.781335	-538.046617	-78.326933	-459.723608	-538.102904	-78.367922	-459.739325	2.17
3.2	-538.180623	-78.401083	-459.781219	-538.047887	-78.326820	-459.723390	-538.104282	-78.367802	-459.739057	1.21
3.3	-538.180955	-78.401070	-459.781172	-538.048229	-78.326772	-459.723304	-538.104662	-78.367751	-459.738953	0.93
3.4	-538.181165	-78.401058	-459.781131	-538.048446	-78.326731	-459.723232	-538.104910	-78.367708	-459.738866	0.73
3.5	-538.181287	-78.401047	-459.781095	-538.048575	-78.326697	-459.723173	-538.105064	-78.367673	-459.738794	0.60
3.6	-538.181346	-78.401036	-459.781064	-538.048646	-78.326670	-459.723125	-538.105156	-78.367645	-459.738735	0.52
3.7	-538.181361	-78.401025	-459.781036	-538.048679	-78.326650	-459.723085	-538.105206	-78.367623	-459.738688	0.47
3.8	-538.181347	-78.401014	-459.781011	-538.048688	-78.326634	-459.723053	-538.105229	-78.367608	-459.738650	0.44
3.9	-538.181315	-78.401005	-459.780989	-538.048683	-78.326623	-459.723027	-538.105236	-78.367596	-459.738619	0.43
4.0	-538.181273	-78.400996	-459.780969	-538.048669	-78.326614	-459.723006	-538.105232	-78.367587	-459.738593	0.43
4.2	-538.181177	-78.400983	-459.780936	-538.048632	-78.326600	-459.722971	-538.105208	-78.367574	-459.738553	0.45
4.4	-538.181090	-78.400974	-459.780908	-538.048592	-78.326588	-459.722943	-538.105176	-78.367563	-459.738520	0.48
4.8	-538.180975	-78.400964	-459.780869	-538.048532	-78.326566	-459.722898	-538.105116	-78.367541	-459.738466	0.51
5.2	-538.180938	-78.400958	-459.780845	-538.048511	-78.326550	-459.722863	-538.105087	-78.367525	-459.738423	0.52
5.6	-538.180953	-78.400954	-459.780830	-538.048523	-78.326539	-459.722835	-538.105091	-78.367514	-459.738389	0.50
6.0	-538.180995	-78.400951	-459.780819	-538.048558	-78.326531	-459.722813	-538.105117	-78.367506	-459.738362	0.46
6.4	-538.181050	-78.400950	-459.780811	-538.048604	-78.326525	-459.722797	-538.105156	-78.367500	-459.738342	0.43
6.8	-538.181109	-78.400949	-459.780805	-538.048656	-78.326521	-459.722785	-538.105201	-78.367496	-459.738327	0.39
7.2	-538.181167	-78.400948	-459.780801	-538.048709	-78.326518	-459.722776	-538.105249	-78.367493	-459.738317	0.35
7.6	-538.181222	-78.400947	-459.780798	-538.048761	-78.326516	-459.722772	-538.105298	-78.367491	-459.738311	0.31
8.0	-538.181272	-78.400947	-459.780796	-538.048811	-78.326515	-459.722769	-538.105345	-78.367490	-459.738307	0.28

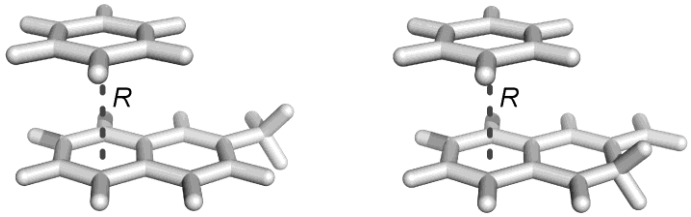

Table A.17: SCS-MP2/AVTZ absolute energies (hartree) and interaction energies (kcal mol^{-1}) for the interaction of benzene with isomers 1 and 2.

	2-methylnaphthalene (**1**)				2-methylene-2,3-dihydronaphthalene (**2**)				
R	Dimer	Monomer	Benzene	Eint	Dimer	Monomer	Benzene	Eint	Difference
2.0	-655.544019	-424.250448	-231.724892	270.66	-655.501716	-424.145614	-231.724938	231.45	39.21
2.4	-655.824154	-424.246717	-231.721673	90.51	-655.739011	-424.141866	-231.721723	78.17	12.34
2.8	-655.931519	-424.244759	-231.719927	20.81	-655.831810	-424.139901	-231.719970	17.61	3.20
3.2	-655.960656	-424.243822	-231.719014	1.37	-655.857260	-424.138962	-231.719042	0.47	0.90
3.3	-655.963140	-424.243654	-231.718840	-0.41	-655.859365	-424.138794	-231.718866	-1.07	0.66
3.4	-655.964653	-424.243501	-231.718682	-1.55	-655.860605	-424.138642	-231.718704	-2.05	0.50
3.5	-655.965474	-424.243361	-231.718538	-2.24	-655.861231	-424.138502	-231.718557	-2.62	0.37
3.6	-655.965812	-424.243231	-231.718406	-2.62	-655.861428	-424.138373	-231.718423	-2.91	0.29
3.7	-655.965818	-424.243112	-231.718286	-2.77	-655.861333	-424.138253	-231.718301	-3.00	0.22
3.8	-655.965605	-424.243000	-231.718176	-2.78	-655.861047	-424.138143	-231.718189	-2.96	0.18
3.9	-655.965254	-424.242897	-231.718075	-2.69	-655.860643	-424.138040	-231.718086	-2.83	0.15
4.0	-655.964822	-424.242801	-231.717982	-2.53	-655.860174	-424.137944	-231.717992	-2.66	0.12
4.4	-655.962952	-424.242491	-231.717688	-1.74	-655.858230	-424.137635	-231.717694	-1.82	0.08
4.8	-655.961487	-424.242292	-231.717500	-1.06	-655.856738	-424.137436	-231.717504	-1.13	0.07
5.2	-655.960560	-424.242183	-231.717397	-0.62	-655.855794	-424.137326	-231.717399	-0.67	0.06
5.6	-655.960019	-424.242127	-231.717343	-0.34	-655.855239	-424.137270	-231.717344	-0.39	0.05
6.0	-655.959706	-424.242098	-231.717312	-0.19	-655.854915	-424.137240	-231.717313	-0.23	0.04

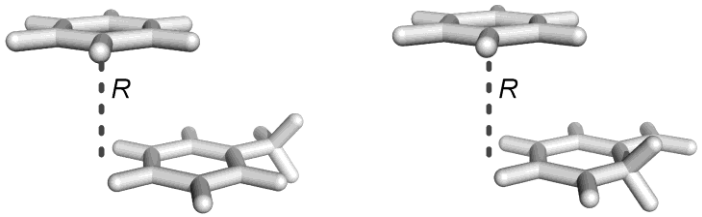

Table A.18: SCS-MP2/AVTZ absolute energies (hartree) and interaction energies (kcal mol^{-1}) for the interaction of benzene with toluene and 2-methylene-2,3-dihydrobenzene.

	Toluene				2-methylene-2,3-dihydrobenzene				
R	Dimer	Monomer	Benzene	Eint	Dimer	Monomer	Benzene	Eint	Difference
2.0	-502.494142	-270.945143	-231.721509	108.25	-502.432146	-270.861853	-231.721559	94.92	13.33
2.4	-502.615014	-270.943398	-231.719766	30.21	-502.535515	-270.860103	-231.719817	27.86	2.35
2.8	-502.652652	-270.942455	-231.718826	5.41	-502.569764	-270.859159	-231.718868	5.19	0.23
3.2	-502.661819	-270.941925	-231.718294	-1.00	-502.578454	-270.858633	-231.718322	-0.94	-0.06
3.3	-502.662409	-270.941824	-231.718192	-1.50	-502.579041	-270.858533	-231.718217	-1.44	-0.06
3.4	-502.662668	-270.941732	-231.718099	-1.78	-502.579311	-270.858442	-231.718121	-1.72	-0.06
3.5	-502.662697	-270.941648	-231.718013	-1.90	-502.579360	-270.858359	-231.718033	-1.86	-0.04
3.6	-502.662573	-270.941572	-231.717935	-1.92	-502.579258	-270.858283	-231.717953	-1.90	-0.03
3.7	-502.662350	-270.941501	-231.717864	-1.87	-502.579057	-270.858214	-231.717879	-1.86	-0.01
3.8	-502.662068	-270.941436	-231.717798	-1.78	-502.578796	-270.858150	-231.717812	-1.78	0.00
3.9	-502.661756	-270.941377	-231.717738	-1.66	-502.578501	-270.858091	-231.717750	-1.67	0.01
4.0	-502.661433	-270.941323	-231.717683	-1.52	-502.578193	-270.858037	-231.717694	-1.55	0.02
4.4	-502.660247	-270.941151	-231.717510	-0.99	-502.577043	-270.857865	-231.717517	-1.04	0.05
4.8	-502.659405	-270.941044	-231.717403	-0.60	-502.576208	-270.857758	-231.717407	-0.65	0.05
5.2	-502.658886	-270.940985	-231.717345	-0.35	-502.575683	-270.857698	-231.717347	-0.40	0.05
5.6	-502.658582	-270.940953	-231.717314	-0.20	-502.575369	-270.857666	-231.717315	-0.24	0.05
6.0	-502.658404	-270.940934	-231.717297	-0.11	-502.575181	-270.857647	-231.717298	-0.15	0.04

The geometries in the above complexes are such that distances between all conserved atoms are identical to those in the complexes of benzene with isomers **1** and **2** on the previous page. Note that at the equilibrium distance of the dimers of benzene with isomers **1** and **2**, there is essentially no difference between the interaction of benzene with the methyl-substituted and methylene-substituted rings.

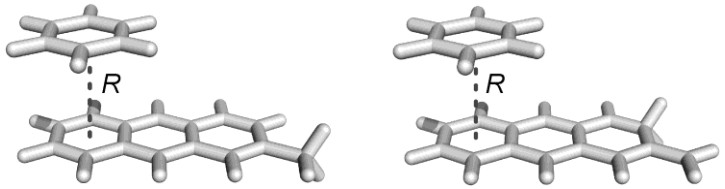

Table A.19: SCS-MP2/AVTZ absolute energies (hartree) and interaction energies (kcal mol^{-1}) for the interaction of benzene with 2-methylanthracene and 2-methylene-2,3-dihydroanthracene.

	2-methylanthracene				2-methylene-2,3-dihydroanthracene				
R	Dimer	Monomer	Benzene	Eint	Dimer	Monomer	Benzene	Eint	Difference
2.0	-808.850954	-577.542317	-231.724940	261.23	-808.775290	-577.426301	-231.724945	235.92	25.32
2.4	-809.122794	-577.538564	-231.721717	86.27	-809.018005	-577.422537	-231.721723	79.23	7.05
2.8	-809.225681	-577.536592	-231.719970	19.38	-809.112438	-577.420561	-231.719975	17.63	1.75
3.2	-809.253609	-577.535642	-231.719048	0.68	-809.138318	-577.419612	-231.719052	0.22	0.46
3.3	-809.255943	-577.535471	-231.718872	-1.00	-809.140445	-577.419441	-231.718875	-1.34	0.33
3.4	-809.257338	-577.535315	-231.718711	-2.08	-809.141690	-577.419285	-231.718714	-2.32	0.24
3.5	-809.258064	-577.535172	-231.718564	-2.72	-809.142308	-577.419143	-231.718566	-2.89	0.17
3.6	-809.258323	-577.535040	-231.718429	-3.05	-809.142489	-577.419011	-231.718432	-3.17	0.12
3.7	-809.258263	-577.534918	-231.718307	-3.16	-809.142374	-577.418890	-231.718309	-3.25	0.09
3.8	-809.257994	-577.534805	-231.718195	-3.13	-809.142065	-577.418777	-231.718196	-3.20	0.06
3.9	-809.257594	-577.534700	-231.718092	-3.01	-809.141636	-577.418672	-231.718093	-3.06	0.04
4.0	-809.257121	-577.534602	-231.717997	-2.84	-809.141142	-577.418575	-231.717999	-2.87	0.03
4.4	-809.255121	-577.534288	-231.717697	-1.97	-809.139103	-577.418261	-231.717698	-1.97	0.01
4.8	-809.253564	-577.534085	-231.717506	-1.24	-809.137537	-577.418058	-231.717507	-1.24	0.00
5.2	-809.252568	-577.533974	-231.717400	-0.75	-809.136537	-577.417946	-231.717400	-0.75	0.00
5.6	-809.251973	-577.533917	-231.717344	-0.45	-809.135943	-577.417889	-231.717344	-0.45	0.00
6.0	-809.251620	-577.533887	-231.717313	-0.26	-809.135591	-577.417858	-231.717313	-0.26	0.00

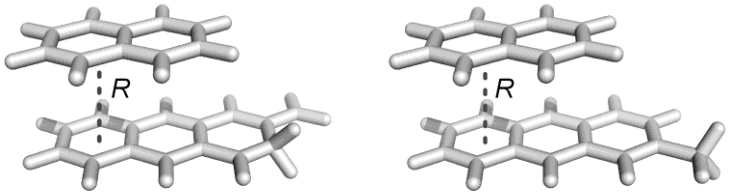

Table A.20: SCS-MP2/AVTZ absolute energies (hartree) and interaction energies (kcal mol^{-1}) for the interaction of naphthalene with 2-methylanthracene and 2-methylene-2,3-dihydroanthracene.

	2-Methylanthracene				2-Methylene-2,3-dihydroanthracene				
R	Dimer	Monomer	Naphthalene	Eint	Dimer	Monomer	Naphthalene	Eint	Difference
2.0	-961.991406	-577.547219	-385.027063	365.76	-961.907743	-577.431220	-385.027108	345.50	20.26
2.4	-962.331428	-577.541364	-385.021729	145.37	-962.257749	-577.425350	-385.021778	118.84	26.54
2.8	-962.505958	-577.538340	-385.018924	32.19	-962.396027	-577.422318	-385.018968	28.40	3.79
3.2	-962.553518	-577.536853	-385.017461	0.50	-962.439104	-577.420827	-385.017491	-0.49	0.99
3.3	-962.557435	-577.536576	-385.017180	-2.31	-962.442581	-577.420550	-385.017206	-3.03	0.72
3.4	-962.559745	-577.536321	-385.016921	-4.08	-962.444569	-577.420295	-385.016944	-4.60	0.52
3.5	-962.560915	-577.536084	-385.016681	-5.11	-962.445516	-577.420058	-385.016701	-5.49	0.38
3.6	-962.561289	-577.535864	-385.016460	-5.63	-962.445731	-577.419838	-385.016477	-5.91	0.28
3.7	-962.561124	-577.535659	-385.016255	-5.78	-962.445453	-577.419633	-385.016270	-5.99	0.21
3.8	-962.560606	-577.535467	-385.016065	-5.69	-962.444854	-577.419441	-385.016078	-5.86	0.16
3.9	-962.559870	-577.535288	-385.015889	-5.45	-962.444061	-577.419263	-385.015901	-5.58	0.13
4.0	-962.559013	-577.535122	-385.015727	-5.12	-962.443164	-577.419097	-385.015737	-5.23	0.10
4.4	-962.555462	-577.534587	-385.015209	-3.56	-962.439538	-577.418562	-385.015215	-3.61	0.06
4.8	-962.552722	-577.534244	-385.014878	-2.26	-962.436773	-577.418217	-385.014881	-2.31	0.05
5.2	-962.550961	-577.534054	-385.014692	-1.39	-962.434999	-577.418026	-385.014694	-1.43	0.04
5.6	-962.549902	-577.533957	-385.014597	-0.85	-962.433930	-577.417930	-385.014598	-0.88	0.03
6.0	-962.549269	-577.533907	-385.014544	-0.51	-962.433288	-577.417878	-385.014545	-0.54	0.03

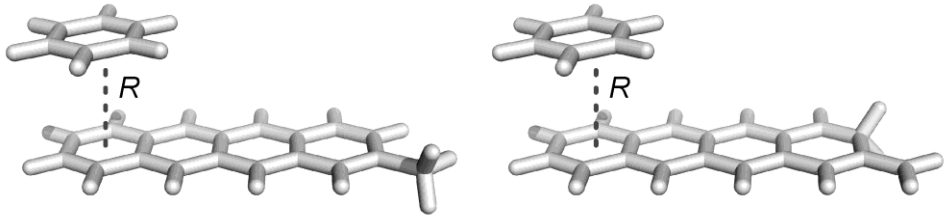

Table A.21: SCS-MP2/AVTZ absolute energies (hartree) and interaction energies (kcal mol^{-1}) for the interaction of benzene with 2-methyltetracene and 2-methylene-2,3-dihydrotetracene.

	2-methyltetracene				2-methylene-2,3-dihydrotetracene				
R	Dimer	Monomer	Benzene	Eint	Dimer	Monomer	Benzene	Eint	Difference
2.0	-962.146780	-730.829820	-231.724951	256.02	-962.049769	-730.709409	-231.724953	241.34	14.68
2.4	-962.413929	-730.826061	-231.721728	84.00	-962.299530	-730.705647	-231.721729	80.22	3.77
2.8	-962.514217	-730.824084	-231.719981	18.73	-962.395271	-730.703671	-231.719982	17.81	0.92
3.2	-962.541512	-730.823131	-231.719056	0.42	-962.421479	-730.702720	-231.719058	0.19	0.24
3.3	-962.543779	-730.822959	-231.718880	-1.22	-962.423636	-730.702548	-231.718881	-1.38	0.17
3.4	-962.545124	-730.822803	-231.718718	-2.26	-962.424900	-730.702392	-231.718719	-2.38	0.12
3.5	-962.545812	-730.822659	-231.718570	-2.88	-962.425530	-730.702249	-231.718571	-2.96	0.08
3.6	-962.546042	-730.822527	-231.718435	-3.19	-962.425718	-730.702118	-231.718436	-3.24	0.05
3.7	-962.545960	-730.822405	-231.718312	-3.29	-962.425606	-730.701996	-231.718313	-3.32	0.03
3.8	-962.545673	-730.822291	-231.718199	-3.25	-962.425297	-730.701883	-231.718200	-3.27	0.02
3.9	-962.545259	-730.822186	-231.718096	-3.12	-962.424867	-730.701778	-231.718096	-3.13	0.01
4.0	-962.544773	-730.822089	-231.718001	-2.94	-962.424369	-730.701680	-231.718002	-2.94	0.00
4.4	-962.542742	-730.821773	-231.717700	-2.05	-962.422314	-730.701366	-231.717700	-2.04	-0.01
4.8	-962.541162	-730.821570	-231.717508	-1.31	-962.420728	-730.701163	-231.717508	-1.29	-0.02
5.2	-962.540147	-730.821458	-231.717401	-0.81	-962.419712	-730.701050	-231.717401	-0.79	-0.02
5.6	-962.539537	-730.821401	-231.717345	-0.50	-962.419102	-730.700993	-231.717345	-0.48	-0.02
6.0	-962.539171	-730.821371	-231.717313	-0.31	-962.418738	-730.700963	-231.717313	-0.29	-0.02

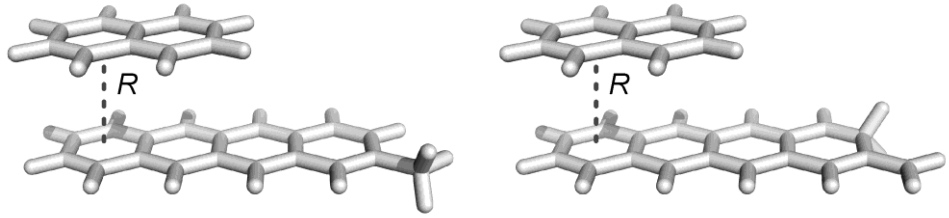

Table A.22: SCS-MP2/AVTZ absolute energies (hartree) and interaction energies (kcal mol^{-1}) for the interaction of naphthalene with isomers 2-methyltetracene and 2-methylene-2,3-dihydrotetracene.

	2-methyltetracene				2-methylene-2,3-dihydrotetracene				
R	Dimer	Monomer	Naphthalene	Eint	Dimer	Monomer	Naphthalene	Eint	Difference
2.0	-1115.274575	-730.834795	-385.027113	368.56	-1115.184765	-730.714381	-385.027120	349.36	19.20
2.4	-1115.632403	-730.828918	-385.021775	136.98	-1115.538825	-730.708501	-385.021781	120.14	16.84
2.8	-1115.796143	-730.825878	-385.018969	30.56	-1115.678934	-730.705462	-385.018974	28.55	2.01
3.2	-1115.842317	-730.824375	-385.017496	-0.28	-1115.722652	-730.703963	-385.017500	-0.75	0.47
3.3	-1115.846066	-730.824094	-385.017211	-2.99	-1115.726164	-730.703683	-385.017215	-3.30	0.32
3.4	-1115.848244	-730.823836	-385.016949	-4.68	-1115.728173	-730.703425	-385.016952	-4.89	0.21
3.5	-1115.849307	-730.823596	-385.016707	-5.65	-1115.729116	-730.703186	-385.016710	-5.79	0.14
3.6	-1115.849594	-730.823373	-385.016483	-6.11	-1115.729317	-730.702964	-385.016486	-6.19	0.08
3.7	-1115.849355	-730.823165	-385.016276	-6.22	-1115.729018	-730.702756	-385.016278	-6.27	0.04
3.8	-1115.848774	-730.822970	-385.016084	-6.10	-1115.728395	-730.702562	-385.016086	-6.12	0.02
3.9	-1115.847984	-730.822789	-385.015906	-5.83	-1115.727575	-730.702382	-385.015908	-5.83	0.00
4.0	-1115.847083	-730.822622	-385.015743	-5.47	-1115.726650	-730.702214	-385.015744	-5.45	-0.02
4.4	-1115.843387	-730.822081	-385.015219	-3.82	-1115.722920	-730.701674	-385.015220	-3.78	-0.04
4.8	-1115.840544	-730.821733	-385.014884	-2.46	-1115.720074	-730.701326	-385.014884	-2.42	-0.04
5.2	-1115.838705	-730.821540	-385.014696	-1.55	-1115.718239	-730.701133	-385.014696	-1.51	-0.04
5.6	-1115.837587	-730.821443	-385.014599	-0.97	-1115.717126	-730.701035	-385.014599	-0.94	-0.03
6.0	-1115.836908	-730.821391	-385.014545	-0.61	-1115.716453	-730.700983	-385.014545	-0.58	-0.03

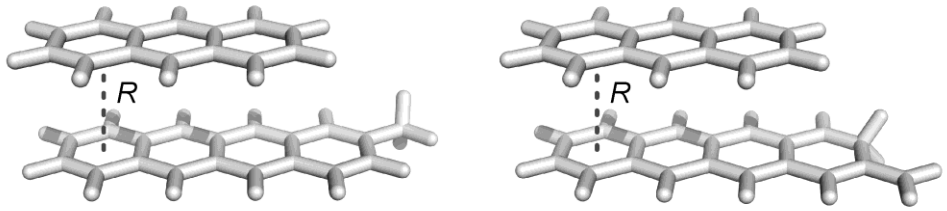

Table A.23: SCS-MP2/AVTZ absolute energies (hartree) and interaction energies (kcal mol^{-1}) for the interaction of anthracene with isomers 2-methyltetracene and 2-methylene-2,3-dihydrotetracene.

	2-methyltetracene				2-methylene-2,3-dihydrotetracene				
R	Dimer	Monomer	Anthracene	Eint	Dimer	Monomer	Anthracene	Eint	Difference
2.0	-1268.385658	-730.839707	-538.323469	487.90	-1268.238606	-730.719292	-538.323513	504.64	-16.74
2.4	-1268.901018	-730.831729	-538.316017	154.82	-1268.817574	-730.711312	-538.316065	131.65	23.17
2.8	-1269.071303	-730.827642	-538.312150	42.98	-1268.955414	-730.707229	-538.312194	40.17	2.81
3.2	-1269.136972	-730.825601	-538.310135	-0.77	-1269.017660	-730.705192	-538.310166	-1.44	0.67
3.3	-1269.142259	-730.825213	-538.309744	-4.58	-1269.022582	-730.704805	-538.309771	-5.02	0.44
3.4	-1269.145312	-730.824854	-538.309383	-6.95	-1269.025386	-730.704447	-538.309406	-7.24	0.29
3.5	-1269.146780	-730.824520	-538.309047	-8.29	-1269.026695	-730.704114	-538.309067	-8.48	0.19
3.6	-1269.147148	-730.824207	-538.308734	-8.92	-1269.026938	-730.703802	-538.308752	-9.03	0.11
3.7	-1269.146772	-730.823914	-538.308443	-9.05	-1269.026476	-730.703509	-538.308458	-9.10	0.06
3.8	-1269.145914	-730.823640	-538.308173	-8.85	-1269.025560	-730.703236	-538.308186	-8.87	0.02
3.9	-1269.144768	-730.823385	-538.307922	-8.45	-1269.024371	-730.702981	-538.307934	-8.44	0.00
4.0	-1269.143459	-730.823148	-538.307691	-7.92	-1269.023037	-730.702745	-538.307701	-7.90	-0.02
4.4	-1269.138146	-730.822386	-538.306950	-5.53	-1269.017693	-730.701982	-538.306956	-5.49	-0.04
4.8	-1269.134076	-730.821896	-538.306475	-3.58	-1269.013626	-730.701491	-538.306478	-3.55	-0.03
5.2	-1269.131440	-730.821623	-538.306208	-2.26	-1269.010998	-730.701218	-538.306210	-2.24	-0.02
5.6	-1269.129832	-730.821485	-538.306070	-1.43	-1269.009395	-730.701078	-538.306071	-1.41	-0.02
6.0	-1269.128853	-730.821412	-538.305996	-0.91	-1269.008420	-730.701004	-538.305997	-0.89	-0.02

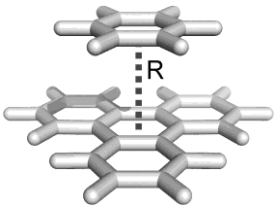

Table A.24: SCS-MP2/AVTZ absolute energies (hartree) and interaction energies (kcal mol^{-1}) for the interaction of benzene with triphenylene.

R	Dimer	Monomer	Benzene	Eint
2.0	-922.933615	-691.626102	-231.725981	262.59
2.4	-923.221509	-691.621204	-231.722649	76.77
2.8	-923.319875	-691.618671	-231.720832	12.32
3.2	-923.343398	-691.617375	-231.719713	-3.96
3.3	-923.344780	-691.617128	-231.719486	-5.12
3.4	-923.345297	-691.616897	-231.719276	-5.73
3.5	-923.345224	-691.616682	-231.719084	-5.93
3.6	-923.344759	-691.616481	-231.718908	-5.88
3.7	-923.344051	-691.616292	-231.718748	-5.65
3.8	-923.343203	-691.616117	-231.718602	-5.32
3.9	-923.342289	-691.615953	-231.718469	-4.94
4.0	-923.341362	-691.615803	-231.718349	-4.52
4.4	-923.338037	-691.615319	-231.717974	-2.98
4.8	-923.335701	-691.615011	-231.717741	-1.85
5.2	-923.334244	-691.614840	-231.717608	-1.13
5.6	-923.333374	-691.614754	-231.717536	-0.68
6.0	-923.332858	-691.614712	-231.717495	-0.41

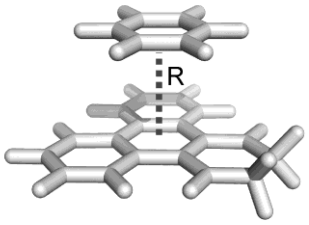

Table A.25: SCS-MP2/AVTZ absolute energies (hartree) and interaction energies (kcal mol^{-1}) for the interaction of benzene with 2,3-dihydrotriphenylene.

R	Dimer	Monomer	Benzene	Eint
2.0	-924.073568	-692.737221	-231.726101	244.57
2.4	-924.344959	-692.732346	-231.722763	69.12
2.8	-924.434007	-692.729826	-231.720926	10.51
3.2	-924.454936	-692.728537	-231.719775	-4.16
3.3	-924.456075	-692.728292	-231.719540	-5.17
3.4	-924.456430	-692.728064	-231.719323	-5.67
3.5	-924.456252	-692.727852	-231.719125	-5.82
3.6	-924.455724	-692.727654	-231.718943	-5.73
3.7	-924.454981	-692.727468	-231.718778	-5.48
3.8	-924.454117	-692.727295	-231.718628	-5.14
3.9	-924.453200	-692.727134	-231.718491	-4.75
4.0	-924.452279	-692.726984	-231.718368	-4.35
4.4	-924.449012	-692.726506	-231.717984	-2.84
4.8	-924.446737	-692.726199	-231.717746	-1.75
5.2	-924.445326	-692.726029	-231.717612	-1.06
5.6	-924.444489	-692.725943	-231.717538	-0.63
6.0	-924.443995	-692.725900	-231.717496	-0.38

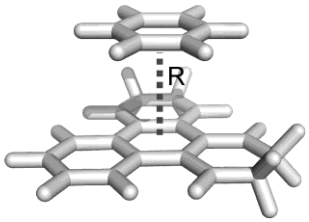

Table A.26: SCS-MP2/AVTZ absolute energies (hartree) and interaction energies (kcal mol^{-1}) for the interaction of benzene with 2,3,6,7-tetrahydrotriphenylene.

R	Dimer	Monomer	Benzene	Eint
2.0	-925.211469	-693.854886	-231.726208	231.94
2.4	-925.470197	-693.850042	-231.722873	64.46
2.8	-925.553546	-693.847539	-231.721018	9.42
3.2	-925.572787	-693.846260	-231.719833	-4.20
3.3	-925.573765	-693.846018	-231.719590	-5.12
3.4	-925.574014	-693.845795	-231.719366	-5.56
3.5	-925.573768	-693.845587	-231.719161	-5.66
3.6	-925.573202	-693.845392	-231.718974	-5.54
3.7	-925.572440	-693.845209	-231.718805	-5.29
3.8	-925.571571	-693.845039	-231.718650	-4.95
3.9	-925.570659	-693.844880	-231.718511	-4.56
4.0	-925.569748	-693.844733	-231.718384	-4.16
4.4	-925.566543	-693.844260	-231.717993	-2.69
4.8	-925.564330	-693.843957	-231.717751	-1.65
5.2	-925.562967	-693.843788	-231.717614	-0.98
5.6	-925.562164	-693.843702	-231.717540	-0.58
6.0	-925.561694	-693.843658	-231.717497	-0.34

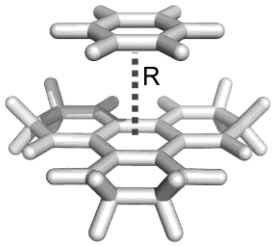

Table A.27: SCS-MP2/AVTZ absolute energies (hartree) and interaction energies (kcal mol^{-1}) for the interaction of benzene with 2,3,6,7,10,11-hexahydrotriphenylene.

R	Dimer	Monomer	Benzene	Eint
2.0	-926.337665	-694.968078	-231.726242	223.80
2.4	-926.587304	-694.963313	-231.722940	62.09
2.8	-926.667405	-694.960873	-231.721083	9.13
3.2	-926.685808	-694.959639	-231.719877	-3.95
3.3	-926.686728	-694.959406	-231.719628	-4.83
3.4	-926.686950	-694.959190	-231.719399	-5.25
3.5	-926.686699	-694.958988	-231.719190	-5.35
3.6	-926.686142	-694.958798	-231.718999	-5.24
3.7	-926.685398	-694.958620	-231.718826	-4.99
3.8	-926.684553	-694.958454	-231.718668	-4.66
3.9	-926.683669	-694.958298	-231.718526	-4.30
4.0	-926.682786	-694.958154	-231.718397	-3.91
4.4	-926.679692	-694.957687	-231.718000	-2.51
4.8	-926.677564	-694.957389	-231.717755	-1.52
5.2	-926.676262	-694.957222	-231.717617	-0.89
5.6	-926.675502	-694.957136	-231.717541	-0.52
6.0	-926.675061	-694.957092	-231.717498	-0.30

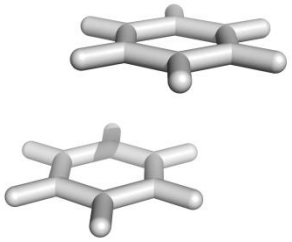

Table A.28: Estimated CCSD(T)/AVTZ absolute energies (hartree) and interaction energies (kcal mol^{-1}) for parallel displaced benzene dimer. Vertical displacement = 1.69 Å, horizontal displacement = 3.52 Å.

CCSD(T)/AVDZ	Dimer	MonA	MonB	Eint
Ethene1	-463.238136	-231.61725	-231.617255	-2.28
MP2/AVDZ	Dimer	MonA	MonB	
Ethene1	-463.088929	-231.54121	-231.541209	-4.09
MP2/AVTZ	Dimer	MonA	MonB	
Ethene1	-463.498566	-231.74576	-231.745765	-4.42
			Total Corrected Eint	**-2.60**

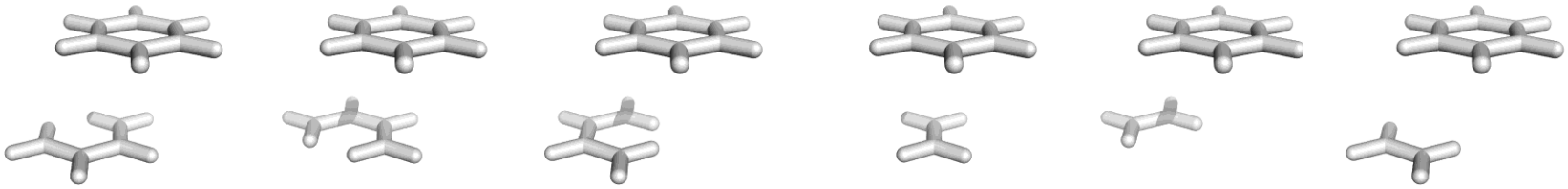

Table A.29: Estimated CCSD(T)/AVTZ absolute energies (hartree) and interaction energies (kcal mol^{-1}) for the parallel displaced dimer of benzene with dissected benzene. Vertical displacement = 1.69 Å, horizontal displacement = 3.52 Å.

CCSD(T)/AVDZ	Dimer	MonA	MonB	Eint	CCSD(T)/AVDZ	Dimer	MonA	MonB	Eint
Ethene1	-309.985934	-78.368461	-231.616151	-0.83	Butadiene1	-387.164886	-155.544932	-231.616934	-1.90
Ethene2	-309.985020	-78.368209	-231.615600	-0.76	Butadiene2	-387.164886	-155.544932	-231.616934	-1.90
Ethene3	-309.985020	-78.368209	-231.615600	-0.76	Butadiene3	-387.163875	-155.544479	-231.616332	-1.92
			Total	-2.35					**-5.71**
MP2/AVDZ	Dimer	MonA	MonB		MP2/AVDZ	Dimer	MonA	MonB	
Ethene1	-309.870456	-78.327469	-231.540166	-1.77	Butadiene1	-387.021944	-155.475706	-231.540899	-3.35
Ethene2	-309.868723	-78.327220	-231.539629	-1.18	Butadiene2	-387.021944	-155.475706	-231.540899	-3.35
Ethene3	-309.868723	-78.327220	-231.539629	-1.18	Butadiene3	-387.020241	-155.475280	-231.540338	-2.90
			Total	-4.12					**-9.60**
MP2/AVTZ	Dimer	MonA	MonB		MP2/AVTZ	Dimer	MonA	MonB	
Ethene1	-310.149977	-78.401380	-231.745339	-2.04	Butadiene1	-387.369480	-155.618067	-231.745606	-3.64
Ethene2	-310.148485	-78.401265	-231.745115	-1.32	Butadiene2	-387.369480	-155.618067	-231.745606	-3.64
Ethene3	-310.148485	-78.401265	-231.745115	-1.32	Butadiene3	-387.368280	-155.617900	-231.745420	-3.11
			Total	-4.69					-10.40
		Total Corrected Eint		**-2.91**			Total Corrected Eint		**-6.51**

Dissected benzene Eint = -3.60

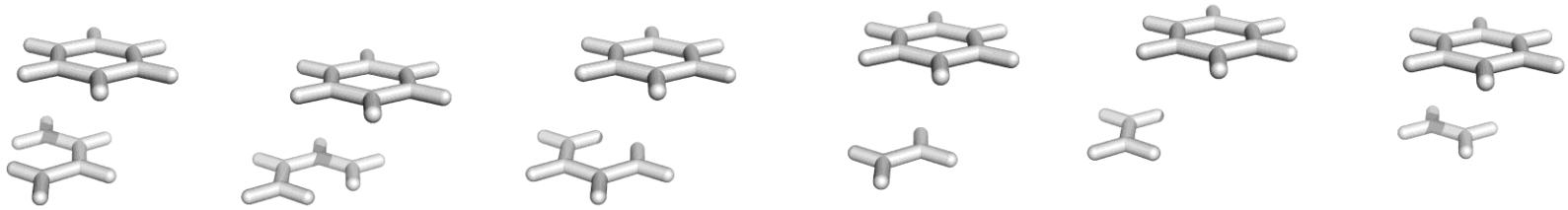

Table A.30: Estimated CCSD(T)/AVTZ absolute energies (hartree) and interaction energies (kcal mol^{-1}) for the parallel displaced dimer of benzene with regioisomer of dissected benzene. Vertical displacement = 1.69 Å, horizontal displacement = 3.52 Å.

CCSD(T)/AVDZ	Dimer	MonA	MonB	Eint	CCSD(T)/AVDZ	Dimer	MonA	MonB	Eint
Ethene1	-309.985213	-78.368460	-231.616028	-0.45	Butadiene1	-387.164140	-155.545065	-231.617013	-1.29
Ethene2	-309.984793	-78.368046	-231.615389	-0.85	Butadiene2	-387.163933	-155.544679	-231.616629	-1.65
Ethene3	-309.985213	-78.368460	-231.616028	-0.45	Butadiene3	-387.163933	-155.544679	-231.616629	-1.65
			Total	**-1.76**				Total	**-4.59**
MP2/AVDZ	Dimer	MonA	MonB		MP2/AVDZ	Dimer	MonA	MonB	
Ethene1	-309.869294	-78.327462	-231.540034	-1.13	Butadiene1	-387.021177	-155.475839	-231.540979	-2.74
Ethene2	-309.868335	-78.327060	-231.539430	-1.16	Butadiene2	-387.020446	-155.475464	-231.540609	-2.74
Ethene3	-309.869294	-78.327462	-231.540034	-1.13	Butadiene3	-387.020446	-155.475464	-231.540609	-2.74
			Total	**-3.41**				Total	**-8.22**
MP2/AVTZ	Dimer	MonA	MonB		MP2/AVTZ	Dimer	MonA	MonB	
Ethene1	-310.148820	-78.401359	-231.745275	-1.37	Butadiene1	-387.368650	-155.618110	-231.745629	-3.08
Ethene2	-310.148242	-78.401201	-231.745024	-1.27	Butadiene2	-387.368266	-155.617972	-231.745515	-3.00
Ethene3	-310.148820	-78.401359	-231.745275	-1.37	Butadiene3	-387.368266	-155.617972	-231.745515	-3.00
			Total	**-4.01**				Total	**-9.08**
			Total Corrected Eint	**-2.36**				Total Corrected Eint	**-5.44**

Dissected benzene Eint = -3.09

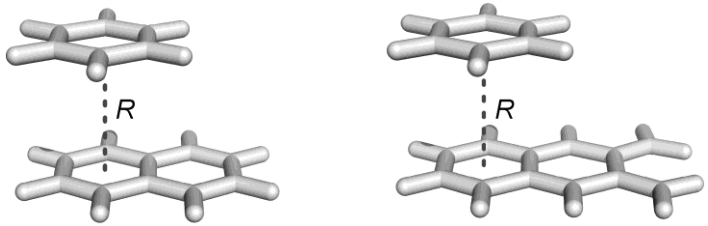

Table A.31: Estimated CCSD(T)/AVTZ absolute energies (hartree) and interaction energies (kcal mol^{-1}) for the interaction of benzene with naphthalene and 2,3-dimethylene-2,3-dihydronaphthalene.

	naphthalene				2,3-dimethylene-2,3-dihydronaphthalene				
R	Dimer	Monomer	Anthracene	Complex	Dimer	Monomer	Anthracene	Complex	Difference
2.0	-616.319393	-385.022868	-231.724840	268.77	-693.536093	-462.186010	-231.724903	235.20	33.57
2.4	-616.596475	-385.019135	-231.721623	90.54	-693.780528	-462.182238	-231.721685	77.43	13.11
2.8	-616.703799	-385.017170	-231.719878	20.86	-693.872597	-462.180253	-231.719942	17.32	3.55
3.2	-616.733000	-385.016235	-231.718978	1.39	-693.897865	-462.179300	-231.719027	0.29	1.10
3.3	-616.735499	-385.016068	-231.718808	-0.39	-693.899951	-462.179129	-231.718853	-1.24	0.85
3.4	-616.737025	-385.015916	-231.718654	-1.54	-693.901176	-462.178974	-231.718693	-2.20	0.66
3.5	-616.737859	-385.015777	-231.718513	-2.24	-693.901788	-462.178832	-231.718548	-2.77	0.53
3.6	-616.738207	-385.015649	-231.718385	-2.62	-693.901973	-462.178701	-231.718416	-3.05	0.43
3.7	-616.738223	-385.015530	-231.718267	-2.78	-693.901867	-462.178579	-231.718295	-3.13	0.36
3.8	-616.738017	-385.015419	-231.718160	-2.78	-693.901570	-462.178467	-231.718184	-3.09	0.30
3.9	-616.737672	-385.015317	-231.718061	-2.69	-693.901156	-462.178362	-231.718082	-2.96	0.26
4.0	-616.737245	-385.015221	-231.717970	-2.54	-693.900676	-462.178266	-231.717989	-2.77	0.23
4.4	-616.735388	-385.014912	-231.717681	-1.75	-693.898692	-462.177953	-231.717692	-1.91	0.16
4.8	-616.733928	-385.014714	-231.717497	-1.08	-693.897165	-462.177751	-231.717503	-1.20	0.12
5.2	-616.733001	-385.014605	-231.717395	-0.63	-693.896192	-462.177640	-231.717398	-0.72	0.10
5.6	-616.732459	-385.014550	-231.717342	-0.36	-693.895615	-462.177585	-231.717343	-0.43	0.07
6.0	-616.732145	-385.014521	-231.717311	-0.20	-693.895273	-462.177556	-231.717312	-0.25	0.06

APPENDIX B

Table B.1: Linear Fit Parameters for B97-D vs CCSD(T)

X	slope	intercept	R^2
BH_2	1.04	–0.04	0.71
CH_3	1.21	–0.05	0.86
NH_2	1.07	–0.10	0.94
OH	1.04	–0.10	0.98
F	1.09	–0.15	0.99

Table B.2: Linear Fit Parameters for SAPT0 Total Energies vs CCSD(T)

X	slope	intercept	R^2
BH_2	1.27	0.02	0.94
CH_3	1.37	–0.01	0.98
NH_2	1.18	0.01	0.99
OH	1.15	0.03	1.00
F	1.16	0.04	1.00

Table B.3: Correlations between pairs of parameters: Hammett constants (σ_m), molar refractivity (MR), and interaction distance (r).

X	MR,r	σ_m,MR	σ_m,r
BH_2	0.26	0.02	0.33
CH_3	0.32	0.02	0.31
NH_2	0.16	0.02	0.55
OH	0.12	0.02	0.73
F	0.07	0.02	0.81

Table B.4: Hammett Constants and Molar Refractivities by Aryl Substituent

Y	MR	σ_m
H	1.03	0
CCH	9.55	0.21
CF_3	5.02	0.43
CH_2OH	7.19	0
CH_3	5.65	–0.07
CHO	6.88	0.35
CN	6.33	0.56
$COCH_3$	11.18	0.38
$COOCH_3$	12.87	0.37
COOH	6.93	0.37
F	0.92	0.34
$N(CH_3)_2$	15.55	–0.15
NH_2	5.42	–0.16
$NHCH_3$	10.33	–0.3
NHOH	7.22	–0.04
NO_2	7.36	0.71
NO	5.2	0.62
OCF_3	7.86	0.38
OH	2.85	0.12
OCH_3	7.87	0.12
SCH_3	13.82	0.15
SH	9.22	0.25

Table B.5: Interaction energies (kcal mol^{-1}), components of SAPT0 interaction energies (kcal mol^{-1}), and optimized interaction distances (Å) for BH_3···C_6H_5Y dimers.

Y	Electronic	Exchange	Induction	Dispersion	SAPT0 AVDZ	CCSD(T) AVTZ	B97-D TZV(2d,2p)	r
H	–0.720	2.451	–0.310	–2.644	–1.223	–0.973	–1.010	3.910
CCH	–0.819	2.496	–0.274	–2.799	–1.397	–1.098	–1.141	3.901
CF_3	–0.853	2.527	–0.241	–2.776	–1.344	–1.101	–1.256	3.899
CH_2OH	–0.783	2.568	–0.335	–2.834	–1.384	–1.102	–1.205	3.893
CH_3	–0.764	2.529	–0.333	–2.800	–1.367	–1.086	–1.186	3.889
CHO	–0.891	2.487	–0.248	–2.744	–1.397	–1.122	–1.172	3.906
CN	–0.826	2.345	–0.215	–2.659	–1.355	–1.102	–1.120	3.924
$COCH_3$	–0.711	2.483	–0.261	–2.792	–1.281	–1.030	–1.088	3.907
$COOCH_3$	–0.867	2.549	–0.269	–2.822	–1.409	–1.133	–1.207	3.896
COOH	–0.776	2.465	–0.247	–2.744	–1.302	–1.056	–1.113	3.908
F	–0.826	2.509	–0.266	–2.658	–1.241	–1.011	–1.125	3.899
$N(CH_3)_2$	–0.836	2.783	–0.395	–3.012	–1.460	–1.161	–1.297	3.864
NH_2	–0.736	2.299	–0.321	–2.648	–1.407	–1.147	–1.228	3.927
$NHCH_3$	–0.841	2.663	–0.373	–2.893	–1.444	–1.157	–1.271	3.877
NHOH	–0.725	2.528	–0.321	–2.800	–1.318	–1.058	–1.157	3.893
NO_2	–0.864	2.399	–0.212	–2.681	–1.358	–1.113	–1.133	3.917
NO	–0.733	2.120	–0.202	–2.520	–1.335	–1.095	–1.119	3.959
OCF_3	–0.821	2.517	–0.252	–2.774	–1.330	–1.100	–1.222	3.898
OH	–0.676	2.382	–0.295	–2.646	–1.236	–1.004	–1.106	3.918
OCH_3	–0.871	2.629	–0.337	–2.844	–1.423	–1.153	–1.250	3.886
SCH_3	–0.890	2.558	–0.307	–2.899	–1.537	–1.231	–1.301	3.890
SH	–0.878	2.515	–0.285	–2.823	–1.470	–1.180	–1.230	3.896

Table B.6: Interaction energies (kcal mol^{-1}), components of SAPT0 interaction energies (kcal mol^{-1}), and optimized interaction distances (Å) for CH_4···C_6H_5Y dimers.

Y	Electronic	Exchange	Induction	Dispersion	SAPT0 AVDZ	CCSD(T) AVTZ	B97-D TZV(2d,2p)	r
H	–0.961	2.387	–0.298	–2.875	–1.747	–1.379	–1.537	3.735
CCH	–1.012	2.657	–0.290	–3.191	–1.837	–1.413	–1.585	3.694
CF_3	–1.011	2.698	–0.255	–3.172	–1.740	–1.375	–1.678	3.690
CH_2OH	–1.162	2.894	–0.366	–3.312	–1.947	–1.501	–1.759	3.670
CH_3	–1.115	2.727	–0.350	–3.195	–1.934	–1.499	–1.718	3.691
CHO	–0.997	2.650	–0.261	–3.128	–1.736	–1.356	–1.524	3.698
CN	–0.948	2.555	–0.234	–3.073	–1.699	–1.332	–1.500	3.706
$COCH_3$	–1.061	2.730	–0.284	–3.235	–1.850	–1.442	–1.640	3.688
$COOCH_3$	–1.024	2.685	–0.279	–3.191	–1.809	–1.417	–1.631	3.692
COOH	–1.005	2.652	–0.264	–3.146	–1.763	–1.383	–1.580	3.696
F	–1.030	2.678	–0.280	–3.030	–1.661	–1.313	–1.538	3.691
$N(CH_3)_2$	–1.211	3.035	–0.415	–3.453	–2.044	–1.596	–1.859	3.655
NH_2	–1.109	2.782	–0.368	–3.206	–1.900	–1.489	–1.731	3.679
$NHCH_3$	–1.172	2.928	–0.397	–3.343	–1.983	–1.551	–1.789	3.663
NHOH	–1.113	2.813	–0.349	–3.253	–1.902	–1.487	–1.715	3.674
NO_2	–0.926	2.550	–0.226	–3.065	–1.666	–1.331	–1.493	3.706
NO	–0.953	2.572	–0.242	–3.066	–1.688	–1.319	–1.453	3.706
OCF_3	–1.035	2.732	–0.270	–3.185	–1.757	–1.397	–1.661	3.685
OH	–1.090	2.724	–0.327	–3.115	–1.808	–1.428	–1.649	3.688
OCH_3	–1.144	2.853	–0.353	–3.256	–1.901	–1.495	–1.720	3.676
SCH_3	–1.067	2.767	–0.325	–3.331	–1.957	–1.527	–1.736	3.680
SH	–1.056	2.711	–0.305	–3.248	–1.898	–1.484	–1.676	3.685

Table B.7: Interaction energies (kcal mol^{-1}), components of SAPT0 interaction energies (kcal mol^{-1}), and optimized interaction distances (Å) for NH_3···C_6H_5Y dimers.

Y	Electronic	Exchange	Induction	Dispersion	SAPT0 AVDZ	CCSD(T) AVTZ	B97-D TZV(2d,2p)	r
H	–2.051	3.404	–0.595	–3.322	–2.563	–2.077	–2.807	3.473
CCH	–1.975	3.433	–0.567	–3.533	–2.642	–2.105	–2.865	3.461
CF_3	–1.704	3.396	–0.512	–3.463	–2.283	–1.851	–2.770	3.466
CH_2OH	–2.254	3.805	–0.673	–3.694	–2.815	–2.289	–3.173	3.434
CH_3	–2.177	3.658	–0.653	–3.586	–2.758	–2.227	–3.047	3.449
CHO	–1.748	3.322	–0.517	–3.419	–2.363	–1.920	–2.683	3.474
CN	–1.575	3.185	–0.479	–3.353	–2.221	–1.781	–2.548	3.482
$COCH_3$	–1.877	3.521	–0.561	–3.582	–2.498	–2.034	–2.854	3.456
$COOCH_3$	–1.944	3.522	–0.560	–3.565	–2.548	–2.081	–2.890	3.454
COOH	–1.887	3.557	–0.550	–3.555	–2.435	–1.982	–2.824	3.450
F	–1.876	3.455	–0.550	–3.348	–2.320	–1.894	–2.722	3.460
$N(CH_3)_2$	–2.485	3.976	–0.745	–3.813	–3.067	–2.544	–3.501	3.422
NH_2	–2.405	3.865	–0.694	–3.666	–2.900	–2.372	–3.238	3.426
$NHCH_3$	–2.211	3.680	–0.688	–3.611	–2.830	–2.335	–3.214	3.445
NHOH	–2.189	3.663	–0.646	–3.605	–2.778	–2.276	–3.111	3.441
NO_2	–1.533	3.270	–0.479	–3.399	–2.142	–1.766	–2.596	3.471
NO	–1.694	3.320	–0.505	–3.406	–2.285	–1.836	–2.638	3.470
OCF_3	–1.830	3.470	–0.538	–3.500	–2.398	–1.968	–2.857	3.458
OH	–2.075	3.609	–0.619	–3.481	–2.566	–2.113	–2.925	3.450
OCH_3	–2.154	3.723	–0.650	–3.615	–2.696	–2.222	–3.063	3.443
SCH_3	–2.078	3.592	–0.619	–3.697	–2.802	–2.273	–3.074	3.447
SH	–2.059	3.520	–0.590	–3.595	–2.725	–2.211	–2.964	3.452

Table B.8: Interaction energies (kcal mol^{-1}), components of SAPT0 interaction energies (kcal mol^{-1}), and optimized interaction distances (Å) for OH_2···C_6H_5Y dimers.

Y	Electronic	Exchange	Induction	Dispersion	SAPT0 AVDZ	CCSD(T) AVTZ	B97-D TZV(2d,2p)	r
H	–2.939	3.778	–1.047	–3.177	–3.386	–2.863	–4.093	3.299
CCH	–2.719	3.703	–1.013	–3.319	–3.348	–2.795	–4.052	3.297
CF_3	–2.167	3.664	–0.948	–3.269	–2.720	–2.310	–3.763	3.300
CH_2OH	–3.464	4.010	–1.129	–3.417	–4.000	–3.378	–4.744	3.279
CH_3	–3.021	3.923	–1.112	–3.362	–3.572	–3.016	–4.311	3.288
CHO	–2.402	3.674	–0.966	–3.253	–2.946	–2.479	–3.674	3.301
CN	–1.922	3.482	–0.904	–3.175	–2.520	–2.114	–3.374	3.312
$COCH_3$	–2.753	3.785	–1.012	–3.346	–3.327	–2.812	–4.070	3.293
$COOCH_3$	–2.516	3.724	–0.997	–3.309	–3.098	–2.653	–3.976	3.297
COOH	–2.329	3.676	–0.970	–3.268	–2.891	–2.466	–3.778	3.300
F	–2.462	3.633	–0.972	–3.121	–2.922	–2.497	–3.830	3.304
$N(CH_3)_2$	–3.494	3.997	–1.181	–3.451	–4.128	–3.589	–5.019	3.283
NH_2	–3.355	3.854	–1.110	–3.321	–3.932	–3.385	–4.732	3.288
$NHCH_3$	–3.291	3.935	–1.150	–3.372	–3.878	–3.352	–4.762	3.286
NHOH	–3.037	3.819	–1.088	–3.341	–3.647	–3.137	–4.491	3.288
NO_2	–1.554	3.414	–0.878	–3.144	–2.163	–1.889	–3.189	3.317
NO	–1.999	3.475	–0.912	–3.156	–2.592	–2.152	–3.353	3.315
OCF_3	–2.304	3.684	–0.975	–3.269	–2.865	–2.448	–3.866	3.298
OH	–3.072	3.851	–1.068	–3.258	–3.546	–3.044	–4.406	3.291
OCH_3	–3.240	3.920	–1.106	–3.345	–3.771	–3.235	–4.592	3.288
SCH_3	–2.479	3.769	–1.064	–3.394	–3.167	–2.716	–4.062	3.293
SH	–2.890	3.772	–1.043	–3.366	–3.527	–2.990	–4.266	3.290

Table B.9: Interaction energies (kcal mol^{-1}), components of SAPT0 interaction energies (kcal mol^{-1}), and optimized interaction distances (Å) for $FH^{\cdots}C_6H_5Y$ dimers.

Y	Electronic	Exchange	Induction	Dispersion	SAPT0 AVDZ	CCSD(T) AVTZ	B97-D TZV(2d,2p)	r
H	–3.905	3.721	–1.852	–2.674	–4.711	–4.122	–5.978	3.159
CCH	–2.961	3.555	–1.821	–2.735	–3.962	–3.480	–5.334	3.165
CF_3	–2.149	3.473	–1.715	–2.684	–3.073	–2.699	–4.786	3.171
CH_2OH	–4.193	3.905	–1.967	–2.846	–5.102	–4.423	–6.444	3.144
CH_3	–4.307	3.985	–1.988	–2.857	–5.168	–4.492	–6.438	3.140
CHO	–2.394	3.469	–1.742	–2.668	–3.335	–2.970	–4.710	3.173
CN	–1.648	3.329	–1.673	–2.620	–2.611	–2.332	–4.162	3.181
$COCH_3$	–2.858	3.682	–1.834	–2.782	–3.792	–3.366	–5.194	3.157
$COOCH_3$	–2.777	3.556	–1.792	–2.726	–3.738	–3.357	–5.279	3.166
COOH	–2.488	3.505	–1.756	–2.692	–3.432	–3.082	–5.012	3.170
F	–2.839	3.548	–1.757	–2.616	–3.665	–3.262	–5.249	3.167
$N(CH_3)_2$	–4.594	4.022	–2.065	–2.932	–5.569	–4.996	–7.124	3.136
NH_2	–4.122	3.800	–1.944	–2.777	–5.044	–4.484	–6.580	3.150
$NHCH_3$	–4.373	3.879	–1.998	–2.841	–5.333	–4.765	–6.873	3.145
NHOH	–3.863	3.738	–1.913	–2.780	–4.818	–4.244	–6.347	3.152
NO_2	–1.218	3.292	–1.644	–2.606	–2.176	–2.126	–3.997	3.182
NO	–1.956	3.306	–1.681	–2.598	–2.929	–2.549	–4.162	3.186
OCF_3	–2.491	3.536	–1.761	–2.697	–3.413	–3.012	–5.088	3.166
OH	–3.735	3.819	–1.905	–2.748	–4.569	–4.060	–6.091	3.150
OCH_3	–3.998	3.873	–1.951	–2.811	–4.888	–4.336	–6.370	3.148
SCH_3	–3.556	3.690	–1.900	–2.824	–4.590	–4.065	–6.105	3.155
SH	–3.229	3.601	–1.844	–2.757	–4.229	–3.737	–5.716	3.161

APPENDIX C

Table C.1: Counterpoise (CP) and non-CP-corrected estimated CCSD(T)/AVTZ interaction energies (kcal mol^{-1}) for dimers of benzene (Bz), borazine (Bn), and triazine (Tz).

		E_{int}(CP-corrected)	E_{int}(non-CP-corrected)
Bz	Bz	-1.6	-2.7
	Bn	-2.2	-3.6
	Tz	-3.1	-4.4
Bn(B)	Bn(B)	-1.8	-2.9
	Bn(N)	-3.3	-4.9
	Tz(C)	-2.7	-3.9
Tz(C)	Bn(N)	-3.1	-4.4
	Tz(C)	-1.5	-2.5
	Tz(N)	-3.8	-5.1

Table C.2: Slopes and correlation coefficients (r) for orthogonal regression analyses of SAPT0 energy components for substituted dimers of the type A-X···A vs B-X···A where A ≠ B.[a]

		Electrostatic		Exchange		Induction		Dispersion		SAPT0	
A	B	Slope	r	Slope	r	Slope	r	Slope	r	Slope	r
						R = 3.5 Å					
Bz	Bn(B)	0.98	0.98	0.59	0.76	-0.09	-0.10	0.89	0.99	0.94	0.96
	Bn(N)	1.02	0.98	0.92	0.96	-0.29	-0.27	0.95	0.99	1.05	0.98
	Tz(C)	1.08	0.98	0.88	0.79	-1.06	-0.39	1.10	0.98	1.03	0.97
Bn(B)	Bz	1.35	0.93	1.51	0.80	1.92	0.56	1.10	0.99	1.40	0.93
	Bn(N)	1.03	0.95	1.30	0.83	1.05	0.57	1.07	0.98	1.08	0.95
	Tz(C)	1.29	0.94	1.27	0.92	2.42	0.55	1.21	0.99	1.29	0.94
Bn(N)	Bz	0.69	0.90	1.09	0.96	25.52	0.12	1.03	1.00	0.85	0.87
	Bn(B)	0.98	0.91	0.69	0.76	1.17	0.58	0.93	0.98	0.84	0.91
	Tz(C)	0.92	0.93	0.97	0.83	3.76	0.52	1.14	0.98	0.88	0.93
Tz(C)	Bz	0.74	0.92	1.66	0.72	-2.18	-0.38	0.89	0.98	0.91	0.93
	Bn(B)	1.06	0.97	0.83	0.89	0.39	0.37	0.81	0.99	0.99	0.95
	Bn(N)	1.04	0.94	1.26	0.80	0.38	0.62	0.87	0.96	1.01	0.95
						R = R_e					
Bz	Bn(B)	1.05	0.97	1.04	0.86	3.05	0.24	0.80	0.93	1.01	0.98
	Bn(N)	1.25	0.91	1.71	0.52	-17.83	-0.09	1.04	0.77	1.10	0.98
	Tz(C)	1.17	0.96	1.25	0.71	-20.33	-0.08	1.03	0.86	1.18	0.98
Bn(B)	Bz	1.89	0.89	1.28	0.74	1.80	0.62	1.20	0.87	1.36	0.95
	Bn(N)	4.04	0.73	4.53	0.42	15.78	0.22	1.72	0.77	1.54	0.89
	Tz(C)	1.39	0.92	1.10	0.68	2.89	0.55	1.22	0.86	1.30	0.95
Bn(N)	Bz	0.88	0.72	1.42	0.70	8.87	0.24	1.13	0.90	0.94	0.85
	Bn(B)	2.23	0.63	2.93	0.55	3.85	0.56	1.13	0.87	1.39	0.92
	Tz(C)	1.99	0.74	2.82	0.69	5.07	0.61	1.66	0.88	1.30	0.94
Tz(C)	Bz	1.12	0.89	1.18	0.72	-122.20	-0.01	0.80	0.87	1.05	0.97
	Bn(B)	1.46	0.98	0.77	0.59	0.60	0.40	0.59	0.82	1.08	0.97
	Bn(N)	2.58	0.82	2.75	0.57	3.15	0.45	1.00	0.81	1.47	0.95
						R = 4.0 Å					
Bz	Bn(B)	0.94	0.99	0.50	0.71	0.07	0.13	0.90	0.99	0.96	0.98
	Bn(N)	0.97	0.98	0.87	0.95	-0.24	-0.28	0.96	0.99	1.01	0.98
	Tz(C)	0.99	0.98	0.77	0.76	-1.14	-0.49	1.08	0.98	1.04	0.98
Bn(B)	Bz	1.17	0.98	1.84	0.74	4.18	0.44	1.09	0.99	1.14	0.98
	Bn(N)	1.01	0.97	1.41	0.81	1.51	0.46	1.06	0.98	1.03	0.97
	Tz(C)	1.17	0.95	1.27	0.88	4.24	0.44	1.19	0.99	1.24	0.95
Bn(N)	Bz	0.87	0.97	1.15	0.95	-15.70	-0.15	1.03	1.00	0.85	0.96
	Bn(B)	0.97	0.93	0.64	0.74	0.79	0.62	0.93	0.98	0.92	0.94
	Tz(C)	0.94	0.94	0.88	0.84	3.01	0.67	1.12	0.98	0.99	0.95
Tz(C)	Bz	0.78	0.91	2.23	0.70	-1.71	-0.57	0.91	0.98	0.92	0.96
	Bn(B)	1.03	0.96	0.87	0.87	0.08	0.13	0.83	0.99	1.00	0.96
	Bn(N)	1.00	0.95	1.41	0.81	0.30	0.55	0.88	0.97	0.99	0.95

Table C.3: Slopes and correlation coefficients (r) for total least squares analyses of SAPT0 interaction energies for A-X···B vs C-X···D (R = 3.5 Å)

		C-X···Bn(N)							
		Bz-X		Bn(B)-X		Bn(N)-X		Tz-X	
B	A-X	Slope	r	Slope	r	Slope	r	Slope	r
Bz	Bz-X	0.45	0.71	0.53	0.95	0.62	0.92	0.56	0.96
	Bn(B)-X	0.44	0.59	0.57	0.96	0.64	0.83	0.59	0.94
	Bn(N)-X	0.40	0.65	0.50	0.91	0.59	0.93	0.52	0.94
	Tz-X	0.37	0.57	0.51	0.91	0.57	0.83	0.53	0.94
		C-X···Bn(B)							
Bz	Bz-X	0.59	0.86	0.40	0.82	0.46	0.89	0.56	0.91
	Bn(B)-X	0.63	0.86	0.44	0.85	0.48	0.86	0.60	0.93
	Bn(N)-X	0.55	0.84	0.37	0.79	0.44	0.89	0.52	0.89
	Tz-X	0.56	0.84	0.38	0.81	0.44	0.85	0.54	0.92
		C-X···Bn(N)							
Bn(B)	Bz-X	0.74	0.41	0.84	0.79	1.02	0.71	0.88	0.78
	Bn(B)-X	1.43	0.51	1.25	0.79	1.59	0.70	1.29	0.81
	Bn(N)-X	1.23	0.53	1.13	0.81	1.37	0.79	1.17	0.84
	Tz-X	0.90	0.48	0.93	0.85	1.13	0.76	0.97	0.86

Table C.4: Slopes and correlation coefficients (r) for total least squares analyses of SAPT0 interaction energies for A-X···B vs C-X···D (R = 4.0 Å)

		C-X···Bn(N)							
		Bz-X		Bn(B)-X		Bn(N)-X		Tz-X	
B	A-X	Slope	r	Slope	r	Slope	r	Slope	r
Bz	Bz-X	0.44	0.88	0.50	0.95	0.537	0.93	0.54	0.97
	Bn(B)-X	0.45	0.85	0.53	0.96	0.549	0.89	0.57	0.97
	Bn(N)-X	0.43	0.86	0.48	0.91	0.538	0.95	0.53	0.95
	Tz-X	0.40	0.81	0.47	0.91	0.493	0.87	0.51	0.95
		C-X···Bn(B)							
Bz	Bz-X	0.47	0.91	0.40	0.89	0.42	0.92	0.51	0.95
	Bn(B)-X	0.48	0.89	0.42	0.90	0.44	0.89	0.54	0.95
	Bn(N)-X	0.45	0.88	0.38	0.85	0.42	0.92	0.50	0.92
	Tz-X	0.43	0.85	0.37	0.85	0.39	0.86	0.48	0.93
		C-X···Bn(N)							
Bn(B)	Bz-X	0.96	0.82	1.04	0.88	1.15	0.85	1.13	0.88
	Bn(B)-X	1.12	0.83	1.21	0.89	1.34	0.84	1.30	0.89
	Bn(N)-X	1.08	0.84	1.16	0.88	1.27	0.90	1.25	0.90
	Tz-X	0.89	0.83	1.02	0.92	1.07	0.87	1.05	0.94

Table C.5: Correlation coefficients of SAPT0 interaction energies between all pairs of sandwich dimers involving benzene, borazine, and triazine (R = R_e).

		Bz-X	Bz-X	Bz-X	Bz-X	Bz-X	Bn(B)-X	Bn(B)-X	Bn(B)-X	Bn(B)-X	Bn(B)-X	Bn(N)-X	Bn(N)-X	Bn(N)-X	Bn(N)-X	Bn(N)-X	Tz-X	Tz-X		Tz-X	Tz-X
		Bz	Bn(B)	Bn(N)	Tz(C)	Tz(N)	Bz	Bn(B)	Bn(N)	Tz(C)	Tz(N)	Bz	Bn(B)	Bn(N)	Tz(C)	Tz(N)	Bz	Bn(B)	Bn(N)	Tz(C)	Tz(N)
Bz-X	Bz	1.00	0.90	0.74	0.12	-0.24	0.98	0.90	0.92	-0.18	0.33	0.98	0.86	0.93	-0.10	0.12	0.98	0.95	0.94	0.02	0.23
Bz-X	Bn(B)		1.00	0.61	0.14	0.03	0.90	0.95	0.84	-0.18	0.61	0.87	0.94	0.83	-0.16	0.46	0.86	0.97	0.81	0.03	0.50
Bz-X	Bn(N)			1.00	0.66	-0.03	0.70	0.67	0.84	0.48	-0.01	0.75	0.62	0.86	0.58	0.00	0.67	0.67	0.88	0.63	0.05
Bz-X	Tz(C)				1.00	0.04	0.11	0.17	0.39	0.92	-0.30	0.16	0.12	0.39	0.91	-0.08	0.00	0.12	0.32	0.97	-0.19
Bz-X	Tz(N)					1.00	-0.24	0.02	-0.24	0.15	0.63	-0.26	0.07	-0.21	0.07	0.83	-0.30	-0.10	-0.20	0.14	0.80
Bn(B)-X	Bz						1.00	0.92	0.93	-0.19	0.35	0.95	0.81	0.90	-0.13	0.15	0.98	0.95	0.92	0.00	0.24
Bn(B)-X	Bn(B)							1.00	0.84	-0.12	0.54	0.88	0.89	0.85	-0.09	0.39	0.87	0.95	0.85	0.07	0.45
Bn(B)-X	Bn(N)								1.00	0.09	0.20	0.89	0.76	0.92	0.16	0.08	0.89	0.89	0.96	0.28	0.11
Bn(B)-X	Tz(C)									1.00	-0.43	-0.15	-0.18	0.09	0.95	-0.15	-0.28	-0.20	0.06	0.97	-0.25
Bn(B)-X	Tz(N)										1.00	0.29	0.57	0.21	-0.51	0.91	0.30	0.48	0.19	-0.33	0.95
Bn(N)-X	Bz											1.00	0.87	0.96	-0.04	0.06	0.96	0.93	0.93	0.05	0.20
Bn(N)-X	Bn(B)												1.00	0.83	-0.11	0.42	0.82	0.93	0.80	0.02	0.49
Bn(N)-X	Bn(N)													1.00	0.19	0.05	0.88	0.88	0.94	0.28	0.15
Bn(N)-X	Tz(C)														1.00	-0.25	-0.19	-0.14	0.16	0.95	-0.35
Bn(N)-X	Tz(N)															1.00	0.07	0.31	0.04	-0.08	0.95
Tz-X	Bz																1.00	0.94	0.92	-0.10	0.18
Tz-X	Bn(B)																	1.00	0.89	0.00	0.37
Tz-X	Bn(N)																		1.00	0.25	0.13
Tz-X	Tz(C)																			1.00	-0.18
Tz-X	Tz(N)																				1.00

Table C.6: Correlation coefficients of the electrostatic components of the SAPT0 interaction energies between all pairs of sandwich dimers involving benzene, borazine, and triazine (R = 4.0 Å).

		Bz-X	Bz-X	Bz-X	Bz-X	Bz-X	Bn(B)-X	Bn(B)-X	Bn(B)-X	Bn(B)-X	Bn(B)-X	Bn(N)-X	Bn(N)-X	Bn(N)-X	Bn(N)-X	Bn(N)-X	Tz-X	Tz-X		Tz-X	Tz-X
		Bz	Bn(B)	Bn(N)	Tz(C)	Tz(N)	Bz	Bn(B)	Bn(N)	Tz(C)	Tz(N)	Bz	Bn(B)	Bn(N)	Tz(C)	Tz(N)	Bz	Bn(B)	Bn(N)	Tz(C)	Tz(N)
Bz-X	Bz	1.00	0.93	0.95	-0.45	-0.52	0.99	0.94	0.95	-0.57	0.03	0.98	0.94	0.94	-0.54	-0.21	0.98	0.90	0.96	-0.58	-0.19
Bz-X	Bn(B)		1.00	0.79	-0.69	-0.22	0.91	0.98	0.81	-0.81	0.37	0.91	0.98	0.80	-0.79	0.13	0.91	0.94	0.83	-0.80	-0.15
Bz-X	Bn(N)			1.00	-0.21	-0.66	0.94	0.82	0.97	-0.32	-0.23	0.94	0.81	0.97	-0.27	-0.43	0.94	0.77	0.98	-0.34	-0.40
Bz-X	Tz(C)				1.00	-0.47	-0.43	-0.67	-0.21	0.96	-0.82	-0.42	-0.69	-0.21	0.93	-0.66	-0.46	-0.66	-0.31	0.91	-0.68
Bz-X	Tz(N)					1.00	-0.53	-0.25	-0.67	-0.32	0.79	-0.52	-0.22	-0.64	-0.34	0.89	-0.51	-0.28	-0.59	-0.26	-0.90
Bn(B)-X	Bz						1.00	0.94	0.97	-0.55	-0.01	0.95	0.90	0.91	-0.52	-0.20	0.98	0.91	0.96	-0.57	-0.21
Bn(B)-X	Bn(B)							1.00	0.84	-0.76	0.29	0.90	0.97	0.80	-0.74	0.09	0.93	0.95	0.86	-0.76	-0.10
Bn(B)-X	Bn(N)								1.00	-0.34	-0.22	0.91	0.80	0.93	-0.32	-0.38	0.94	0.81	0.97	-0.38	-0.39
Bn(B)-X	Tz(C)									1.00	-0.80	-0.54	-0.78	-0.33	0.98	-0.60	-0.58	-0.76	-0.41	0.96	-0.61
Bn(B)-X	Tz(N)										1.00	0.02	0.35	-0.18	-0.82	0.92	0.01	0.26	-0.14	-0.74	0.95
Bn(N)-X	Bz											1.00	0.94	0.97	-0.51	-0.26	0.95	0.86	0.94	-0.54	-0.19
Bn(N)-X	Bn(B)												1.00	0.84	-0.76	0.08	0.91	0.92	0.84	-0.77	-0.14
Bn(N)-X	Bn(N)													1.00	-0.30	-0.42	0.90	0.76	0.94	-0.35	-0.35
Bn(N)-X	Tz(C)														1.00	-0.66	-0.53	-0.72	-0.36	0.95	-0.66
Bn(N)-X	Tz(N)															1.00	-0.22	0.05	-0.34	-0.55	0.96
Tz-X	Bz																1.00	0.92	0.97	-0.60	-0.21
Tz-X	Bn(B)																	1.00	0.83	-0.80	-0.04
Tz-X	Bn(N)																		1.00	-0.42	-0.34
Tz-X	Tz(C)																			1.00	-0.55
Tz-X	Tz(N)																				1.00

Table C.7: Correlation coefficients of the non-electrostatic components of the SAPT0 interaction energies between all pairs of sandwich dimers involving benzene, borazine, and triazine (R = 4.0 Å).

		Bz-X	Bz-X	Bz-X	Bz-X	Bz-X	Bn(B)-X	Bn(B)-X	Bn(B)-X	Bn(B)-X	Bn(B)-X	Bn(N)-X	Bn(N)-X	Bn(N)-X	Bn(N)-X	Bn(N)-X	Tz-X	Tz-X		Tz-X	Tz-X
		Bz	Bn(B)	Bn(N)	Tz(C)	Tz(N)	Bz	Bn(B)	Bn(N)	Tz(C)	Tz(N)	Bz	Bn(B)	Bn(N)	Tz(C)	Tz(N)	Bz	Bn(B)	Bn(N)	Tz(C)	Tz(N)
Bz-X	Bz	1.00	0.97	0.99	0.97	0.99	0.93	0.92	0.91	0.93	0.93	0.98	0.93	0.97	0.95	0.96	0.91	0.86	0.87	0.89	0.90
Bz-X	Bn(B)		1.00	0.94	0.98	0.96	0.95	0.95	0.95	0.94	0.94	0.99	0.98	0.98	0.97	0.98	0.97	0.95	0.95	0.95	0.95
Bz-X	Bn(N)			1.00	0.96	0.99	0.92	0.90	0.90	0.92	0.92	0.96	0.90	0.95	0.93	0.95	0.88	0.82	0.84	0.86	0.88
Bz-X	Tz(C)				1.00	0.99	0.96	0.94	0.95	0.97	0.96	0.98	0.96	0.98	0.99	0.99	0.95	0.91	0.92	0.95	0.95
Bz-X	Tz(N)					1.00	0.95	0.93	0.93	0.96	0.95	0.97	0.93	0.97	0.97	0.98	0.92	0.87	0.88	0.91	0.92
Bn(B)-X	Bz						1.00	1.00	1.00	0.99	0.99	0.94	0.94	0.94	0.96	0.96	0.96	0.93	0.95	0.96	0.97
Bn(B)-X	Bn(B)							1.00	1.00	0.99	0.99	0.93	0.94	0.94	0.95	0.95	0.97	0.95	0.96	0.97	0.98
Bn(B)-X	Bn(N)								1.00	0.99	0.99	0.93	0.94	0.94	0.96	0.95	0.97	0.94	0.96	0.97	0.98
Bn(B)-X	Tz(C)									1.00	1.00	0.93	0.93	0.94	0.97	0.97	0.95	0.92	0.94	0.97	0.97
Bn(B)-X	Tz(N)										1.00	0.93	0.92	0.93	0.96	0.96	0.95	0.92	0.94	0.97	0.97
Bn(N)-X	Bz											1.00	0.98	1.00	0.98	0.99	0.96	0.93	0.93	0.94	0.94
Bn(N)-X	Bn(B)												1.00	0.99	0.97	0.97	0.98	0.97	0.97	0.96	0.96
Bn(N)-X	Bn(N)													1.00	0.99	0.99	0.96	0.94	0.94	0.95	0.95
Bn(N)-X	Tz(C)														1.00	1.00	0.96	0.94	0.95	0.97	0.97
Bn(N)-X	Tz(N)															1.00	0.96	0.93	0.94	0.96	0.97
Tz-X	Bz																1.00	0.98	0.99	0.99	0.99
Tz-X	Bn(B)																	1.00	0.99	0.97	0.97
Tz-X	Bn(N)																		1.00	0.99	0.99
Tz-X	Tz(C)																			1.00	1.00
Tz-X	Tz(N)																				1.00

Table C.8: SAPT0 interaction energies (kcal mol^{-1}) for monosubstituted dimers of benzene, borazine, and triazine (R = R_e).

	Bz-X	Bz-X	Bz-X	Bz-X	Bz-X	Bn(B)-X	Bn(B)-X	Bn(B)-X	Bn(B)-X	Bn(B)-X	Bn(N)-X	Bn(N)-X	Bn(N)-X	Bn(N)-X	Bn(N)-X	Tz-X	Tz-X	Tz-X	Tz-X	Tz-X
X	Bz	BnB	BnN	Tz	TzN	Bz	BnB	BnN	Tz	TzN	Bz	BnB	BnN	Tz	TzN	Bz	BnB	BnN	Tz	TzN
H	-1.37	-1.86	-1.82	-3.19	-3.19	-1.82	-0.63	-3.09	-1.89	-3.19	-1.82	-3.08	-0.62	-3.19	-1.89	-3.19	-1.89	-3.19	-1.04	-4.22
BF2	-2.38	-2.48	-2.27	-3.17	-3.59	-2.67	-1.25	-3.47	-1.73	-4.11	-3.16	-3.96	-1.34	-3.07	-2.35	-4.25	-2.50	-3.83	-0.91	-5.35
CCH	-2.49	-2.48	-2.77	-3.96	-3.34	-2.64	-1.03	-3.99	-2.36	-3.34	-3.47	-4.00	-1.67	-4.18	-1.92	-4.15	-2.50	-4.10	-1.59	-4.56
CF3	-2.96	-2.61	-2.88	-3.54	-3.41	-3.40	-1.38	-4.46	-2.02	-3.67	-3.68	-3.81	-1.59	-3.63	-2.08	-4.95	-2.67	-4.55	-1.30	-4.83
CH2OH	-2.02	-2.40	-2.41	-3.46	-4.17	-2.32	-1.07	-3.49	-1.97	-4.08	-2.59	-3.77	-1.11	-3.62	-2.71	-3.82	-2.37	-3.72	-1.20	-5.40
CH3	-1.82	-2.13	-2.38	-3.61	-3.80	-2.16	-0.80	-3.60	-2.20	-3.70	-2.37	-3.53	-1.03	-3.75	-2.37	-3.55	-2.16	-3.75	-1.35	-4.92
CHO	-2.64	-2.56	-2.58	-3.52	-3.39	-2.84	-1.15	-3.96	-1.95	-3.82	-3.39	-3.99	-1.51	-3.53	-2.11	-4.47	-2.53	-4.18	-1.27	-4.90
CN	-3.06	-2.60	-2.95	-3.78	-3.04	-3.25	-1.23	-4.33	-2.17	-3.26	-3.99	-4.19	-1.85	-3.96	-1.80	-5.03	-2.70	-4.59	-1.51	-4.42
COCH3	-2.75	-2.81	-2.80	-3.79	-3.75	-3.04	-1.42	-4.18	-2.21	-4.09	-3.52	-4.35	-1.63	-3.85	-2.46	-4.62	-2.75	-4.45	-1.56	-5.24
COOCH3	-2.68	-2.81	-2.57	-3.49	-3.83	-2.95	-1.28	-4.03	-1.91	-4.17	-3.41	-4.42	-1.41	-3.44	-2.54	-4.53	-2.78	-4.17	-1.21	-5.45
COOH	-2.67	-2.76	-2.55	-3.40	-3.66	-3.02	-1.40	-3.98	-1.85	-4.06	-3.49	-4.29	-1.49	-3.30	-2.43	-4.59	-2.77	-4.18	-1.11	-5.30
F	-2.01	-1.88	-2.36	-3.21	-3.03	-2.31	-0.77	-3.50	-1.89	-2.98	-2.77	-3.42	-1.12	-3.54	-1.53	-4.06	-2.10	-3.89	-1.02	-4.05
NH2	-1.71	-2.01	-2.43	-3.46	-4.08	-1.82	-0.79	-3.09	-2.19	-3.53	-2.37	-3.56	-0.95	-3.83	-2.26	-3.32	-1.92	-3.53	-1.41	-5.17
NHCH3	-1.97	-2.22	-2.72	-3.77	-4.45	-2.20	-0.95	-3.61	-2.54	-3.99	-2.69	-3.71	-1.24	-4.18	-2.57	-3.62	-2.23	-3.95	-1.67	-5.60
NO2	-3.51	-2.97	-3.03	-3.45	-3.45	-3.77	-1.50	-4.61	-1.88	-3.87	-4.09	-4.55	-1.84	-3.51	-2.32	-5.67	-3.17	-4.90	-1.22	-5.11
NO	-2.85	-2.61	-2.68	-3.51	-3.25	-3.03	-1.15	-4.06	-1.92	-3.62	-3.33	-3.96	-1.45	-3.52	-2.13	-4.64	-2.57	-4.24	-1.22	-4.75
OCF3	-2.77	-2.51	-2.84	-3.44	-3.67	-3.11	-1.30	-3.96	-2.00	-3.65	-3.54	-4.06	-1.56	-3.79	-2.13	-4.75	-2.65	-4.32	-1.28	-4.90
OH	-1.81	-1.90	-2.44	-3.42	-3.38	-2.04	-0.78	-3.38	-2.15	-3.13	-2.54	-3.43	-1.07	-3.87	-1.71	-3.63	-2.02	-3.78	-1.23	-4.28
OME	-1.98	-2.17	-2.63	-3.65	-3.74	-2.27	-0.97	-3.73	-2.36	-3.44	-2.69	-3.76	-1.24	-4.10	-2.10	-3.76	-2.21	-4.03	-1.54	-4.74
SCH3	-2.52	-2.52	-3.08	-4.46	-3.60	-2.89	-1.27	-4.21	-3.05	-3.24	-3.18	-3.87	-1.55	-4.78	-2.07	-4.24	-2.52	-4.40	-2.21	-4.58
SH	-2.37	-2.29	-2.87	-4.14	-3.32	-2.72	-1.09	-3.94	-2.71	-3.04	-3.03	-3.64	-1.50	-4.49	-1.90	-4.08	-2.42	-4.10	-1.84	-4.31
SiF3	-3.00	-2.69	-2.64	-3.24	-3.76	-3.38	-1.27	-4.05	-1.79	-4.17	-3.66	-4.04	-1.57	-3.08	-2.43	-4.95	-2.73	-4.36	-1.06	-5.58
SiH3	-2.23	-2.39	-2.51	-3.58	-3.88	-2.73	-1.13	-3.90	-2.16	-4.06	-2.83	-3.79	-1.35	-3.59	-2.52	-3.98	-2.38	-3.93	-1.35	-5.38

Table C.9: SAPT0 interaction energies (kcal mol^{-1}) for monosubstituted dimers of benzene, borazine, and triazine (R = 3.5 Å).

X	Bz-X Bz	Bz-X BnB	Bz-X BnN	Bz-X Tz	Bz-X TzN	Bn(B)-X Bz	Bn(B)-X BnB	Bn(B)-X BnN	Bn(B)-X Tz	Bn(B)-X TzN	Bn(N)-X Bz	Bn(N)-X BnB	Bn(N)-X BnN	Bn(N)-X Tz	Bn(N)-X TzN	Tz-X Bz	Tz-X BnB	Tz-X BnN	Tz-X Tz	Tz-X TzN
H	-0.20	-1.37	-1.37	-2.97	-2.97	-1.37	0.19	-3.21	-1.61	-3.19	-1.37	-3.21	0.19	-3.19	-1.61	-2.97	-1.61	-3.19	-0.37	-4.22
BF2	-1.43	-2.25	-1.80	-2.97	-3.44	-2.27	-0.48	-3.66	-1.43	-4.05	-2.93	-4.05	-0.67	-3.08	-2.23	-4.12	-2.44	-3.85	-0.38	-5.15
CCH	-1.88	-2.18	-2.55	-3.88	-3.19	-2.35	-0.31	-3.98	-2.26	-3.35	-3.43	-4.05	-1.35	-4.10	-1.72	-4.08	-2.29	-4.04	-1.22	-4.51
CF3	-2.24	-2.22	-2.61	-3.40	-3.27	-3.19	-0.56	-4.43	-1.84	-3.63	-3.50	-4.04	-1.28	-3.62	-1.96	-4.89	-2.48	-4.51	-0.85	-4.71
CH2OH	-1.24	-2.10	-2.17	-3.31	-4.11	-2.01	-0.42	-3.63	-1.81	-4.05	-2.41	-3.94	-0.64	-3.60	-2.62	-3.71	-2.27	-3.74	-0.74	-5.23
CH3	-0.95	-1.80	-2.13	-3.46	-3.70	-1.81	-0.18	-3.65	-2.04	-3.67	-2.12	-3.69	-0.53	-3.73	-2.22	-3.42	-1.96	-3.71	-0.93	-4.81
CHO	-1.88	-2.29	-2.28	-3.39	-3.25	-2.56	-0.49	-3.96	-1.73	-3.78	-3.26	-4.08	-1.05	-3.54	-1.99	-4.39	-2.42	-4.14	-0.81	-4.76
CN	-2.41	-2.30	-2.71	-3.69	-2.88	-2.98	-0.47	-4.30	-2.05	-3.26	-4.03	-4.23	-1.64	-3.93	-1.59	-4.98	-2.57	-4.53	-1.11	-4.35
COCH3	-2.06	-2.56	-2.51	-3.68	-3.64	-2.74	-0.72	-4.18	-2.02	-4.03	-3.38	-4.34	-1.24	-3.83	-2.36	-4.56	-2.65	-4.39	-1.20	-5.05
COOCH3	-1.99	-2.63	-2.30	-3.37	-3.72	-2.71	-0.76	-4.02	-1.71	-4.12	-3.31	-4.36	-1.05	-3.45	-2.49	-4.48	-2.74	-4.15	-0.76	-5.22
COOH	-2.00	-2.54	-2.24	-3.26	-3.55	-2.72	-0.67	-3.99	-1.61	-4.00	-3.36	-4.29	-1.04	-3.34	-2.33	-4.53	-2.67	-4.13	-0.65	-5.09
F	-1.18	-1.47	-2.12	-3.01	-2.86	-1.99	0.03	-3.61	-1.68	-3.00	-2.54	-3.52	-0.63	-3.54	-1.27	-3.96	-1.91	-3.84	-0.52	-3.99
NH2	-0.87	-1.61	-2.26	-3.30	-4.04	-1.42	-0.13	-3.31	-2.09	-3.58	-2.13	-3.63	-0.56	-3.79	-2.18	-3.27	-1.73	-3.69	-1.26	-4.97
NHCH3	-1.21	-1.86	-2.63	-3.65	-4.42	-1.91	-0.53	-3.74	-2.49	-4.00	-2.44	-3.87	-0.87	-4.12	-2.48	-3.51	-2.11	-3.95	-1.34	-5.33
NO2	-2.96	-2.79	-2.83	-3.34	-3.34	-3.65	-0.97	-4.55	-1.67	-3.81	-4.03	-4.49	-1.49	-3.48	-2.21	-5.65	-3.09	-4.81	-0.81	-4.88
NO	-2.19	-2.37	-2.42	-3.40	-3.10	-2.79	-0.49	-4.09	-1.70	-3.59	-3.21	-4.05	-1.00	-3.52	-1.93	-4.57	-2.47	-4.20	-0.73	-4.62
OCF3	-2.12	-2.16	-2.66	-3.28	-3.58	-2.91	-0.70	-4.08	-1.86	-3.68	-3.39	-4.14	-1.18	-3.77	-2.00	-4.69	-2.51	-4.30	-0.85	-4.78
OH	-1.00	-1.44	-2.25	-3.26	-3.26	-1.70	0.01	-3.52	-2.00	-3.14	-2.32	-3.53	-0.63	-3.84	-1.49	-3.52	-1.78	-3.72	-0.79	-4.21
OME	-1.24	-1.76	-2.48	-3.52	-3.67	-1.99	-0.30	-3.79	-2.29	-3.48	-2.48	-3.81	-0.81	-4.03	-1.92	-3.68	-2.04	-3.97	-1.17	-4.62
SCH3	-1.92	-2.12	-2.95	-4.40	-3.48	-2.59	-0.48	-4.26	-2.99	-3.25	-3.03	-3.97	-1.34	-4.67	-1.95	-4.20	-2.35	-4.34	-1.97	-4.55
SH	-1.74	-1.86	-2.70	-4.07	-3.19	-2.41	-0.23	-4.02	-2.61	-3.04	-2.91	-3.73	-1.15	-4.39	-1.66	-4.01	-2.09	-4.05	-1.51	-4.30
SiF3	-2.14	-2.42	-2.34	-3.02	-3.65	-3.16	-0.80	-4.24	-1.56	-4.12	-3.51	-4.22	-1.14	-3.21	-2.42	-4.87	-2.66	-4.40	-0.51	-5.31
SiH3	-1.34	-2.13	-2.14	-3.41	-3.78	-2.38	-0.53	-3.91	-1.95	-4.01	-2.60	-3.93	-0.73	-3.61	-2.43	-3.85	-2.25	-3.93	-0.86	-5.22

Table C.10: SAPT0 interaction energies (kcal mol^{-1}) for monosubstituted dimers of benzene, borazine, and triazine (R = 4.0 Å).

X	Bz-X Bz	Bz-X BnB	Bz-X BnN	Bz-X Tz	Bz-X TzN	Bn(B)-X Bz	Bn(B)-X BnB	Bn(B)-X BnN	Bn(B)-X Tz	Bn(B)-X TzN	Bn(N)-X Bz	Bn(N)-X BnB	Bn(N)-X BnN	Bn(N)-X Tz	Bn(N)-X TzN	Tz-X Bz	Tz-X BnB	Tz-X BnN	Tz-X Tz	Tz-X TzN
H	-1.36	-1.82	-1.82	-2.79	-2.79	-1.82	-1.22	-2.26	-1.97	-2.33	-1.82	-2.26	-1.22	-2.33	-1.97	-2.79	-1.97	-2.33	-1.03	-2.89
BF2	-2.31	-2.36	-2.24	-2.77	-3.05	-2.54	-1.67	-2.63	-1.88	-2.81	-2.96	-2.83	-1.82	-2.26	-2.26	-3.65	-2.51	-2.83	-1.04	-3.39
CCH	-2.35	-2.32	-2.48	-3.27	-2.85	-2.42	-1.56	-2.71	-2.35	-2.42	-3.07	-2.81	-2.06	-2.81	-1.92	-3.41	-2.40	-2.80	-1.50	-3.05
CF3	-2.78	-2.45	-2.64	-3.02	-2.88	-3.12	-1.79	-3.05	-2.12	-2.51	-3.29	-2.91	-2.14	-2.59	-2.08	-4.13	-2.65	-3.19	-1.33	-3.12
CH2OH	-1.92	-2.28	-2.22	-2.96	-3.42	-2.20	-1.62	-2.51	-2.08	-2.86	-2.39	-2.72	-1.63	-2.54	-2.52	-3.19	-2.40	-2.64	-1.23	-3.48
CH3	-1.75	-2.10	-2.19	-3.07	-3.17	-2.06	-1.44	-2.51	-2.23	-2.61	-2.23	-2.55	-1.59	-2.64	-2.29	-3.00	-2.20	-2.60	-1.36	-3.21
CHO	-2.53	-2.39	-2.45	-2.99	-2.89	-2.67	-1.67	-2.76	-2.04	-2.63	-3.11	-2.85	-1.99	-2.51	-2.09	-3.77	-2.51	-2.96	-1.29	-3.15
CN	-2.88	-2.43	-2.70	-3.16	-2.61	-3.00	-1.70	-2.99	-2.24	-2.30	-3.62	-2.96	-2.34	-2.73	-1.79	-4.18	-2.63	-3.21	-1.46	-2.89
COCH3	-2.60	-2.54	-2.58	-3.17	-3.14	-2.78	-1.81	-2.90	-2.23	-2.80	-3.14	-2.98	-2.09	-2.69	-2.33	-3.85	-2.65	-3.10	-1.53	-3.34
COOCH3	-2.50	-2.55	-2.41	-2.95	-3.21	-2.71	-1.82	-2.77	-2.02	-2.86	-3.04	-2.98	-1.93	-2.44	-2.41	-3.73	-2.66	-2.91	-1.23	-3.46
COOH	-2.54	-2.50	-2.40	-2.88	-3.08	-2.75	-1.78	-2.76	-1.95	-2.77	-3.10	-2.94	-1.93	-2.36	-2.30	-3.79	-2.62	-2.91	-1.16	-3.36
F	-1.95	-1.92	-2.17	-2.78	-2.60	-2.22	-1.31	-2.48	-1.98	-2.16	-2.54	-2.46	-1.64	-2.48	-1.67	-3.42	-2.18	-2.68	-1.08	-2.68
NH2	-1.65	-2.02	-2.18	-2.98	-3.32	-1.80	-1.39	-2.31	-2.23	-2.60	-2.23	-2.53	-1.57	-2.65	-2.25	-2.77	-2.00	-2.50	-1.52	-3.30
NHCH3	-1.88	-2.23	-2.43	-3.24	-3.58	-2.09	-1.63	-2.58	-2.48	-2.85	-2.46	-2.74	-1.81	-2.91	-2.48	-3.04	-2.34	-2.75	-1.62	-3.54
NO2	-3.23	-2.68	-2.78	-2.87	-2.87	-3.45	-2.00	-3.15	-1.98	-2.59	-3.60	-3.09	-2.24	-2.45	-2.17	-4.63	-2.92	-3.38	-1.24	-3.18
NO	-2.69	-2.42	-2.51	-2.96	-2.77	-2.83	-1.68	-2.83	-2.01	-2.50	-3.04	-2.81	-1.93	-2.49	-2.05	-3.88	-2.54	-2.98	-1.22	-3.06
OCF3	-2.61	-2.41	-2.57	-2.95	-3.04	-2.88	-1.82	-2.85	-2.10	-2.60	-3.15	-2.92	-2.04	-2.65	-2.12	-3.93	-2.62	-3.05	-1.30	-3.18
OH	-1.74	-1.90	-2.18	-2.94	-2.84	-1.96	-1.29	-2.40	-2.17	-2.29	-2.34	-2.44	-1.60	-2.66	-1.82	-3.05	-2.07	-2.57	-1.25	-2.83
OME	-1.88	-2.09	-2.33	-3.11	-3.11	-2.13	-1.47	-2.57	-2.34	-2.50	-2.43	-2.62	-1.72	-2.80	-2.10	-3.12	-2.23	-2.71	-1.48	-3.09
SCH3	-2.35	-2.36	-2.68	-3.64	-3.02	-2.60	-1.70	-2.94	-2.83	-2.39	-2.78	-2.78	-2.05	-3.21	-2.11	-3.49	-2.48	-3.01	-2.00	-3.10
SH	-2.25	-2.21	-2.53	-3.43	-2.83	-2.51	-1.56	-2.79	-2.59	-2.25	-2.72	-2.65	-1.94	-3.03	-1.92	-3.40	-2.34	-2.85	-1.71	-2.93
SiF3	-2.86	-2.57	-2.61	-2.83	-3.14	-3.21	-1.93	-3.05	-1.98	-2.81	-3.43	-3.03	-2.16	-2.38	-2.37	-4.21	-2.74	-3.21	-1.15	-3.47
SiH3	-2.16	-2.33	-2.37	-3.08	-3.26	-2.55	-1.70	-2.77	-2.22	-2.81	-2.68	-2.77	-1.82	-2.61	-2.43	-3.39	-2.42	-2.82	-1.36	-3.47

Table C.11: SAPT0 electrostatic component (kcal mol^{-1}) for monosubstituted dimers of benzene, borazine, and triazine (R = R_e).

X	Bz-X Bz	Bz-X BnB	Bz-X BnN	Bz-X Tz	Bz-X TzN	Bn(B)-X Bz	Bn(B)-X BnB	Bn(B)-X BnN	Bn(B)-X Tz	Bn(B)-X TzN	Bn(N)-X Bz	Bn(N)-X BnB	Bn(N)-X BnN	Bn(N)-X Tz	Bn(N)-X TzN	Tz-X Bz	Tz-X BnB	Tz-X BnN	Tz-X Tz	Tz-X TzN
H	0.47	-1.09	-1.25	-1.91	-1.93	-1.28	-0.24	-6.30	-1.10	-2.82	-1.28	-6.34	-0.24	-2.81	-1.10	-1.91	-1.10	-2.81	0.81	-3.05
BF2	-0.39	-2.11	-1.54	-1.88	-2.30	-1.77	-0.54	-6.86	-0.66	-4.36	-2.71	-8.02	-0.74	-2.46	-1.46	-3.13	-1.74	-3.79	1.19	-4.72
CCH	-0.16	-1.51	-1.86	-2.42	-1.56	-1.77	-0.33	-7.31	-1.46	-3.01	-3.21	-6.90	-1.06	-4.09	-0.48	-2.68	-1.20	-3.92	0.70	-2.98
CF3	-1.11	-1.59	-2.13	-2.15	-1.97	-2.97	-0.55	-7.98	-0.95	-3.62	-3.15	-7.25	-1.33	-3.15	-1.00	-3.73	-1.63	-4.93	0.97	-3.52
CH2OH	0.27	-1.64	-1.56	-1.94	-2.89	-1.54	-0.48	-6.91	-0.95	-4.28	-1.94	-7.59	-0.43	-3.15	-1.59	-2.44	-1.48	-4.08	1.07	-4.31
CH3	0.37	-1.47	-1.63	-2.19	-2.50	-1.35	-0.32	-6.90	-1.27	-3.50	-1.68	-7.17	-0.48	-3.82	-1.29	-2.11	-1.13	-3.69	0.78	-3.73
CHO	-0.52	-1.79	-1.89	-1.89	-1.68	-2.17	-0.54	-6.72	-0.90	-3.81	-3.06	-7.61	-0.97	-3.47	-1.05	-3.03	-1.55	-4.02	0.94	-3.75
CN	-1.00	-1.66	-2.19	-2.16	-1.19	-2.53	-0.48	-7.33	-1.28	-2.25	-4.20	-7.10	-1.52	-4.00	-0.39	-3.83	-1.57	-4.79	0.77	-2.88
COCH3	-0.43	-1.74	-1.73	-2.18	-2.12	-1.89	-0.45	-7.23	-0.98	-3.73	-2.70	-7.54	-0.90	-3.63	-1.17	-2.88	-1.48	-3.98	0.84	-4.05
COOCH3	-0.53	-2.04	-1.73	-1.90	-2.41	-2.17	-0.65	-7.01	-0.73	-4.46	-2.86	-7.77	-0.80	-3.14	-1.42	-3.26	-1.69	-4.33	1.18	-4.52
COOH	-0.49	-1.89	-1.72	-1.81	-2.13	-2.03	-0.54	-7.01	-0.67	-3.96	-2.90	-7.88	-0.81	-3.35	-1.30	-3.11	-1.61	-4.04	1.18	-4.40
F	-0.15	-1.36	-1.91	-1.99	-1.82	-1.93	-0.29	-7.73	-1.14	-2.96	-2.31	-6.47	-0.76	-3.98	-0.50	-3.14	-1.31	-4.18	0.88	-2.97
NH2	0.51	-1.31	-1.86	-2.22	-3.15	-1.05	-0.32	-6.86	-1.44	-3.98	-1.70	-6.14	-0.55	-3.67	-1.35	-1.94	-0.93	-3.71	0.63	-4.63
NHCH3	0.44	-1.50	-2.31	-2.48	-3.34	-1.25	-0.50	-7.20	-1.56	-4.22	-1.66	-7.07	-0.73	-3.80	-1.48	-1.94	-1.25	-4.60	0.67	-5.32
NO2	-1.76	-2.12	-2.27	-2.01	-2.01	-3.51	-0.84	-7.81	-0.64	-3.86	-3.73	-7.75	-1.18	-2.69	-1.04	-4.26	-1.87	-4.94	1.18	-4.03
NO	-0.83	-1.89	-2.01	-1.80	-1.90	-2.53	-0.56	-7.72	-0.88	-3.70	-3.04	-7.64	-0.91	-3.45	-0.87	-3.23	-1.61	-4.34	1.00	-3.61
OCF3	-0.63	-1.67	-2.22	-1.91	-2.25	-2.65	-0.71	-7.75	-0.96	-4.06	-2.92	-6.92	-0.99	-3.67	-0.90	-3.67	-1.66	-4.74	1.01	-3.53
OH	0.24	-1.11	-1.88	-2.13	-2.11	-1.43	-0.17	-7.52	-1.36	-3.03	-1.98	-6.38	-0.66	-4.27	-0.64	-2.40	-1.06	-4.05	0.73	-3.11
OME	0.22	-1.16	-2.03	-2.14	-2.30	-1.49	-0.23	-7.53	-1.50	-3.71	-1.83	-6.64	-0.60	-3.75	-0.84	-2.20	-1.08	-4.57	0.68	-3.39
SCH3	-0.02	-1.14	-2.20	-2.91	-1.72	-1.64	-0.27	-7.96	-1.99	-2.37	-2.15	-6.58	-1.04	-4.95	-0.64	-2.29	-1.22	-4.41	0.21	-2.62
SH	-0.02	-1.24	-2.12	-2.55	-1.44	-1.92	-0.32	-7.61	-1.79	-1.90	-2.58	-5.86	-0.97	-4.55	-0.42	-2.38	-1.07	-3.92	0.41	-2.61
SiF3	-1.19	-2.21	-2.27	-1.69	-2.63	-3.05	-0.98	-7.84	-0.69	-4.97	-3.54	-7.90	-1.25	-3.38	-1.74	-4.01	-1.97	-4.89	1.23	-5.22
SiH3	0.06	-1.90	-1.59	-1.90	-2.59	-1.74	-0.57	-6.08	-1.04	-3.93	-2.30	-7.32	-0.64	-3.41	-1.56	-2.45	-1.45	-3.92	0.94	-4.25

Table C.12: SAPT0 exchange-repulsion component (kcal mol^{-1}) for monosubstituted dimers of benzene, borazine, and triazine (R = R_e).

X	Bz-X Bz	Bz-X BnB	Bz-X BnN	Bz-X Tz	Bz-X TzN	Bn(B)-X Bz	Bn(B)-X BnB	Bn(B)-X BnN	Bn(B)-X Tz	Bn(B)-X TzN	Bn(N)-X Bz	Bn(N)-X BnB	Bn(N)-X BnN	Bn(N)-X Tz	Bn(N)-X TzN	Tz-X Bz	Tz-X BnB	Tz-X BnN	Tz-X Tz	Tz-X TzN
H	3.09	4.90	5.36	4.34	4.38	5.42	4.25	12.02	4.26	5.75	5.42	12.10	4.28	5.73	4.25	4.34	4.26	5.73	0.99	4.68
BF2	3.53	6.55	5.55	5.07	4.98	5.45	4.27	13.17	4.31	7.83	6.50	14.57	4.54	6.12	4.79	6.02	5.47	7.55	2.69	7.10
CCH	3.51	5.87	6.01	5.23	4.51	5.91	4.58	13.38	5.06	6.96	7.78	13.18	5.20	8.01	4.16	5.72	4.51	7.70	2.53	5.29
CF3	4.63	5.45	6.05	5.39	5.11	6.83	4.23	13.82	4.69	7.53	6.87	13.72	5.70	6.98	4.85	6.19	5.08	8.86	2.71	5.99
CH2OH	3.66	6.31	6.22	5.21	5.81	6.16	4.86	13.58	4.85	8.09	6.86	14.62	5.04	7.10	4.93	5.90	5.45	8.80	2.60	6.49
CH3	3.51	6.21	6.12	5.13	5.46	5.84	4.89	13.18	4.81	7.04	6.38	13.95	4.98	7.87	4.67	5.31	4.79	7.63	2.68	5.89
CHO	3.59	5.96	5.99	4.50	4.19	6.15	4.61	12.27	4.51	7.45	7.15	14.12	4.94	7.66	4.70	5.47	5.12	7.55	2.54	6.16
CN	3.92	5.61	5.95	4.66	3.85	6.02	4.31	12.68	4.88	5.24	8.52	13.15	5.60	8.09	4.03	6.27	4.91	8.48	2.47	5.35
COCH3	3.87	5.96	5.81	5.26	5.11	5.73	4.39	13.39	4.65	7.28	6.87	14.10	5.17	7.98	4.80	5.63	5.21	7.64	2.86	6.83
COOCH3	4.21	6.49	6.13	5.11	5.43	6.34	4.97	13.05	4.61	8.43	7.19	14.16	5.23	7.57	4.97	6.53	5.45	8.73	2.57	7.17
COOH	3.63	5.96	5.87	4.84	4.87	5.60	4.24	12.92	4.39	7.41	6.81	14.29	4.85	8.06	4.72	5.69	4.98	7.87	2.61	7.00
F	3.21	5.48	5.82	4.57	4.67	5.76	4.07	13.78	4.34	6.51	5.94	12.10	4.62	7.76	3.97	5.51	4.47	7.48	2.31	5.24
NH2	4.54	6.09	7.93	5.52	6.43	7.14	6.35	15.55	5.77	8.21	5.81	14.53	6.16	9.64	5.01	6.55	6.17	10.80	3.64	7.27
NHCH3	3.92	6.70	7.81	6.19	6.81	6.36	5.66	14.37	5.47	8.66	6.45	14.12	5.75	7.62	5.32	5.77	5.66	9.91	3.11	8.92
NO2	5.16	6.08	6.14	5.26	5.26	7.35	4.78	13.43	4.32	7.73	7.54	13.84	5.02	6.35	4.50	6.26	4.97	8.64	2.59	6.97
NO	3.87	6.02	6.01	4.25	5.15	6.39	4.54	13.73	4.42	7.53	7.17	14.13	4.89	7.56	4.15	5.44	5.04	8.02	2.26	6.08
OCF3	3.87	5.86	6.54	5.02	5.34	6.77	4.83	14.18	4.78	8.50	6.88	12.85	5.22	7.82	4.62	6.60	5.17	8.94	2.67	5.92
OH	3.21	5.28	6.10	4.83	5.02	5.66	4.13	13.96	4.60	6.72	6.16	12.28	4.87	8.05	4.24	5.11	4.32	7.71	2.47	5.30
OME	3.71	5.48	6.69	4.95	5.26	6.05	4.49	14.14	5.09	8.12	6.25	12.89	4.99	7.18	4.44	5.27	4.72	9.08	2.57	5.76
SCH3	3.95	5.47	6.81	5.90	5.08	5.81	4.55	14.67	5.41	6.47	6.77	13.27	5.95	9.09	4.86	5.34	5.23	8.71	3.24	5.16
SH	3.45	5.57	6.44	5.13	4.36	6.12	4.46	13.90	5.16	5.20	7.34	11.70	5.31	8.30	4.13	5.03	4.29	7.54	2.76	5.01
SiF3	4.66	6.62	6.75	4.87	5.81	7.18	5.50	14.35	4.65	9.33	7.66	14.49	5.51	8.51	5.65	6.94	5.80	9.24	2.63	8.22
SiH3	3.43	6.84	5.85	4.71	5.65	5.88	5.09	11.55	4.72	7.55	7.01	14.10	4.84	7.65	5.21	5.59	5.45	8.09	2.56	6.46

Table C.13: SAPT0 induction component (kcal mol^{-1}) for monosubstituted dimers of benzene, borazine, and triazine (R = R_e).

X	Bz-X Bz	Bz-X BnB	Bz-X BnN	Bz-X Tz	Bz-X TzN	Bn(B)-X Bz	Bn(B)-X BnB	Bn(B)-X BnN	Bn(B)-X Tz	Bn(B)-X TzN	Bn(N)-X Bz	Bn(N)-X BnB	Bn(N)-X BnN	Bn(N)-X Tz	Bn(N)-X TzN	Tz-X Bz	Tz-X BnB	Tz-X BnN	Tz-X Tz	Tz-X TzN
H	-0.23	-0.33	-0.36	-0.29	-0.29	-0.36	-0.15	-1.01	-0.20	-0.44	-0.36	-1.02	-0.15	-0.44	-0.20	-0.29	-0.20	-0.44	-0.05	-0.32
BF2	-0.20	-0.38	-0.29	-0.28	-0.26	-0.40	-0.19	-1.19	-0.22	-0.65	-0.46	-1.36	-0.18	-0.49	-0.24	-0.48	-0.37	-0.69	-0.19	-0.59
CCH	-0.25	-0.36	-0.38	-0.33	-0.29	-0.41	-0.18	-1.15	-0.26	-0.55	-0.61	-1.24	-0.24	-0.70	-0.23	-0.40	-0.24	-0.62	-0.16	-0.40
CF3	-0.25	-0.30	-0.32	-0.29	-0.26	-0.50	-0.18	-1.27	-0.24	-0.61	-0.53	-1.24	-0.25	-0.58	-0.26	-0.53	-0.35	-0.84	-0.23	-0.52
CH2OH	-0.30	-0.45	-0.47	-0.38	-0.43	-0.44	-0.21	-1.18	-0.27	-0.67	-0.50	-1.29	-0.24	-0.59	-0.28	-0.44	-0.32	-0.73	-0.17	-0.51
CH3	-0.27	-0.41	-0.44	-0.35	-0.38	-0.39	-0.18	-1.12	-0.24	-0.56	-0.43	-1.17	-0.20	-0.62	-0.23	-0.35	-0.23	-0.59	-0.15	-0.41
CHO	-0.22	-0.35	-0.32	-0.26	-0.23	-0.45	-0.19	-1.11	-0.23	-0.61	-0.56	-1.34	-0.22	-0.65	-0.25	-0.45	-0.33	-0.69	-0.19	-0.51
CN	-0.23	-0.32	-0.32	-0.26	-0.21	-0.44	-0.18	-1.16	-0.25	-0.42	-0.75	-1.37	-0.31	-0.76	-0.26	-0.55	-0.37	-0.83	-0.22	-0.49
COCH3	-0.25	-0.37	-0.35	-0.32	-0.30	-0.44	-0.20	-1.23	-0.25	-0.61	-0.54	-1.33	-0.25	-0.68	-0.27	-0.46	-0.34	-0.69	-0.21	-0.56
COOCH3	-0.24	-0.38	-0.34	-0.30	-0.30	-0.44	-0.19	-1.15	-0.23	-0.68	-0.52	-1.29	-0.21	-0.61	-0.25	-0.48	-0.32	-0.75	-0.17	-0.55
COOH	-0.22	-0.34	-0.31	-0.27	-0.26	-0.40	-0.16	-1.15	-0.22	-0.59	-0.51	-1.33	-0.21	-0.66	-0.24	-0.45	-0.31	-0.70	-0.18	-0.56
F	-0.20	-0.30	-0.35	-0.25	-0.27	-0.38	-0.14	-1.19	-0.20	-0.50	-0.46	-1.10	-0.20	-0.64	-0.21	-0.44	-0.27	-0.68	-0.17	-0.43
NH2	-0.31	-0.42	-0.55	-0.41	-0.52	-0.40	-0.22	-1.15	-0.30	-0.69	-0.44	-0.99	-0.22	-0.58	-0.26	-0.39	-0.22	-0.60	-0.16	-0.58
NHCH3	-0.36	-0.48	-0.66	-0.47	-0.57	-0.46	-0.27	-1.25	-0.33	-0.75	-0.46	-1.17	-0.26	-0.60	-0.29	-0.44	-0.32	-0.83	-0.22	-0.74
NO2	-0.29	-0.36	-0.33	-0.27	-0.27	-0.59	-0.24	-1.33	-0.25	-0.68	-0.64	-1.39	-0.26	-0.57	-0.27	-0.66	-0.46	-0.97	-0.29	-0.70
NO	-0.23	-0.34	-0.31	-0.24	-0.27	-0.45	-0.17	-1.25	-0.22	-0.61	-0.54	-1.32	-0.20	-0.62	-0.21	-0.46	-0.33	-0.74	-0.18	-0.51
OCF3	-0.23	-0.30	-0.37	-0.27	-0.30	-0.46	-0.18	-1.23	-0.24	-0.67	-0.53	-1.14	-0.24	-0.64	-0.25	-0.53	-0.32	-0.81	-0.20	-0.50
OH	-0.25	-0.33	-0.44	-0.31	-0.36	-0.39	-0.16	-1.20	-0.24	-0.54	-0.46	-1.08	-0.21	-0.66	-0.23	-0.37	-0.22	-0.64	-0.15	-0.41
OME	-0.29	-0.36	-0.50	-0.34	-0.39	-0.42	-0.19	-1.23	-0.27	-0.66	-0.46	-1.12	-0.22	-0.58	-0.24	-0.39	-0.25	-0.76	-0.16	-0.45
SCH3	-0.31	-0.39	-0.50	-0.42	-0.39	-0.44	-0.23	-1.27	-0.33	-0.55	-0.53	-1.20	-0.29	-0.80	-0.29	-0.41	-0.32	-0.70	-0.23	-0.43
SH	-0.26	-0.36	-0.44	-0.35	-0.32	-0.44	-0.21	-1.18	-0.30	-0.43	-0.56	-1.05	-0.24	-0.72	-0.24	-0.37	-0.26	-0.60	-0.19	-0.40
SiF3	-0.25	-0.37	-0.34	-0.26	-0.30	-0.56	-0.26	-1.39	-0.26	-0.82	-0.57	-1.36	-0.25	-0.71	-0.30	-0.61	-0.43	-0.93	-0.23	-0.75
SiH3	-0.23	-0.43	-0.37	-0.30	-0.35	-0.42	-0.21	-1.01	-0.24	-0.62	-0.46	-1.23	-0.18	-0.60	-0.26	-0.41	-0.31	-0.68	-0.16	-0.50

Table C.14: SAPT0 dispersion component (kcal mol^{-1}) for monosubstituted dimers of benzene, borazine, and triazine (R = R_e).

X	Bz-X Bz	Bz-X BnB	Bz-X BnN	Bz-X Tz	Bz-X TzN	Bn(B)-X Bz	Bn(B)-X BnB	Bn(B)-X BnN	Bn(B)-X Tz	Bn(B)-X TzN	Bn(N)-X Bz	Bn(N)-X BnB	Bn(N)-X BnN	Bn(N)-X Tz	Bn(N)-X TzN	Tz-X Bz	Tz-X BnB	Tz-X BnN	Tz-X Tz	Tz-X TzN
H	-4.70	-5.34	-5.57	-5.32	-5.34	-5.61	-4.50	-7.80	-4.84	-5.68	-5.60	-7.83	-4.51	-5.68	-4.84	-5.32	-4.84	-5.68	-2.78	-5.52
BF2	-5.32	-6.55	-5.99	-6.08	-6.01	-5.95	-4.81	-8.59	-5.16	-6.94	-6.49	-9.15	-4.95	-6.24	-5.44	-6.66	-5.86	-6.89	-4.59	-7.15
CCH	-5.59	-6.47	-6.55	-6.44	-6.00	-6.37	-5.11	-8.90	-5.70	-6.74	-7.44	-9.05	-5.57	-7.39	-5.37	-6.78	-5.58	-7.26	-4.67	-6.48
CF3	-6.24	-6.17	-6.48	-6.49	-6.30	-6.76	-4.89	-9.02	-5.51	-6.97	-6.87	-9.04	-5.70	-6.87	-5.67	-6.88	-5.76	-7.65	-4.76	-6.78
CH2OH	-5.64	-6.62	-6.60	-6.36	-6.67	-6.51	-5.24	-8.99	-5.61	-7.23	-7.01	-9.50	-5.48	-6.98	-5.77	-6.84	-6.02	-7.70	-4.70	-7.09
CH3	-5.44	-6.46	-6.44	-6.20	-6.38	-6.26	-5.19	-8.75	-5.50	-6.68	-6.65	-9.14	-5.34	-7.18	-5.52	-6.40	-5.59	-7.09	-4.66	-6.67
CHO	-5.48	-6.38	-6.36	-5.87	-5.66	-6.37	-5.03	-8.41	-5.33	-6.85	-6.94	-9.17	-5.27	-7.07	-5.51	-6.47	-5.78	-7.03	-4.56	-6.81
CN	-5.75	-6.24	-6.39	-6.02	-5.49	-6.30	-4.88	-8.53	-5.53	-5.82	-7.57	-8.87	-5.61	-7.29	-5.18	-6.92	-5.68	-7.44	-4.53	-6.40
COCH3	-5.93	-6.66	-6.53	-6.55	-6.43	-6.44	-5.16	-9.12	-5.63	-7.03	-7.15	-9.58	-5.66	-7.52	-5.82	-6.90	-6.14	-7.43	-5.05	-7.46
COOCH3	-6.11	-6.88	-6.63	-6.41	-6.56	-6.69	-5.41	-8.91	-5.56	-7.46	-7.23	-9.52	-5.63	-7.26	-5.85	-7.33	-6.22	-7.82	-4.78	-7.55
COOH	-5.60	-6.48	-6.38	-6.16	-6.14	-6.19	-4.93	-8.73	-5.35	-6.92	-6.89	-9.38	-5.32	-7.35	-5.61	-6.72	-5.84	-7.30	-4.71	-7.35
F	-4.87	-5.71	-5.92	-5.54	-5.61	-5.76	-4.42	-8.37	-4.90	-6.04	-5.95	-7.95	-4.78	-6.69	-4.80	-5.99	-4.98	-6.51	-4.04	-5.88
NH2	-5.33	-6.26	-6.67	-6.34	-6.84	-6.12	-5.05	-8.75	-5.57	-7.07	-6.60	-8.36	-5.43	-6.89	-5.66	-6.30	-5.34	-7.00	-4.55	-7.23
NHCH3	-5.97	-6.94	-7.57	-7.02	-7.35	-6.86	-5.85	-9.53	-6.12	-7.69	-7.03	-9.59	-6.00	-7.39	-6.12	-7.01	-6.32	-8.43	-5.23	-8.46
NO2	-6.62	-6.58	-6.57	-6.42	-6.42	-7.01	-5.20	-8.90	-5.31	-7.07	-7.25	-9.24	-5.42	-6.60	-5.51	-7.01	-5.82	-7.64	-4.70	-7.34
NO	-5.67	-6.40	-6.36	-5.72	-6.23	-6.43	-4.95	-8.83	-5.24	-6.84	-6.92	-9.14	-5.22	-7.00	-5.19	-6.39	-5.68	-7.18	-4.30	-6.72
OCF3	-5.78	-6.39	-6.79	-6.29	-6.46	-6.78	-5.24	-9.16	-5.58	-7.42	-6.97	-8.85	-5.56	-7.30	-5.61	-7.15	-5.84	-7.72	-4.75	-6.80
OH	-5.01	-5.74	-6.22	-5.81	-5.93	-5.88	-4.58	-8.63	-5.16	-6.28	-6.26	-8.25	-5.06	-7.00	-5.08	-5.97	-5.05	-6.79	-4.28	-6.07
OME	-5.62	-6.13	-6.80	-6.13	-6.31	-6.41	-5.04	-9.11	-5.68	-7.19	-6.65	-8.89	-5.41	-6.94	-5.46	-6.43	-5.61	-7.78	-4.62	-6.65
SCH3	-6.13	-6.46	-7.20	-7.02	-6.57	-6.62	-5.32	-9.65	-6.13	-6.79	-7.27	-9.35	-6.17	-8.12	-6.00	-6.88	-6.21	-8.00	-5.42	-6.69
SH	-5.54	-6.25	-6.76	-6.37	-5.92	-6.49	-5.02	-9.05	-5.77	-5.91	-7.24	-8.44	-5.61	-7.52	-5.36	-6.36	-5.38	-7.13	-4.82	-6.31
SiF3	-6.22	-6.74	-6.77	-6.15	-6.64	-6.94	-5.53	-9.18	-5.49	-7.71	-7.20	-9.27	-5.59	-7.50	-6.04	-7.27	-6.13	-7.78	-4.69	-7.83
SiH3	-5.49	-6.91	-6.40	-6.09	-6.59	-6.46	-5.44	-8.37	-5.60	-7.07	-7.07	-9.33	-5.37	-7.22	-5.90	-6.72	-6.07	-7.42	-4.69	-7.09

Table C.15: SAPT0 electrostatic component (kcal mol^{-1}) for monosubstituted dimers of benzene, borazine, and triazine (R = 3.5 Å).

X	Bz-X Bz	Bz-X BnB	Bz-X BnN	Bz-X Tz	Bz-X TzN	Bn(B)-X Bz	Bn(B)-X BnB	Bn(B)-X BnN	Bn(B)-X Tz	Bn(B)-X TzN	Bn(N)-X Bz	Bn(N)-X BnB	Bn(N)-X BnN	Bn(N)-X Tz	Bn(N)-X TzN	Tz-X Bz	Tz-X BnB	Tz-X BnN	Tz-X Tz	Tz-X TzN
H	-2.22	-2.41	-2.41	-3.20	-3.20	-2.41	-0.76	-3.24	-1.47	-2.66	-2.41	-3.24	-0.76	-2.66	-1.47	-3.20	-1.47	-2.66	0.63	-3.07
BF2	-3.10	-2.87	-2.63	-2.82	-3.37	-2.99	-1.13	-3.41	-1.00	-3.24	-3.51	-3.62	-1.22	-2.11	-1.67	-3.91	-1.84	-2.95	1.04	-3.60
CCH	-2.83	-2.41	-2.73	-3.26	-2.58	-2.82	-0.82	-3.53	-1.63	-2.34	-3.40	-3.27	-1.37	-2.74	-0.74	-3.53	-1.55	-2.89	0.44	-2.72
CF3	-3.57	-2.73	-3.06	-2.90	-2.86	-3.72	-1.12	-3.95	-1.17	-2.61	-3.90	-3.59	-1.61	-2.42	-1.18	-4.57	-1.91	-3.45	0.80	-2.98
CH2OH	-2.32	-2.51	-2.42	-2.82	-3.63	-2.49	-0.96	-3.18	-1.17	-3.05	-2.58	-3.34	-0.80	-2.37	-1.78	-3.25	-1.63	-2.66	0.88	-3.49
CH3	-2.24	-2.34	-2.53	-3.15	-3.38	-2.37	-0.75	-3.27	-1.50	-2.76	-2.49	-3.21	-0.87	-2.67	-1.55	-3.08	-1.40	-2.72	0.55	-3.19
CHO	-3.17	-2.67	-2.77	-2.97	-2.91	-3.10	-1.01	-3.55	-1.16	-2.84	-3.54	-3.46	-1.35	-2.38	-1.23	-3.98	-1.72	-3.08	0.76	-3.07
CN	-3.52	-2.57	-3.02	-3.13	-2.38	-3.51	-0.98	-3.86	-1.44	-2.29	-4.07	-3.43	-1.72	-2.60	-0.66	-4.45	-1.77	-3.36	0.56	-2.56
COCH3	-2.98	-2.65	-2.70	-3.01	-3.03	-2.99	-0.98	-3.52	-1.22	-2.86	-3.31	-3.42	-1.23	-2.41	-1.34	-3.79	-1.65	-3.04	0.65	-3.08
COOCH3	-2.97	-2.72	-2.54	-2.73	-3.17	-3.03	-1.05	-3.43	-0.96	-3.01	-3.30	-3.49	-1.09	-2.09	-1.53	-3.78	-1.76	-2.84	1.03	-3.33
COOH	-3.13	-2.76	-2.61	-2.72	-3.10	-3.17	-1.09	-3.50	-0.95	-2.98	-3.49	-3.53	-1.19	-2.08	-1.47	-3.97	-1.81	-2.94	1.04	-3.29
F	-2.81	-2.28	-2.77	-2.99	-2.78	-2.90	-0.78	-3.51	-1.41	-2.36	-3.15	-3.23	-1.15	-2.70	-0.78	-3.92	-1.56	-3.05	0.70	-2.61
NH2	-2.08	-2.24	-2.55	-3.01	-3.65	-2.10	-0.79	-3.07	-1.60	-2.75	-2.47	-3.20	-0.87	-2.74	-1.49	-2.93	-1.19	-2.72	0.20	-3.38
NHCH3	-2.20	-2.39	-2.75	-3.16	-3.82	-2.13	-0.83	-3.12	-1.63	-2.80	-2.64	-3.38	-1.07	-2.92	-1.65	-2.86	-1.43	-2.74	0.43	-3.42
NO2	-3.81	-2.81	-2.96	-2.69	-2.69	-3.94	-1.23	-3.90	-0.88	-2.67	-3.98	-3.59	-1.49	-2.10	-1.22	-4.84	-2.02	-3.38	1.07	-2.89
NO	-3.36	-2.66	-2.82	-2.91	-2.68	-3.34	-1.01	-3.68	-1.14	-2.66	-3.49	-3.44	-1.28	-2.37	-1.18	-4.16	-1.77	-3.12	0.84	-2.93
OCF3	-3.23	-2.62	-2.90	-2.74	-3.01	-3.37	-1.16	-3.62	-1.14	-2.61	-3.56	-3.55	-1.32	-2.48	-1.08	-4.24	-1.88	-3.20	0.84	-2.95
OH	-2.41	-2.16	-2.70	-3.11	-3.03	-2.45	-0.68	-3.30	-1.60	-2.38	-2.78	-3.13	-1.03	-2.88	-0.90	-3.36	-1.37	-2.86	0.52	-2.75
OME	-2.33	-2.21	-2.68	-3.13	-3.20	-2.39	-0.69	-3.28	-1.62	-2.46	-2.65	-3.16	-0.97	-2.85	-1.10	-3.15	-1.32	-2.80	0.44	-2.86
SCH3	-2.60	-2.28	-2.87	-3.57	-2.60	-2.85	-0.86	-3.69	-2.13	-2.01	-2.87	-3.16	-1.25	-3.17	-0.80	-3.42	-1.49	-3.06	-0.08	-2.51
SH	-2.75	-2.32	-2.89	-3.48	-2.55	-2.99	-0.93	-3.71	-1.99	-2.05	-3.05	-3.21	-1.32	-3.12	-0.73	-3.62	-1.59	-3.09	0.09	-2.56
SiF3	-3.68	-3.04	-3.00	-2.67	-3.39	-3.70	-1.35	-3.81	-0.93	-3.12	-4.04	-3.83	-1.60	-2.10	-1.74	-4.55	-2.09	-3.36	1.09	-3.60
SiH3	-2.73	-2.67	-2.68	-3.07	-3.47	-2.85	-1.04	-3.47	-1.32	-3.00	-3.02	-3.47	-1.14	-2.49	-1.73	-3.46	-1.65	-2.89	0.71	-3.52

Table C.16: SAPT0 exchange-repulsion component (kcal mol^{-1}) for monosubstituted dimers of benzene, borazine, and triazine (R = 3.5 Å).

X	Bz-X Bz	Bz-X BnB	Bz-X BnN	Bz-X Tz	Bz-X TzN	Bn(B)-X Bz	Bn(B)-X BnB	Bn(B)-X BnN	Bn(B)-X Tz	Bn(B)-X TzN	Bn(N)-X Bz	Bn(N)-X BnB	Bn(N)-X BnN	Bn(N)-X Tz	Bn(N)-X TzN	Tz-X Bz	Tz-X BnB	Tz-X BnN	Tz-X Tz	Tz-X TzN
H	11.29	8.55	8.55	7.70	7.70	8.54	6.74	6.13	5.61	5.40	8.54	6.13	6.74	5.40	5.61	7.70	5.61	5.40	4.77	4.71
BF2	11.45	8.55	8.67	7.66	7.71	8.80	6.94	6.32	5.73	5.53	8.58	6.10	6.74	5.30	5.54	8.02	5.81	5.65	4.89	4.87
CCH	11.01	8.36	8.27	7.36	7.36	8.68	6.93	6.23	5.64	5.42	8.25	5.96	6.43	5.08	5.26	7.82	5.82	5.53	4.78	4.73
CF3	11.37	8.62	8.50	7.43	7.48	8.74	6.97	6.21	5.56	5.36	8.75	6.38	6.81	5.28	5.52	8.20	6.10	5.75	4.87	4.85
CH2OH	11.29	8.68	8.51	7.62	7.62	8.75	7.04	6.29	5.69	5.49	8.56	6.27	6.71	5.33	5.54	7.99	6.00	5.66	4.88	4.84
CH3	11.29	8.62	8.51	7.67	7.67	8.64	6.88	6.21	5.65	5.45	8.55	6.19	6.71	5.37	5.59	7.84	5.82	5.53	4.82	4.78
CHO	11.13	8.33	8.38	7.41	7.45	8.63	6.80	6.16	5.59	5.39	8.40	5.99	6.57	5.16	5.39	7.86	5.74	5.52	4.77	4.75
CN	10.90	8.16	8.15	7.19	7.22	8.58	6.77	6.12	5.51	5.31	8.20	5.84	6.37	4.99	5.20	7.76	5.68	5.44	4.68	4.65
COCH3	11.20	8.41	8.45	7.47	7.51	8.69	6.87	6.22	5.63	5.43	8.45	6.05	6.63	5.20	5.43	7.93	5.81	5.60	4.81	4.79
COOCH3	11.07	8.28	8.34	7.38	7.42	8.61	6.78	6.15	5.57	5.38	8.32	5.93	6.51	5.11	5.34	7.81	5.68	5.49	4.74	4.72
COOH	11.04	8.24	8.31	7.33	7.39	8.60	6.77	6.14	5.56	5.37	8.30	5.90	6.49	5.09	5.32	7.81	5.68	5.48	4.73	4.71
F	10.76	8.12	8.02	7.24	7.22	8.30	6.51	5.90	5.38	5.19	8.11	5.76	6.29	5.00	5.20	7.43	5.40	5.15	4.51	4.45
NH2	11.20	8.64	8.41	7.65	7.61	8.67	6.93	6.28	5.68	5.48	8.45	6.15	6.61	5.31	5.50	7.56	5.61	5.33	4.64	4.72
NHCH3	11.74	9.22	8.91	8.01	7.98	8.81	7.11	6.42	5.73	5.54	9.05	6.78	7.16	5.72	5.92	8.21	6.31	5.92	5.04	4.98
NO2	10.70	7.93	7.99	7.07	7.07	8.44	6.58	5.98	5.39	5.20	8.16	5.78	6.34	4.96	5.19	7.64	5.50	5.31	4.56	4.54
NO	10.90	8.13	8.18	7.22	7.26	8.50	6.68	6.05	5.48	5.29	8.32	5.93	6.50	5.11	5.34	7.73	5.62	5.40	4.67	4.64
OCF3	11.11	8.51	8.31	7.33	7.32	8.63	6.86	6.21	5.49	5.30	8.49	6.21	6.62	5.16	5.36	7.98	5.97	5.67	4.75	4.70
OH	10.91	8.32	8.15	7.41	7.38	8.39	6.63	6.01	5.46	5.27	8.23	5.90	6.41	5.13	5.33	7.50	5.52	5.25	4.59	4.54
OME	11.13	8.51	8.35	7.55	7.53	8.46	6.69	6.08	5.50	5.32	8.42	6.07	6.58	5.25	5.46	7.66	5.66	5.39	4.68	4.63
SCH3	11.26	8.75	8.50	7.57	7.51	8.98	7.31	6.55	5.84	5.59	8.61	6.39	6.75	5.35	5.51	8.16	6.22	5.88	5.00	4.92
SH	11.17	8.68	8.40	7.49	7.43	8.94	7.28	6.49	5.81	5.56	8.55	6.36	6.69	5.30	5.45	8.11	6.19	5.81	4.97	4.88
SiF3	11.63	8.81	8.76	7.66	7.71	8.91	7.10	6.37	5.71	5.51	8.93	6.51	6.98	5.43	5.67	8.31	6.20	5.85	4.99	4.97
SiH3	11.66	8.93	8.84	7.85	7.87	8.91	7.15	6.43	5.81	5.60	8.91	6.54	7.01	5.54	5.76	8.22	6.18	5.83	5.04	4.99

Table C.17: SAPT0 induction component (kcal mol^{-1}) for monosubstituted dimers of benzene, borazine, and triazine (R = 3.5 Å).

X	Bz-X Bz	Bz-X BnB	Bz-X BnN	Bz-X Tz	Bz-X TzN	Bn(B)-X Bz	Bn(B)-X BnB	Bn(B)-X BnN	Bn(B)-X Tz	Bn(B)-X TzN	Bn(N)-X Bz	Bn(N)-X BnB	Bn(N)-X BnN	Bn(N)-X Tz	Bn(N)-X TzN	Tz-X Bz	Tz-X BnB	Tz-X BnN	Tz-X Tz	Tz-X TzN
H	-0.51	-0.52	-0.52	-0.46	-0.46	-0.52	-0.23	-0.49	-0.26	-0.42	-0.52	-0.49	-0.23	-0.42	-0.26	-0.46	-0.26	-0.42	-0.25	-0.32
BF2	-0.45	-0.50	-0.43	-0.41	-0.39	-0.60	-0.29	-0.54	-0.29	-0.45	-0.59	-0.54	-0.26	-0.42	-0.28	-0.60	-0.38	-0.53	-0.32	-0.42
CCH	-0.51	-0.49	-0.49	-0.44	-0.44	-0.56	-0.26	-0.51	-0.29	-0.43	-0.64	-0.55	-0.29	-0.44	-0.29	-0.51	-0.31	-0.45	-0.28	-0.35
CF3	-0.46	-0.46	-0.43	-0.39	-0.37	-0.61	-0.28	-0.55	-0.28	-0.43	-0.64	-0.56	-0.29	-0.44	-0.29	-0.65	-0.40	-0.56	-0.35	-0.43
CH2OH	-0.60	-0.57	-0.60	-0.51	-0.53	-0.58	-0.29	-0.53	-0.31	-0.46	-0.60	-0.54	-0.30	-0.44	-0.30	-0.56	-0.34	-0.48	-0.30	-0.38
CH3	-0.55	-0.53	-0.57	-0.48	-0.50	-0.54	-0.25	-0.50	-0.28	-0.43	-0.55	-0.49	-0.26	-0.42	-0.27	-0.48	-0.28	-0.42	-0.26	-0.34
CHO	-0.47	-0.48	-0.44	-0.41	-0.39	-0.59	-0.27	-0.54	-0.28	-0.44	-0.63	-0.55	-0.28	-0.44	-0.29	-0.58	-0.36	-0.51	-0.32	-0.40
CN	-0.46	-0.45	-0.43	-0.39	-0.37	-0.59	-0.27	-0.54	-0.28	-0.42	-0.72	-0.62	-0.35	-0.48	-0.32	-0.64	-0.41	-0.56	-0.36	-0.43
COCH3	-0.51	-0.51	-0.48	-0.44	-0.42	-0.61	-0.29	-0.55	-0.30	-0.46	-0.64	-0.56	-0.30	-0.44	-0.30	-0.59	-0.37	-0.52	-0.32	-0.40
COOCH3	-0.47	-0.48	-0.44	-0.41	-0.39	-0.57	-0.25	-0.51	-0.27	-0.42	-0.58	-0.51	-0.26	-0.41	-0.26	-0.55	-0.33	-0.48	-0.29	-0.37
COOH	-0.46	-0.47	-0.42	-0.40	-0.38	-0.57	-0.25	-0.52	-0.27	-0.42	-0.60	-0.52	-0.27	-0.41	-0.27	-0.57	-0.34	-0.50	-0.31	-0.38
F	-0.46	-0.43	-0.47	-0.38	-0.40	-0.51	-0.22	-0.47	-0.25	-0.39	-0.59	-0.50	-0.26	-0.41	-0.27	-0.55	-0.32	-0.48	-0.29	-0.37
NH2	-0.63	-0.56	-0.66	-0.53	-0.60	-0.56	-0.29	-0.52	-0.32	-0.46	-0.56	-0.49	-0.27	-0.42	-0.28	-0.48	-0.28	-0.42	-0.27	-0.39
NHCH3	-0.69	-0.61	-0.73	-0.57	-0.65	-0.60	-0.32	-0.55	-0.34	-0.48	-0.60	-0.54	-0.32	-0.45	-0.32	-0.58	-0.35	-0.50	-0.33	-0.43
NO2	-0.48	-0.46	-0.42	-0.36	-0.36	-0.66	-0.31	-0.58	-0.31	-0.46	-0.69	-0.58	-0.32	-0.45	-0.31	-0.75	-0.49	-0.65	-0.42	-0.50
NO	-0.47	-0.46	-0.41	-0.39	-0.37	-0.58	-0.25	-0.52	-0.27	-0.42	-0.61	-0.52	-0.26	-0.42	-0.27	-0.59	-0.36	-0.52	-0.32	-0.40
OCF3	-0.47	-0.43	-0.47	-0.38	-0.40	-0.57	-0.25	-0.51	-0.27	-0.41	-0.63	-0.53	-0.29	-0.42	-0.28	-0.61	-0.36	-0.53	-0.33	-0.41
OH	-0.53	-0.47	-0.56	-0.44	-0.49	-0.53	-0.25	-0.49	-0.28	-0.42	-0.58	-0.50	-0.27	-0.42	-0.28	-0.50	-0.28	-0.44	-0.27	-0.35
OME	-0.57	-0.51	-0.60	-0.47	-0.52	-0.55	-0.26	-0.51	-0.29	-0.44	-0.59	-0.51	-0.29	-0.42	-0.29	-0.52	-0.29	-0.45	-0.28	-0.36
SCH3	-0.61	-0.57	-0.60	-0.52	-0.54	-0.62	-0.35	-0.55	-0.36	-0.48	-0.64	-0.57	-0.32	-0.47	-0.32	-0.57	-0.37	-0.48	-0.35	-0.41
SH	-0.56	-0.53	-0.55	-0.48	-0.49	-0.59	-0.32	-0.52	-0.33	-0.46	-0.63	-0.56	-0.30	-0.46	-0.31	-0.55	-0.35	-0.46	-0.33	-0.39
SiF3	-0.46	-0.49	-0.44	-0.41	-0.39	-0.67	-0.33	-0.60	-0.31	-0.48	-0.64	-0.59	-0.30	-0.45	-0.30	-0.70	-0.46	-0.62	-0.38	-0.48
SiH3	-0.51	-0.55	-0.52	-0.47	-0.47	-0.59	-0.29	-0.54	-0.29	-0.45	-0.57	-0.53	-0.26	-0.43	-0.28	-0.55	-0.35	-0.49	-0.30	-0.39

Table C.18: SAPT0 dispersion component (kcal mol^{-1}) for monosubstituted dimers of benzene, borazine, and triazine (R = 3.5 Å).

X	Bz-X	Bz-X	Bz-X	Bz-X	Bz-X	Bn(B)-X	Bn(B)-X	Bn(B)-X	Bn(B)-X	Bn(B)-X	Bn(N)-X	Bn(N)-X	Bn(N)-X	Bn(N)-X	Bn(N)-X	Tz-X	Tz-X	Tz-X	Tz-X	Tz-X
	Bz	BnB	BnN	Tz	TzN	Bz	BnB	BnN	Tz	TzN	Bz	BnB	BnN	Tz	TzN	Bz	BnB	BnN	Tz	TzN
H	-8.76	-6.98	-6.98	-7.00	-7.00	-6.98	-5.56	-5.61	-5.50	-5.52	-6.98	-5.61	-5.56	-5.52	-5.50	-7.00	-5.50	-5.52	-5.52	-5.54
BF2	-9.33	-7.44	-7.41	-7.39	-7.39	-7.48	-6.00	-6.02	-5.87	-5.89	-7.42	-6.00	-5.93	-5.83	-5.81	-7.63	-6.02	-6.02	-5.99	-6.00
CCH	-9.56	-7.64	-7.61	-7.55	-7.53	-7.64	-6.16	-6.17	-5.99	-6.00	-7.64	-6.20	-6.12	-5.99	-5.96	-7.86	-6.25	-6.23	-6.16	-6.16
CF3	-9.58	-7.65	-7.61	-7.54	-7.52	-7.60	-6.13	-6.13	-5.95	-5.96	-7.72	-6.27	-6.19	-6.05	-6.01	-7.87	-6.26	-6.24	-6.16	-6.16
CH2OH	-9.60	-7.70	-7.66	-7.60	-7.58	-7.68	-6.20	-6.21	-6.02	-6.03	-7.79	-6.33	-6.24	-6.12	-6.09	-7.90	-6.29	-6.27	-6.19	-6.20
CH3	-9.46	-7.55	-7.53	-7.49	-7.48	-7.54	-6.06	-6.08	-5.91	-5.93	-7.64	-6.19	-6.11	-6.01	-5.98	-7.70	-6.11	-6.10	-6.04	-6.06
CHO	-9.37	-7.48	-7.45	-7.41	-7.41	-7.49	-6.01	-6.04	-5.87	-5.89	-7.49	-6.06	-5.99	-5.88	-5.86	-7.68	-6.08	-6.08	-6.02	-6.04
CN	-9.33	-7.44	-7.41	-7.37	-7.35	-7.46	-5.99	-6.01	-5.84	-5.86	-7.43	-6.02	-5.95	-5.83	-5.80	-7.65	-6.06	-6.05	-5.99	-6.00
COCH3	-9.77	-7.82	-7.78	-7.71	-7.69	-7.83	-6.32	-6.33	-6.13	-6.14	-7.89	-6.41	-6.33	-6.18	-6.15	-8.11	-6.45	-6.44	-6.34	-6.35
COOCH3	-9.63	-7.70	-7.66	-7.60	-7.58	-7.72	-6.23	-6.23	-6.05	-6.06	-7.74	-6.29	-6.21	-6.07	-6.04	-7.97	-6.34	-6.31	-6.24	-6.24
COOH	-9.45	-7.55	-7.52	-7.47	-7.46	-7.58	-6.10	-6.12	-5.95	-5.96	-7.57	-6.14	-6.07	-5.94	-5.92	-7.80	-6.19	-6.18	-6.12	-6.13
F	-8.67	-6.88	-6.90	-6.89	-6.90	-6.87	-5.48	-5.53	-5.40	-5.43	-6.91	-5.55	-5.51	-5.44	-5.42	-6.91	-5.43	-5.46	-5.44	-5.46
NH2	-9.36	-7.46	-7.46	-7.41	-7.41	-7.44	-5.98	-6.00	-5.84	-5.85	-7.54	-6.09	-6.03	-5.93	-5.91	-7.41	-5.87	-5.88	-5.82	-5.93
NHCH3	-10.06	-8.08	-8.06	-7.93	-7.92	-7.99	-6.49	-6.49	-6.25	-6.26	-8.25	-6.73	-6.64	-6.46	-6.43	-8.28	-6.64	-6.62	-6.47	-6.47
NO2	-9.36	-7.45	-7.44	-7.37	-7.37	-7.49	-6.02	-6.04	-5.86	-5.88	-7.53	-6.09	-6.02	-5.90	-5.87	-7.70	-6.09	-6.09	-6.02	-6.03
NO	-9.27	-7.38	-7.36	-7.32	-7.32	-7.37	-5.91	-5.94	-5.78	-5.80	-7.43	-6.01	-5.94	-5.84	-5.81	-7.55	-5.97	-5.97	-5.92	-5.93
OCF3	-9.52	-7.62	-7.60	-7.50	-7.49	-7.60	-6.14	-6.17	-5.95	-5.96	-7.70	-6.26	-6.19	-6.03	-6.00	-7.82	-6.24	-6.24	-6.12	-6.12
OH	-8.97	-7.13	-7.14	-7.11	-7.12	-7.10	-5.68	-5.73	-5.58	-5.61	-7.20	-5.79	-5.74	-5.66	-5.64	-7.16	-5.65	-5.67	-5.63	-5.65
OME	-9.46	-7.55	-7.55	-7.47	-7.48	-7.51	-6.04	-6.08	-5.89	-5.91	-7.66	-6.20	-6.14	-6.01	-5.99	-7.67	-6.09	-6.10	-6.01	-6.03
SCH3	-9.97	-8.02	-7.98	-7.88	-7.86	-8.11	-6.58	-6.58	-6.35	-6.35	-8.13	-6.63	-6.53	-6.38	-6.34	-8.37	-6.71	-6.68	-6.55	-6.55
SH	-9.59	-7.69	-7.65	-7.60	-7.58	-7.76	-6.28	-6.28	-6.09	-6.09	-7.78	-6.32	-6.23	-6.11	-6.07	-7.95	-6.35	-6.31	-6.24	-6.24
SiF3	-9.63	-7.71	-7.66	-7.60	-7.58	-7.70	-6.21	-6.20	-6.03	-6.03	-7.75	-6.31	-6.22	-6.08	-6.05	-7.93	-6.31	-6.28	-6.21	-6.21
SiH3	-9.76	-7.84	-7.77	-7.73	-7.70	-7.85	-6.35	-6.33	-6.15	-6.15	-7.92	-6.45	-6.34	-6.22	-6.18	-8.05	-6.43	-6.38	-6.31	-6.31

Table C.19: SAPT0 electrostatic component (kcal mol^{-1}) for monosubstituted dimers of benzene, borazine, and triazine (R = 4.0 Å).

X	Bz-X Bz	Bz-X BnB	Bz-X BnN	Bz-X Tz	Bz-X TzN	Bn(B)-X Bz	Bn(B)-X BnB	Bn(B)-X BnN	Bn(B)-X Tz	Bn(B)-X TzN	Bn(N)-X Bz	Bn(N)-X BnB	Bn(N)-X BnN	Bn(N)-X Tz	Bn(N)-X TzN	Tz-X Bz	Tz-X BnB	Tz-X BnN	Tz-X Tz	Tz-X TzN
H	0.58	-0.09	-0.09	-0.88	-0.88	-0.10	0.21	-0.67	-0.32	-0.62	-0.10	-0.67	0.21	-0.62	-0.32	-0.88	-0.32	-0.62	0.80	-1.04
BF2	-0.14	-0.41	-0.34	-0.65	-0.96	-0.57	-0.03	-0.84	-0.04	-0.91	-0.97	-0.99	-0.17	-0.33	-0.40	-1.41	-0.57	-0.84	1.05	-1.29
CCH	0.14	-0.15	-0.30	-0.94	-0.53	-0.32	0.18	-0.80	-0.41	-0.42	-0.81	-0.79	-0.19	-0.71	0.11	-1.01	-0.35	-0.69	0.71	-0.84
CF3	-0.43	-0.37	-0.57	-0.75	-0.64	-1.06	-0.08	-1.16	-0.18	-0.52	-1.16	-0.96	-0.35	-0.52	-0.09	-1.78	-0.61	-1.09	0.89	-0.90
CH2OH	0.56	-0.13	-0.05	-0.65	-1.11	-0.09	0.13	-0.59	-0.12	-0.84	-0.16	-0.71	0.22	-0.44	-0.49	-0.81	-0.54	-0.54	0.98	-1.27
CH3	0.61	-0.04	-0.12	-0.86	-0.95	-0.03	0.24	-0.65	-0.34	-0.66	-0.12	-0.64	0.17	-0.63	-0.34	-0.73	-0.25	-0.59	0.76	-1.08
CHO	-0.21	-0.34	-0.43	-0.78	-0.70	-0.65	0.01	-0.92	-0.16	-0.68	-1.00	-0.92	-0.24	-0.51	-0.15	-1.45	-0.51	-0.91	0.86	-0.99
CN	-0.52	-0.35	-0.64	-0.92	-0.39	-0.97	-0.02	-1.14	-0.35	-0.35	-1.43	-0.97	-0.52	-0.68	0.19	-1.81	-0.59	-1.11	0.73	-0.70
COCH3	-0.04	-0.30	-0.36	-0.79	-0.77	-0.54	0.05	-0.88	-0.19	-0.70	-0.80	-0.86	-0.14	-0.51	-0.22	-1.29	-0.45	-0.85	0.81	-1.00
COOCH3	-0.01	-0.34	-0.24	-0.61	-0.88	-0.54	0.00	-0.80	-0.02	-0.81	-0.76	-0.91	-0.04	-0.31	-0.36	-1.24	-0.51	-0.72	1.05	-1.17
COOH	-0.15	-0.39	-0.32	-0.62	-0.84	-0.67	-0.04	-0.87	-0.02	-0.78	-0.93	-0.96	-0.12	-0.32	-0.32	-1.40	-0.56	-0.80	1.05	-1.14
F	0.07	-0.16	-0.37	-0.83	-0.64	-0.49	0.12	-0.87	-0.33	-0.44	-0.71	-0.79	-0.11	-0.70	0.06	-1.43	-0.47	-0.89	0.80	-0.78
NH2	0.72	0.00	-0.08	-0.78	-1.09	0.19	0.26	-0.51	-0.37	-0.69	-0.13	-0.66	0.17	-0.66	-0.32	-0.57	-0.12	-0.55	0.53	-1.21
NHCH3	0.74	-0.01	-0.13	-0.84	-1.15	0.19	0.26	-0.52	-0.39	-0.70	-0.14	-0.68	0.12	-0.74	-0.37	-0.51	-0.20	-0.52	0.71	-1.20
NO2	-0.79	-0.54	-0.66	-0.60	-0.60	-1.33	-0.22	-1.22	-0.03	-0.58	-1.38	-1.07	-0.39	-0.37	-0.16	-2.14	-0.78	-1.18	1.03	-0.89
NO	-0.38	-0.39	-0.50	-0.77	-0.59	-0.84	-0.03	-1.02	-0.16	-0.58	-0.96	-0.92	-0.21	-0.50	-0.14	-1.60	-0.57	-0.95	0.90	-0.93
OCF3	-0.21	-0.33	-0.45	-0.67	-0.76	-0.80	-0.08	-0.94	-0.14	-0.58	-0.95	-0.94	-0.19	-0.55	-0.09	-1.57	-0.59	-0.94	0.92	-0.94
OH	0.44	-0.03	-0.24	-0.88	-0.76	-0.11	0.25	-0.69	-0.42	-0.47	-0.37	-0.67	0.03	-0.78	0.00	-0.97	-0.30	-0.71	0.71	-0.85
OME	0.53	-0.01	-0.19	-0.87	-0.85	-0.04	0.26	-0.66	-0.42	-0.51	-0.25	-0.65	0.10	-0.75	-0.11	-0.78	-0.23	-0.64	0.67	-0.91
SCH3	0.39	-0.02	-0.30	-1.13	-0.50	-0.27	0.22	-0.86	-0.69	-0.20	-0.33	-0.61	-0.02	-0.93	0.10	-0.85	-0.24	-0.72	0.41	-0.67
SH	0.25	-0.07	-0.34	-1.08	-0.48	-0.40	0.16	-0.90	-0.62	-0.23	-0.48	-0.67	-0.09	-0.91	0.13	-1.02	-0.32	-0.77	0.51	-0.70
SiF3	-0.55	-0.51	-0.58	-0.59	-0.92	-1.12	-0.19	-1.13	-0.03	-0.80	-1.31	-1.08	-0.39	-0.32	-0.39	-1.84	-0.69	-1.09	1.08	-1.23
SiH3	0.26	-0.21	-0.25	-0.79	-0.97	-0.39	0.08	-0.81	-0.23	-0.75	-0.48	-0.78	-0.01	-0.52	-0.40	-0.98	-0.37	-0.70	0.87	-1.22

Table C.20: SAPT0 exchange-repulsion component (kcal mol^{-1}) for monosubstituted dimers of benzene, borazine, and triazine (R = 4.0 Å).

X	Bz-X Bz	Bz-X BnB	Bz-X BnN	Bz-X Tz	Bz-X TzN	Bn(B)-X Bz	Bn(B)-X BnB	Bn(B)-X BnN	Bn(B)-X Tz	Bn(B)-X TzN	Bn(N)-X Bz	Bn(N)-X BnB	Bn(N)-X BnN	Bn(N)-X Tz	Bn(N)-X TzN	Tz-X Bz	Tz-X BnB	Tz-X BnN	Tz-X Tz	Tz-X TzN
H	2.66	1.92	1.92	1.68	1.68	1.92	1.41	1.29	1.13	1.09	1.92	1.29	1.41	1.09	1.13	1.68	1.13	1.09	0.90	0.90
BF2	2.69	1.91	1.93	1.65	1.66	1.99	1.46	1.34	1.15	1.11	1.93	1.28	1.40	1.05	1.10	1.76	1.17	1.14	0.93	0.93
CCH	2.55	1.83	1.81	1.56	1.56	1.95	1.45	1.31	1.12	1.08	1.82	1.23	1.32	0.99	1.02	1.70	1.16	1.10	0.90	0.90
CF3	2.65	1.89	1.87	1.57	1.59	1.97	1.45	1.31	1.10	1.06	1.97	1.33	1.42	1.04	1.09	1.81	1.22	1.16	0.92	0.92
CH2OH	2.63	1.92	1.89	1.64	1.64	1.96	1.47	1.33	1.13	1.10	1.91	1.30	1.39	1.05	1.10	1.74	1.14	1.14	0.92	0.92
CH3	2.64	1.92	1.89	1.66	1.66	1.94	1.44	1.31	1.13	1.09	1.91	1.29	1.40	1.07	1.11	1.71	1.16	1.11	0.91	0.91
CHO	2.59	1.84	1.85	1.58	1.59	1.94	1.42	1.30	1.11	1.07	1.88	1.24	1.36	1.01	1.06	1.72	1.14	1.11	0.90	0.90
CN	2.51	1.78	1.78	1.51	1.52	1.92	1.40	1.28	1.09	1.05	1.82	1.20	1.30	0.97	1.01	1.69	1.12	1.08	0.87	0.87
COCH3	2.61	1.86	1.87	1.60	1.60	1.96	1.44	1.31	1.12	1.09	1.89	1.26	1.37	1.03	1.07	1.74	1.16	1.13	0.91	0.91
COOCH3	2.57	1.82	1.84	1.57	1.58	1.93	1.41	1.29	1.11	1.07	1.85	1.23	1.34	1.00	1.05	1.70	1.13	1.10	0.89	0.89
COOH	2.56	1.81	1.83	1.56	1.57	1.93	1.41	1.29	1.10	1.07	1.85	1.22	1.33	1.00	1.04	1.70	1.13	1.09	0.89	0.89
F	2.49	1.79	1.76	1.55	1.54	1.85	1.35	1.23	1.06	1.02	1.80	1.19	1.29	0.98	1.01	1.60	1.07	1.02	0.84	0.83
NH2	2.61	1.92	1.86	1.65	1.64	1.94	1.45	1.32	1.13	1.10	1.87	1.27	1.36	1.05	1.08	1.63	1.11	1.05	0.86	0.89
NHCH3	2.81	2.11	2.04	1.78	1.77	2.00	1.51	1.37	1.16	1.12	2.09	1.48	1.55	1.19	1.23	1.84	1.31	1.23	0.98	0.98
NO2	2.46	1.72	1.73	1.48	1.48	1.88	1.36	1.24	1.06	1.02	1.81	1.19	1.30	0.97	1.01	1.66	1.08	1.05	0.84	0.85
NO	2.52	1.78	1.79	1.53	1.54	1.90	1.39	1.26	1.08	1.05	1.85	1.23	1.34	1.00	1.05	1.68	1.12	1.08	0.87	0.88
OCF3	2.60	1.88	1.83	1.56	1.56	1.95	1.44	1.31	1.09	1.05	1.92	1.30	1.38	1.02	1.06	1.77	1.21	1.15	0.90	0.90
OH	2.53	1.84	1.80	1.59	1.58	1.87	1.37	1.25	1.08	1.04	1.83	1.22	1.32	1.01	1.04	1.62	1.09	1.04	0.86	0.85
OME	2.61	1.90	1.86	1.64	1.63	1.89	1.40	1.27	1.10	1.06	1.89	1.27	1.37	1.05	1.08	1.67	1.13	1.08	0.88	0.88
SCH3	2.61	1.92	1.87	1.61	1.60	2.03	1.54	1.40	1.17	1.13	1.92	1.33	1.40	1.06	1.09	1.79	1.25	1.19	0.95	0.95
SH	2.58	1.90	1.84	1.59	1.58	2.02	1.53	1.38	1.17	1.12	1.91	1.33	1.39	1.04	1.07	1.78	1.25	1.18	0.94	0.94
SiF3	2.73	1.95	1.95	1.64	1.65	2.02	1.49	1.35	1.14	1.10	2.02	1.37	1.46	1.07	1.12	1.84	1.25	1.19	0.95	0.95
SiH3	2.75	2.00	1.98	1.70	1.71	2.02	1.51	1.37	1.17	1.13	2.01	1.38	1.47	1.11	1.15	1.81	1.25	1.19	0.96	0.97

Table C.21: SAPT0 induction component (kcal mol^{-1}) for monosubstituted dimers of benzene, borazine, and triazine (R = 4.0 Å).

X	Bz-X Bz	Bz-X BnB	Bz-X BnN	Bz-X Tz	Bz-X TzN	Bn(B)-X Bz	Bn(B)-X BnB	Bn(B)-X BnN	Bn(B)-X Tz	Bn(B)-X TzN	Bn(N)-X Bz	Bn(N)-X BnB	Bn(N)-X BnN	Bn(N)-X Tz	Bn(N)-X TzN	Tz-X Bz	Tz-X BnB	Tz-X BnN	Tz-X Tz	Tz-X TzN
H	-0.21	-0.17	-0.17	-0.15	-0.15	-0.17	-0.06	-0.10	-0.07	-0.09	-0.17	-0.10	-0.06	-0.09	-0.07	-0.15	-0.07	-0.09	-0.05	-0.07
BF2	-0.17	-0.12	-0.11	-0.10	-0.10	-0.19	-0.07	-0.12	-0.07	-0.09	-0.19	-0.12	-0.07	-0.09	-0.07	-0.21	-0.12	-0.14	-0.08	-0.10
CCH	-0.21	-0.15	-0.15	-0.13	-0.14	-0.18	-0.07	-0.11	-0.07	-0.10	-0.21	-0.13	-0.09	-0.10	-0.08	-0.17	-0.08	-0.11	-0.06	-0.08
CF3	-0.18	-0.12	-0.12	-0.10	-0.10	-0.20	-0.08	-0.12	-0.07	-0.10	-0.21	-0.13	-0.09	-0.11	-0.08	-0.24	-0.14	-0.16	-0.11	-0.12
CH2OH	-0.25	-0.19	-0.20	-0.17	-0.18	-0.19	-0.09	-0.13	-0.09	-0.11	-0.20	-0.13	-0.09	-0.11	-0.08	-0.18	-0.12	-0.12	-0.07	-0.09
CH3	-0.23	-0.17	-0.19	-0.16	-0.16	-0.17	-0.07	-0.11	-0.07	-0.10	-0.18	-0.11	-0.07	-0.09	-0.07	-0.15	-0.07	-0.09	-0.05	-0.07
CHO	-0.18	-0.12	-0.12	-0.11	-0.11	-0.19	-0.07	-0.12	-0.07	-0.10	-0.21	-0.13	-0.09	-0.10	-0.08	-0.21	-0.11	-0.14	-0.09	-0.10
CN	-0.18	-0.12	-0.12	-0.10	-0.10	-0.19	-0.08	-0.12	-0.07	-0.09	-0.26	-0.18	-0.12	-0.13	-0.10	-0.25	-0.15	-0.18	-0.11	-0.13
COCH3	-0.20	-0.14	-0.14	-0.12	-0.12	-0.21	-0.09	-0.13	-0.08	-0.11	-0.22	-0.14	-0.10	-0.10	-0.08	-0.22	-0.12	-0.15	-0.09	-0.11
COOCH3	-0.18	-0.13	-0.13	-0.11	-0.11	-0.18	-0.06	-0.11	-0.06	-0.09	-0.19	-0.11	-0.07	-0.08	-0.06	-0.19	-0.09	-0.12	-0.07	-0.08
COOH	-0.17	-0.12	-0.12	-0.10	-0.10	-0.18	-0.06	-0.11	-0.06	-0.09	-0.19	-0.12	-0.08	-0.09	-0.06	-0.20	-0.10	-0.13	-0.08	-0.09
F	-0.18	-0.12	-0.13	-0.10	-0.11	-0.16	-0.05	-0.09	-0.06	-0.08	-0.19	-0.11	-0.07	-0.09	-0.07	-0.19	-0.10	-0.13	-0.08	-0.09
NH2	-0.27	-0.19	-0.21	-0.18	-0.19	-0.19	-0.09	-0.12	-0.09	-0.11	-0.18	-0.10	-0.07	-0.09	-0.07	-0.16	-0.07	-0.10	-0.06	-0.09
NHCH3	-0.30	-0.22	-0.24	-0.20	-0.22	-0.21	-0.10	-0.14	-0.10	-0.12	-0.20	-0.12	-0.09	-0.11	-0.08	-0.20	-0.11	-0.13	-0.09	-0.11
NO2	-0.18	-0.12	-0.11	-0.09	-0.09	-0.23	-0.10	-0.14	-0.08	-0.11	-0.24	-0.15	-0.11	-0.11	-0.09	-0.31	-0.19	-0.23	-0.15	-0.16
NO	-0.17	-0.12	-0.11	-0.10	-0.10	-0.18	-0.06	-0.11	-0.06	-0.09	-0.20	-0.12	-0.07	-0.09	-0.07	-0.22	-0.12	-0.15	-0.09	-0.10
OCF3	-0.18	-0.12	-0.12	-0.10	-0.10	-0.18	-0.07	-0.11	-0.06	-0.09	-0.21	-0.13	-0.09	-0.10	-0.07	-0.22	-0.12	-0.14	-0.09	-0.10
OH	-0.22	-0.15	-0.17	-0.14	-0.15	-0.18	-0.07	-0.11	-0.07	-0.10	-0.19	-0.11	-0.08	-0.10	-0.07	-0.16	-0.08	-0.10	-0.06	-0.08
OME	-0.24	-0.17	-0.19	-0.15	-0.16	-0.19	-0.08	-0.12	-0.08	-0.10	-0.19	-0.12	-0.08	-0.10	-0.08	-0.17	-0.08	-0.11	-0.07	-0.08
SCH3	-0.25	-0.18	-0.19	-0.16	-0.17	-0.21	-0.10	-0.13	-0.10	-0.12	-0.21	-0.13	-0.09	-0.11	-0.09	-0.19	-0.10	-0.12	-0.08	-0.09
SH	-0.22	-0.16	-0.17	-0.14	-0.15	-0.19	-0.09	-0.12	-0.09	-0.11	-0.20	-0.13	-0.08	-0.11	-0.08	-0.18	-0.09	-0.11	-0.07	-0.09
SiF3	-0.18	-0.12	-0.11	-0.10	-0.10	-0.22	-0.10	-0.14	-0.08	-0.10	-0.22	-0.14	-0.09	-0.11	-0.08	-0.26	-0.15	-0.18	-0.11	-0.13
SiH3	-0.20	-0.15	-0.16	-0.13	-0.14	-0.19	-0.07	-0.12	-0.07	-0.10	-0.18	-0.11	-0.07	-0.09	-0.07	-0.18	-0.09	-0.12	-0.06	-0.09

Table C.22: SAPT0 dispersion component (kcal mol^{-1}) for monosubstituted dimers of benzene, borazine, and triazine (R = 4.0 Å).

X	Bz-X Bz	Bz-X BnB	Bz-X BnN	Bz-X Tz	Bz-X TzN	Bn(B)-X Bz	Bn(B)-X BnB	Bn(B)-X BnN	Bn(B)-X Tz	Bn(B)-X TzN	Bn(N)-X Bz	Bn(N)-X BnB	Bn(N)-X BnN	Bn(N)-X Tz	Bn(N)-X TzN	Tz-X Bz	Tz-X BnB	Tz-X BnN	Tz-X Tz	Tz-X TzN
H	-0.21	-0.17	-0.17	-0.15	-0.15	-0.17	-0.06	-0.10	-0.07	-0.09	-0.17	-0.10	-0.06	-0.09	-0.07	-0.15	-0.07	-0.09	-0.05	-0.07
BF2	-0.17	-0.12	-0.11	-0.10	-0.10	-0.19	-0.07	-0.12	-0.07	-0.09	-0.19	-0.12	-0.07	-0.09	-0.07	-0.21	-0.12	-0.14	-0.08	-0.10
CCH	-0.21	-0.15	-0.15	-0.13	-0.14	-0.18	-0.07	-0.11	-0.07	-0.10	-0.21	-0.13	-0.09	-0.10	-0.08	-0.17	-0.08	-0.11	-0.06	-0.08
CF3	-0.18	-0.12	-0.12	-0.10	-0.10	-0.20	-0.08	-0.12	-0.07	-0.10	-0.21	-0.13	-0.09	-0.11	-0.08	-0.24	-0.14	-0.16	-0.11	-0.12
CH2OH	-0.25	-0.19	-0.20	-0.17	-0.18	-0.19	-0.09	-0.13	-0.09	-0.11	-0.20	-0.13	-0.09	-0.11	-0.08	-0.18	-0.12	-0.12	-0.07	-0.09
CH3	-0.23	-0.17	-0.19	-0.16	-0.16	-0.17	-0.07	-0.11	-0.07	-0.10	-0.18	-0.11	-0.07	-0.09	-0.07	-0.15	-0.07	-0.09	-0.05	-0.07
CHO	-0.18	-0.12	-0.12	-0.11	-0.11	-0.19	-0.07	-0.12	-0.07	-0.10	-0.21	-0.13	-0.09	-0.10	-0.08	-0.21	-0.11	-0.14	-0.09	-0.10
CN	-0.18	-0.12	-0.12	-0.10	-0.10	-0.19	-0.08	-0.12	-0.07	-0.09	-0.26	-0.18	-0.12	-0.13	-0.10	-0.25	-0.15	-0.18	-0.11	-0.13
COCH3	-0.20	-0.14	-0.14	-0.12	-0.12	-0.21	-0.09	-0.13	-0.08	-0.11	-0.22	-0.14	-0.10	-0.10	-0.08	-0.22	-0.12	-0.15	-0.09	-0.11
COOCH3	-0.18	-0.13	-0.13	-0.11	-0.11	-0.18	-0.06	-0.11	-0.06	-0.09	-0.19	-0.11	-0.07	-0.08	-0.06	-0.19	-0.09	-0.12	-0.07	-0.08
COOH	-0.17	-0.12	-0.12	-0.10	-0.10	-0.18	-0.06	-0.11	-0.06	-0.09	-0.19	-0.12	-0.08	-0.09	-0.06	-0.20	-0.10	-0.13	-0.08	-0.09
F	-0.18	-0.12	-0.13	-0.10	-0.11	-0.16	-0.05	-0.09	-0.06	-0.08	-0.19	-0.11	-0.07	-0.09	-0.07	-0.19	-0.10	-0.13	-0.08	-0.09
NH2	-0.27	-0.19	-0.21	-0.18	-0.19	-0.19	-0.09	-0.12	-0.09	-0.11	-0.18	-0.10	-0.07	-0.09	-0.07	-0.16	-0.07	-0.10	-0.06	-0.09
NHCH3	-0.30	-0.22	-0.24	-0.20	-0.22	-0.21	-0.10	-0.14	-0.10	-0.12	-0.20	-0.12	-0.09	-0.11	-0.08	-0.20	-0.11	-0.13	-0.09	-0.11
NO2	-0.18	-0.12	-0.11	-0.09	-0.09	-0.23	-0.10	-0.14	-0.08	-0.11	-0.24	-0.15	-0.11	-0.11	-0.09	-0.31	-0.19	-0.23	-0.15	-0.16
NO	-0.17	-0.12	-0.11	-0.10	-0.10	-0.18	-0.06	-0.11	-0.06	-0.09	-0.20	-0.12	-0.07	-0.09	-0.07	-0.22	-0.12	-0.15	-0.09	-0.10
OCF3	-0.18	-0.12	-0.12	-0.10	-0.10	-0.18	-0.07	-0.11	-0.06	-0.09	-0.21	-0.13	-0.09	-0.10	-0.07	-0.22	-0.12	-0.14	-0.09	-0.10
OH	-0.22	-0.15	-0.17	-0.14	-0.15	-0.18	-0.07	-0.11	-0.07	-0.10	-0.19	-0.11	-0.08	-0.10	-0.07	-0.16	-0.08	-0.10	-0.06	-0.08
OME	-0.24	-0.17	-0.19	-0.15	-0.16	-0.19	-0.08	-0.12	-0.08	-0.10	-0.19	-0.12	-0.08	-0.10	-0.08	-0.17	-0.08	-0.11	-0.07	-0.08
SCH3	-0.25	-0.18	-0.19	-0.16	-0.17	-0.21	-0.10	-0.13	-0.10	-0.12	-0.21	-0.13	-0.09	-0.11	-0.09	-0.19	-0.10	-0.12	-0.08	-0.09
SH	-0.22	-0.16	-0.17	-0.14	-0.15	-0.19	-0.09	-0.12	-0.09	-0.11	-0.20	-0.13	-0.08	-0.11	-0.08	-0.18	-0.09	-0.11	-0.07	-0.09
SiF3	-0.18	-0.12	-0.11	-0.10	-0.10	-0.22	-0.10	-0.14	-0.08	-0.10	-0.22	-0.14	-0.09	-0.11	-0.08	-0.26	-0.15	-0.18	-0.11	-0.13
SiH3	-0.20	-0.15	-0.16	-0.13	-0.14	-0.19	-0.07	-0.12	-0.07	-0.10	-0.18	-0.11	-0.07	-0.09	-0.07	-0.18	-0.09	-0.12	-0.06	-0.09

APPENDIX D

Computing the σ- and π-components of the ESP and Q_{zz}

The electrostatic potential of a collection of nuclei and the associated electron density is given by

$$V(\mathbf{r}) = V^{nuc}(\mathbf{r}) + V^{elec}(\mathbf{r}) = \sum_{A}^{nuclei} \frac{Z_A}{|\mathbf{r} - \mathbf{R_A}|} - \int \frac{\rho(\mathbf{r}')}{|\mathbf{r} - \mathbf{r}'|} d\mathbf{r}'$$

where the integral runs over all space. We wish to partition the nuclear charges and $\rho(\mathbf{r})$ into contributions from the σ- and π-sytems, such that

$$V(\mathbf{r}) = V_\sigma(\mathbf{r}) + V_\pi(\mathbf{r}) = \left\lfloor V_\sigma^{nuc}(\mathbf{r}) + V_\sigma^{elec}(\mathbf{r}) \right\rfloor + \left\lfloor V_\pi^{nuc}(\mathbf{r}) + V_\pi^{elec}(\mathbf{r}) \right\rfloor$$

where π-system is defined as the neutral system comprising the π-electrons and corresponding component of the nuclear charge. σ-system is defined similarly.

For planar arenes, this can be accomplished by partitioning the electron density based on the symmetry of the underlying molecular orbitals. For a C_s-symmetric arene in which the mirror-plane corresponds to the molecular plane, the contributions of the σ- and π-electrons to the electrostatic potential can be defined as

$$V_{a'}^{elec}(\mathbf{r}) = -\int \frac{\rho_{a'}(\mathbf{r}')}{|\mathbf{r} - \mathbf{r}'|} d\mathbf{r}' \equiv V_\sigma^{elec}(\mathbf{r})$$

and

$$V_{a''}^{elec}(\mathbf{r}) = -\int \frac{\rho_{a''}(\mathbf{r}')}{|\mathbf{r} - \mathbf{r}'|} d\mathbf{r}' \equiv V_\pi^{elec}(\mathbf{r}),$$

where

$$\rho_{a'}(\mathbf{r}) = 2\sum_{i}^{a'} \left|\phi_i^s(\mathbf{r})\right|^2$$

and

$$\rho_{a''}(\mathbf{r}) = 2\sum_{i}^{a''} \left|\phi_i^s(\mathbf{r})\right|^2$$

in which the sums run over all doubly-occupied molecular orbitals of *a′* or *a″* symmetry.

The σ- and π-contributions to $V^{nuc}(\mathbf{r})$ are evaluated by assigning effective charges to each nucleus *A* ($Z_{s,A}^{eff}$, where s = σ or π) according to the number of electrons contributed to the *σ*- and *π*-systems in a given molecule (*e.g.* in benzene, $Z_{\pi,H}^{eff} = 0$, $Z_{\sigma,H}^{eff}$

= 1, $Z^{eff}_{\pi,C}$ = 1, and $Z^{eff}_{\sigma,C}$ = 5). The nuclear component of the ESP is computed separately for the σ- and π-sytems via

$$V^{nuc}_{\sigma}(\mathbf{r}) = \sum_{A}^{nuclei} \frac{Z^{eff}_{\sigma,A}}{|\mathbf{r} - \mathbf{R_A}|}$$

and

$$V^{nuc}_{\pi}(\mathbf{r}) = \sum_{A}^{nuclei} \frac{Z^{eff}_{\pi,A}}{|\mathbf{r} - \mathbf{R_A}|}$$

The σ- and π-components of Q_{zz} are defined similarly.

Table D.1: Q_{zz} values for the azines (ΔQ), as well as the nuclear (ΔQ_N), σ-electronic [$\Delta Q_e(\sigma)$] and π-electronic [$\Delta Q_e(\pi)$] contributions, all relative to benzene.[a]

	ΔQ	ΔQ_N	ΔQ_e	$\Delta Q_e(\sigma)$	$\Delta Q_e(\pi)$
pyridine	3.0	17.8	–14.9	–14.6	–0.3
pyrazine	6.1	35.0	–29.0	–28.5	–0.5
s-triazine	9.2	53.2	–44.0	–43.3	–0.7
s-tetrazine	11.4	63.8	–52.4	–51.8	–0.6

[a] Computed at the HF/aug-cc-pVTZ level of theory. Q_{zz} values are in Buckinghams.

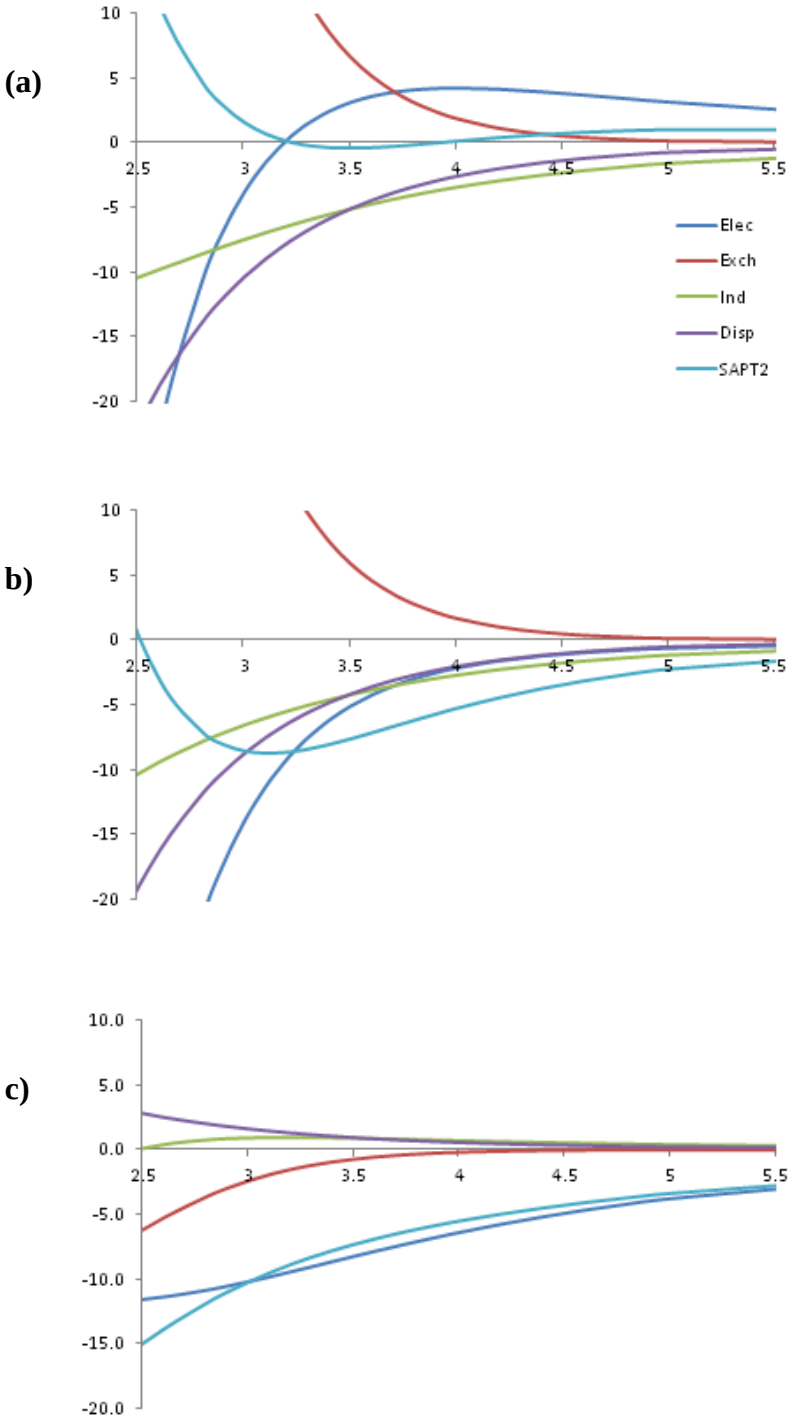

Figure D.1: SAPT2 energy components as a function of anion-arene distance for (a) benzene and (b) s-triazine, as well as the difference between the two plots (c). The difference in the SAPT2 interaction energy closely followed the difference in the electrostatic components. Plots for the other azines look the same, only scaled by the number of nitrogen atoms.